

# **Tunable Nanoparticles for the Local Delivery of Protein Drugs for Improved Vaccination**

**Dissertation**

zur Erlangung des Grades

des Doktors der Naturwissenschaften

der Naturwissenschaftlichen-Technischen Fakultät III

Chemie, Pharmazie, Bio- und Werkstoffwissenschaften

der Universität des Saarlandes

von

**René Rietscher**

Saarbrücken

2015

**Die vorliegende Arbeit wurde in der Zeit von April 2011 bis September 2014 an der Universität des Saarlandes in Saarbrücken angefertigt.**

Tag des Kolloquiums:	11.12.2015
Dekan:	Prof. Dr.-Ing. Dirk Bähre
Berichterstatter:	Prof. Dr. Claus-Michael Lehr
	Prof. Dr. Elmar Heinzle
Vorsitz:	Prof. Dr. Marc Schneider
Akad. Mitarbeiter:	Dr. Stefan Boettcher

Diese Arbeit wurde im Rahmen des BMBF geförderten Projektes  
*„Plattform für effizienten epithelialen Transport für pharmazeutische  
Applikationen durch innovative partikuläre Trägersysteme“*  
(Akronym „PeTrA“, Fördernummer: 13N11454) angefertigt.

# Table of Contents

<b>Summary .....</b>	<b>4</b>
<b>Zusammenfassung .....</b>	<b>5</b>
<b>1. General Introduction .....</b>	<b>6</b>
1.1. Oral vaccination .....	6
1.1.1. Intestinal mucosal immune system .....	7
1.1.2. Specific Immune system .....	9
1.1.3. Adjuvants .....	11
1.1.4. Delivery of protein-particles through the GIT.....	13
1.2. Particulate vaccine/protein delivery systems.....	14
1.2.1. Polymers for passive and active drug targeting.....	16
1.2.2. Preparation methods .....	19
1.2.3. Particle size .....	21
1.2.4. Surface properties of nanoparticles .....	23
1.2.5. Drug loading .....	25
1.2.6. Drug release .....	26
1.3. References .....	28
<b>2. Research Objectives .....</b>	<b>40</b>
<b>3. Impact of hydrophilic-modified PLGA on particle formation, protein loading and release .....</b>	<b>41</b>
3.1. Introduction .....	42
3.2. Materials and methods.....	44
3.2.1. Materials .....	44
3.2.2. Preparation of nanoparticles .....	45
3.2.3. Characterization of nanoparticles.....	45
3.2.4. Determination of Encapsulation efficiency and loading.....	46
3.2.5. In vitro release of protein .....	46
3.2.6. Activity of OVA .....	46
3.2.7. Determination of surface hydrophobicity .....	47
3.2.8. Statistical analysis .....	47

3.3. Results and discussion .....	47
3.3.1. Characterization of nanoparticles.....	48
3.3.2. Loading and of Encapsulation efficiency.....	49
3.3.3. Adsorption and activity studies .....	51
3.3.4. OVA release from the particles.....	54
3.4. Conclusion .....	57
3.5. References .....	58
<b>4. Antigen delivery via hydrophilic PEG-<i>b</i>-PAGE-<i>b</i>-PLGA nanoparticles improves vaccination efficiency.....</b>	<b>62</b>
4.1. Introduction .....	63
4.2. Materials and methods.....	65
4.2.1. Materials .....	65
4.2.2. Fluoresceineamine labeling of PLGA.....	65
4.2.3. Preparation of NPs .....	66
4.2.4. Characterization of NPs .....	68
4.2.5. In vitro release of antigen .....	69
4.2.6. Determination of endotoxin concentrations .....	69
4.2.7. Cytotoxicity assay for NPs .....	69
4.2.8. Stability of NP formulations in different media .....	70
4.2.9. Mice .....	70
4.2.10. Isolation and Differentiation of myeloid antigen presenting cells .....	70
4.2.11. Isolation of CD8 <sup>+</sup> cells (CTLs).....	71
4.2.12. Flow cytometry .....	71
4.2.13. NP-uptake studies .....	71
4.2.14. Evaluation of ovalbumin-NPs.....	71
4.2.15. In vivo experiments.....	72
4.2.16. Statistical analysis .....	72
4.3. Results and discussion .....	73
4.3.1. Characterization of antigen-loaded NPs .....	73
4.3.2. OVA release from antigen-loaded NPs .....	75
4.3.3. Endotoxin levels, cytotoxicity and stability of the formulations .....	77
4.3.4. Determination of a size-uptake relationship in APCs for NPs.....	78
4.3.5. In vitro effect of OVA-loaded NPs on T cells and NPs.....	80

---

4.3.6. PLGA-OVA-NPs improve generation of cytotoxic CD8 T cells in vivo.....	83
4.4. Conclusion .....	84
4.5. References .....	85
<b>5. Semi-Automated Nanoprecipitation-System - an option for operator independent, scalable and size adjustable nanoparticle synthesis .....</b>	<b>89</b>
5.1. Introduction .....	90
5.2. Materials and method .....	91
5.2.1. Materials .....	91
5.2.2. Experimental setup – SAN-System.....	91
5.2.3. Preparation and washing of nanoparticles .....	92
5.2.4. Characterization of nanoparticles.....	93
5.3. Results and Discussion.....	93
5.4. Conclusion .....	96
5.5. References .....	96
<b>6. Overall Conclusion and Outlook.....</b>	<b>98</b>
<b>List of Abbreviations.....</b>	<b>102</b>
<b>Curriculum vitae .....</b>	<b>105</b>
<b>List of Publications.....</b>	<b>106</b>
<b>Acknowledgements .....</b>	<b>108</b>

## Summary

The oral route of vaccination is besides nasal, vaginal or rectal route, one of the most interesting mucosal vaccination routes. Usually a vaccine as live but attenuated, inactivated or even dead pathogen is administered subcutaneously or intramuscularly via injection, to develop immunity to a pathogen. Alternatively, also purified proteins can be used for vaccination. The aim of oral or mucosal vaccination is to achieve a cheap and save mass immunization, with avoidance of needle based systems, no need of clinical environment and lower production cost. Disadvantages that have to be overcome are potential degradation of the vaccine and probably inefficient uptake through the intestinal wall, resulting in low immune responses. The present work evaluates the protection of a protein based vaccine by nanoparticles and delivery through the gastrointestinal tract as a perspective for oral vaccination. The results presented in this thesis show a successful encapsulation and therefore protection of the model protein ovalbumin with the basic polymer poly(D,L-lactide-co-glycolide acid) (PLGA) and further developed PLGA derivatives. These derivatives were found to increase the protein encapsulation up to 50% and release of the protein from nanoparticles from 50 to 100% compared to pure PLGA particles. Furthermore, the polymers introduce passive and active drug targeting properties to PLGA. In *in vitro* and also *in vivo* mice studies an improved efficiency of vaccination could be proven. This was shown by a significant increased T cell activation, with higher interleukin 2 production.

Furthermore, a new and reproducible method for a size-adjustable production of nanoparticles was investigated to study a size-dependent uptake of NPs during vaccination. This technology is a semi-automated system for an operator independent, scalable and size adjustable NP synthesis. By varying certain process parameters the system is able to produce nanoparticles in a size range of 150 to 600 nm with a narrow size distribution.

## Zusammenfassung

Die orale Vakzinierungsroute ist neben der nasalen, vaginalen oder rektalen Route, eine der interessantesten, mukosalen Vakzinierungsrouten. In der Regel wird ein Vakzin lebend, aber abgeschwächt, inaktiviert oder abgetötet subkutan oder intramuskulär verabreicht, um eine Immunität gegen einen Krankheitserreger zu entwickeln. Alternativ können auch gereinigte Proteine für eine Vakzinierung verwendet werden. Das Ziel der oralen, beziehungsweise mukosalen Vakzinierung, ist das Erreichen einer kostengünstigen und sicheren Massenvakzinierung, unter Vermeidung von Nadel basierten Systemen und ohne Notwendigkeit einer klinischen Umgebung. Nachteile, die überwunden werden müssen, sind der potenzielle Abbau des Vakzins und ineffiziente Aufnahme durch die Darmwand, mit daraus resultierenden niedrigen Immunantworten. Die vorliegende Arbeit bewertet den Schutz eines Vakzins durch Nanopartikel (NP) und Transport durch den Gastrointestinaltrakt als Perspektive für die orale Vakzinierung. Die Ergebnisse zeigen eine erfolgreiche Verkapselung und damit Schutz des Modellproteins Ovalbumin mit dem Polymer Polylactid-co-Glycolid (PLGA) und weiteren PLGA-Derivaten. Für diese Derivate wurde eine erhöhte Proteinverkapselung von bis zu 50% und eine erhöhte Freisetzungsrate aus den NP von bis zu 50 bis 100% im Vergleich zu reinen PLGA-Teilchen gefunden. Weiterhin werden mit diesen Polymeren passive und aktive Drug-Targeting-Eigenschaften in das Polymer PLGA eingeführt. *In vitro*, als auch *in vivo*-Studien an Mäusen konnten eine verbesserte Effizienz der Vakzinierung nachweisen. Dies wurde durch eine signifikant höhere T-Zell-Aktivierung, mit einer gesteigerten Interleukin 2-Produktion gezeigt.

Außerdem wurde ein neues und reproduzierbares Verfahren für die Herstellung von NP unterschiedlicher Größe untersucht, um eine größenabhängige Aufnahme von NP während der Vakzinierung zu untersuchen. Diese Technologie ist ein halbautomatisches System für eine Bediener-unabhängige, skalierbare und NP-Synthese mit einstellbarer Größe. Durch das Variieren bestimmter Verfahrensparameter konnte gezeigt werden, dass das System in der Lage ist, NP in einem Größenbereich von 150 bis 600 nm mit einer engen Größenverteilung herzustellen.



# 1. General Introduction

## 1.1. Oral vaccination

Vaccination is in general the use of an antigenic material, a vaccine, to develop immunity to a pathogen, by stimulating the immune system in order to control diseases in a preventive strategy. The first vaccination was realized by Edward Jenner in 1796 [1], who gave cowpox pus to healthy people, to induce a protective immune response against smallpox. This vaccination was so efficient, that in nowadays smallpox has been eradicated, as one of the first infection diseases [2]. But still, especially in developing countries infectious diseases cause most of the mortality among children younger than 5 years [3] and represent substantial health problems in older children and adults. Vaccines are one of the most promising interventions to reduce the burden of specific infections in populations in developing countries [4]. Furthermore the continuous contact with existing pathogens also in first world countries and additionally the emergence of new pathogens over the time requires new and innovative, but also cheap and save vaccination strategies. Especially for immunizing populations in developing countries oral vaccines are of major interest for several reasons. Particularly, contaminated needles and syringes are the main problems both for healthcare workers, as well as for environmental safety in many developing countries where there is a high prevalence of HIV and hepatitis B and C [5,6]. Current licensed vaccines are mostly delivered by subcutaneous (sc) and intramuscular (im) injection, what makes the mass immunization especially in these countries expensive and unsafe, because of the cost intensive production of the syringe that has to be applied by trained personnel [7]. Another negative aspect of the invasive route of delivery, while not using a needle free system, is the increased possibility of needle-based side effects [8]. However, also in first world countries needle and syringe vaccinations can lead to unwanted infection in both patients and healthcare workers. In the US, annually more than one million people suffer from infections from needles, thus causing costly treatments. Also to achieve high immunization coverage in the population, immunization without needles or syringes, by for example oral vaccination, would increase acceptability and consequently compliance. An alternative to the subcutaneous or intramuscular application of vaccines is the mucosal route of vaccine delivery. In particular, oral vaccination is a most attractive and also cost-effective form of preventing

infectious diseases. Over the last few years, there has been exponential increase in interest in needle-free vaccine delivery. Already various vaccine delivery systems have been under investigation for oral [9], nasal [10], ocular [11,12], vaginal [13] and rectal route [14].

For vaccination pathogens like viruses, bacteria, parasites or even fungi can be used in either live, attenuated, inactivated or killed form. Additionally, purified products, like proteins, RNA, and DNA derived from these pathogens, are possible vaccines, inducing an immune response that shows already success [15] but also failures [16] in literature. Still, oral vaccines are largely ineffective, due to degradation in the gastrointestinal tract (GIT) and probably inefficient uptake through the intestinal epithelium, resulting in low immune responses. Considering the oral vaccines available on the market only killed or attenuated microorganisms, that can resist the intestinal degradation, without any need of protection, are so far available [17]. To overcome these limitations, uncountable research groups and companies focus on oral vaccine delivery, because, already existing oral vaccines brought already great benefits for disease control or even eradication of diseases [17]. Focusing on protein based vaccines the greatest challenge is the protection of proteins from the gastrointestinal environment, by the selection of a suitable carrier and adjuvant to boost the immune response. The development of new vaccine delivery systems and suitable vaccine adjuvants can lead to cheaper and efficacious vaccines and increase the immunization rate in poor or undeveloped countries. The use of protective polymeric vaccine carriers, which can additionally function as adjuvants, is maybe one the best options to solve this global issue [18–21]. Another benefit is the avoidance of oral systemic tolerance, which is induced by oral delivery of soluble proteins, caused by T cell anergy, T cell deletion and the induction of suppressor T cells [22]. The whole complexity of oral tolerance was already reviewed elsewhere [23,24]. In order to develop new and complex vaccine strategies, the understanding of how the immune response works, how vaccines stimulate the response to convey protection and how the currently available polymeric delivery systems works, is necessary.

### **1.1.1. Intestinal mucosal immune system**

For the oral delivery of vaccines the GIT is the most important side of action [25]. With a length of approximately 9 meters and a total surface area, including villi and microvilli, of

400 m<sup>2</sup>, compared to only 2.3 m<sup>2</sup> of the skin [26], the GIT is the largest and also most studied compartment of the mucosal immune system. The surface of the GIT, including stomach as well as small and large intestine, is covered by a confluent, protecting layer of mucosa and forms together with a large number of immune cells and types of lymphoid tissue, the gut associated lymphoid tissue (GALT) [27,28]. For oral vaccination the small intestine covered by the mucosa is of great importance, which carries most of the immune cells, like T cells, monocytes/macrophages and B cells. Moreover, 80% of the immunoglobulin and immunoglobulin producing cells are located in the intestinal tract [29].

A mandatory step for starting an immune response, is the internalization and presentation of an antigen (e.g. derived from proteins) by professional antigen presenting cells (APCs), which are located within the intestinal wall [30]. Therefore, the major challenge for polymeric vaccine carriers is the save and efficient delivery of proteins through the mucus and intestinal epithelium to the APCs. Prior to the uptake of polymeric vaccine carriers by APCs, the delivery of the carrier to the intestine, uptake by intestinal cells and subsequent passage through the intestinal epithelium is important. The delivery through the stomach and therefore protection from gastric acid can be easily achieved by encapsulating the polymeric vaccine carriers, in freeze-dried and stable form, in enteric coated tablets or capsules. After the tablet or capsule has reached the intestine, the protective coating gets dissolved, together with the capsule or tablet and the polymeric vaccine carriers will be released. The mucus-covered intestine is a highly specialized tissue, which consists of enterocytes, goblet cells, enteroendocrine cells, M cells and various other cell types [27]. The goblet cells and enteroendocrine cells secrete mucus, which is required for a better float of the bolus as well as peptide hormones, responsible for the digestion of the intestinal content [31,32]. The largest population of cells in the intestine represents enterocytes. They make up approximately 80% of all intestinal epithelial cells, controlling the uptake of fluids, electrolytes and nutrients and are the most important barrier for harmful pathogens and toxic material [33,34].

The paracellular route of uptake in the intestine, through the intercellular space between the epithelial cells is completely blocked or restricted for pathogens, particulate polymeric vaccine carrier or macromolecules, due to the tight junctions. The permeability can be enhanced by selecting an appropriate polymer, like starch [35] or chitosan [36], which

might lead to an opening of tight junctions. However, the uptake and delivery of polymeric vaccine carriers via M cells is more pronounced [37]. The main task of M cells is the collection and transport of possible pathogens no matter whether, macromolecules, bacteria, viruses or particles, from the basolateral lumen [38] to the extracellular space. After crossing the mucus, the pathogens are taken up by phagocytosis or endocytosis and transported in small vesicles through M cells [39]. This whole process is also called transcytosis. Anatomically, the uptake of pathogens in M cells is also facilitated by a thinner protecting glycocalyx, sparse microvilli and apical surface receptors that can be targeted [40,41]. The majority of M cells are thereby located within Peyer's patches [42], which are local aggregations of lymphoid tissue of the small intestine. On the basolateral lumen of the Peyer's patches an increased number of APCs, within a dom-/pocket-like structure [43,44] can be found. Important APCs are dendritic cells (DCs), macrophages and B cells [45,46]. Epithelia cells, membranous microfold (M) cells or enterocytes are also able to present antigens on the cell surface, but are less important targets for vaccination [47].

### **1.1.2. Specific Immune system**

The specific immune response, also known as adaptive immune response, is able to specifically adapt the immune response to a certain pathogen [48]. The main effector cells during this process are highly specialized cells, which recognize specific structures (antigens) of pathogens and can furthermore produce antibodies against particular pathogens. After the first contact of a pathogen with the immune system and the first initial immune response a immunological memory can be created, representing the basis of vaccination [16]. Carriers of the specific immune response are white blood cells, also known as lymphocytes [49]. The specific immune response can be divided furthermore into two main broad classes – the humoral and the cell-mediated immune response [27]. During the humoral immune response the foreign antigen is bound by secreted antibodies from activated B cells leading to the inactivation of the pathogen [49]. In cell-mediated immune responses, T cells recognize their specific antigen only after the pathogen has been internalized, processed to peptide fragments and displayed on the major histocompatibility complex (MHC) of a specific APC [27]. Two MHC classes can be found, first the MHC class I molecule [50,51], which is recognized by CD8<sup>+</sup> cytotoxic T cells, present endogenous produced antigens, from invaded intracellular viruses and bacteria.

The MHC class I is expressed on nearly all cells, except of cells, without a nucleus. Second, the MHC class II molecules [52–54], which are recognized by CD4<sup>+</sup> T helper cells, are present on the cell surface of APCs that engulfed exogenous available pathogens. As we aim with our work, to combat intracellular infections, especially of virus or bacteria infected cells, the focus is on CD8<sup>+</sup> cytotoxic T cells. During CD8 mediated immune responses the T cell receptor (TCR) binds to the MHC molecule and releases after activation, interleukins (for regulation of differentiation and growth of further B and T cells) and cytotoxins (for example release of granulysin, for the apoptosis of the target cell) [16,55]. Especially for the prevention of virus replication, the release of cytotoxins is important. With the release of interleukins other cell types can be activated, leading to the differentiation of B and T cell to long live memory cells. With these memory cells a fast defense reaction, after repeated contact with the pathogen, can be achieved [56,57].

In detail, multiple steps are necessary, after a pathogen or nanoparticulate vaccine system has reached the APC (Figure 1). First the APC is surrounding the whole pathogen or nanoparticulate vaccine system, in an endosomal compartment, called phagosome [58]. After lysis or breaking up the pathogen/nanoparticle (NP), the pathogen is processed into smaller peptides, transported to the endoplasmic reticulum and bound intracellular to MHC class I, forming the MHC class I:peptide complex. This complex is then transported to the surface of the APC, for the recognition by CD8 T cells [59–61]. The binding of the MHC class I:peptide complex on the APC with the antigen-specific T cell receptor (TCR) is the first of three steps for specific T cell immunity. The second mandatory step for the activation of naïve T cells is the co-stimulation of the APC and T cell by expression of costimulatory ligands and receptors (up-regulation of CD80/86 on the cell surface of the APC and T cell) [62]. The upregulation of this costimulatory ligand is followed by the recognition of pathogen-associated molecular patterns (PAMPs) by APC through pattern recognition receptors (PRRs) [63,64]. This evolutionary initiated signaling cascade for cell activation has thereby a direct link to the adaptive and innate immunity. The last step for specific T cell immunity is the cytokine release caused with a T cell activation through cross presentation of the antigen, which can be detected by a CD69 up-regulation [65]. An interesting cytokine, which can be released, is the Interleukin 2 (IL-2), which can induce the proliferation of T cells towards effector T cells and/or memory T cells, what is essential for the fight against a recurring infection.

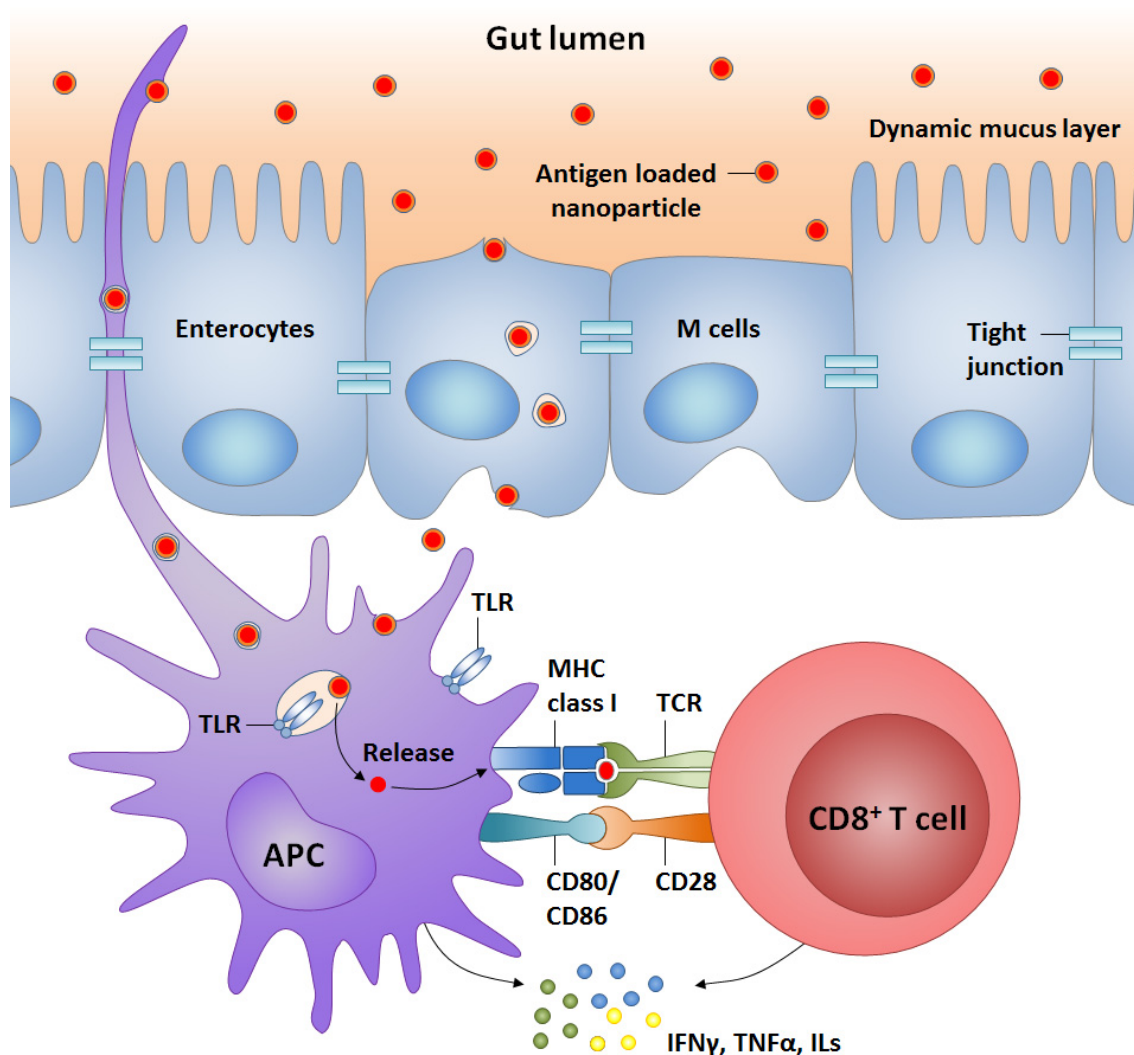


**Figure 1 | Molecular mechanisms of transport and uptake of antigen loaded NPs along the intestinal epithelium.** Antigen loaded NPs (AIN) are directly taken up by APCs or transported by M cells through the intestinal wall, before APCs in the Peyer's Patches can take up the AIN. The antigen is released from AIN and is after further processing presented to CD8<sup>+</sup> cytotoxic T cells (CTLs), by MHC I molecules. As next step the binding of the TCR on the T cell to the MHC class I:peptide complex on the APC takes place. In parallel a co-stimulation of the T cell via upregulation of CD80/86 on APCs and CD28 on T cells happens. The last step is the release of cytokines from both, APCs and T cells.

### 1.1.3. Adjuvants

For vaccination usually adjuvants (from Latin, *adiuvare*: to aid) are used to modify the immunological reaction of the vaccine [66]. The most prominent effect is the boost of immunological responses, with enhanced antigen uptake and higher release of antibodies. Consequently, this results in a longer lasting protection and also minimizes the amount of administered vaccine [67]. Two different ways of actions are known predominantly from adjuvants. First, the adjuvant can cause an irritation by inflammation, what causes an unspecific increase of immune response, boosting the immune response. Therefore, the co-administration of minimal amounts of toxins (e.g. tetanus toxin together with a tetanus

vaccine) is often used. Second, the circulation time of a vaccine in the human body can be increased by forming depot formulations, for example with oil emulsions of paraffin oil, like Freund's adjuvant. For other adjuvants like aluminum hydroxide the type of action is not totally clear. Aluminum alone has no effect on the immunological reaction, but without Aluminum the vaccine/toxin combination would not respond high enough [68]. For our research two types of adjuvants were used, CpG oligodeoxynucleotides (CpG ODN) [69] and Cholera toxin B (CTB) [70,71]. The CpG ODN is a synthetic, single-stranded DNA molecule [72,73], which binds to the endosomal associated PRR-like TLR9, inducing a strong immune response. After CpG ODN uptake the specific immune system is activated, due to its high homology to prokaryotic DNA. The CTB is a protein complex purified from cholera toxin. The main reason described in literature, why CTB has a great adjuvant effect, is the efficient binding to the monosialotetrahexosylganglioside 1 (GM1) receptor that is present on all APCs, as well as most of the M cells. This binding triggers events that results in an improved antigen uptake, with facilitating the antigen presentation [74].

The adjuvants can be either administered together with the vaccine encapsulated and protected within the carrier or co-administered in one formulation [75,76]. However, vaccine formulations containing adjuvants are designed for the initiation of an efficient immune response, but there are of course also many possible side effects [77]. Most often vaccination leads to fever, what is called in clinical trials as reactogenic. This term describes the ability to produce common or so-said “expected” side effects. Other common side effect could be redness, bruising, swelling, and induration that could be increased with the usage of adjuvants [77].

Besides the usage of additional given adjuvant, one should also consider substances, with an intrinsic adjuvant-function. This can be the polymer for the production of a nanoparticulate vaccine carrier or the carrier itself. A benefit can be the use of vaccine carriers without additional adjuvants, what reduces adjuvant induced side effects. One example for an intrinsic adjuvant-function is reported in chapter 4.3.6 for our new unmodified PEG-*b*-PAGE-*b*-PLGA NP loaded with OVA, which shows without adjuvant the same T cell response, compared to an OVA/adjuvant formulation.

#### 1.1.4. Delivery of protein-particles through the GIT

Most of the current available vaccines, as mentioned before, are delivered sc or im, because these vaccines would not survive the harsh conditions of the GIT. Consequently, they cannot be taken up efficiently and induce no immune response [78]. This is due to the fact, that the GIT has developed various morphological and physiological barriers against toxic materials, harmful pathogens, but also against particulate systems and macromolecules, like proteins. These barriers are first, the acid conditions in the stomach and basic conditions in the gut lumen, second the proteolytic enzymes of the stomach and intestines (e.g. cathepsin, pepsin, trypsin,  $\alpha$ -amylase, chymotrypsin), third, the bacterial gut flora, fourth, the mucus layer on gut epithelia cells and fifth the gut epithelia itself [79]. By the delivery of pure proteins as vaccines the mentioned defense systems would lead efficiently to the destruction or even degradation of the protein to a certain extent, consequently the protein is not functional anymore for vaccination [78]. To overcome this problem, we investigate furthermore the integrity and activity of the protein after vaccination. The usage of model proteins in research is very prominent, because therapeutic proteins are very costly and after a first evaluation with the model protein, the work can be adapted to the therapeutic protein.

Representative model proteins are bovine serum albumin (BSA) or ovalbumin (OVA) that are available in high amounts for lower prices and in high purified, medical grade. For integrity and activity studies of the protein the unique 3-dimensional tertiary and sometimes quaternary structure is important [80–82]. This tertiary structure is furthermore characterized by defined primary and secondary structures, describing the amino acid sequence and repeating local structures, like alpha helix and beta sheets, which are additionally stabilized by hydrogen bonds. The tertiary structure characterizes the shape of the whole, single protein with the relationship to other internal secondary structures. A synonymous term for “tertiary structure” is also called fold, which is also known as its native conformation. Especially this native conformation is important for the activity of the protein and has to be kept stable [83]. The quaternary structure is an arrangement of multiple proteins and plays an important role in complex protein structures like, ion channels or enzymes [84]. As mentioned before the use of model proteins can help to evaluate results from method development, however each protein differs from each



other, by their structure, molecular weight and physicochemical properties. Nevertheless, the development of protein/vaccine delivery systems with the help of a model protein, instead of the real therapeutic protein, is only a first hint for successful delivery systems. After the evaluation with the model protein, the system needs to be tested with the therapeutic protein.

For our research the model protein OVA was used. OVA is a glycoprotein, which is the main protein found in egg white and comprises roughly 55-65% of the main protein egg white [85]. The protein consists of 385 amino acids and has a molecular weight of approximately 45 kDa. OVA is a good model protein for method development, but can also be used for preclinical mouse vaccination studies, because mice had never contact with this protein and can therefore induce an immunological response [86,87]. For human vaccination studies the therapeutic protein, Her-2/neu was used. Only a part of the protein Her2 (human epidermal growth factor receptor 2), also called HER/neu, with 630 amino acids and a molecular weight of approximately 73 kDa was used. The over-expression of this receptor is a biomarker for development and progression for specific types of breast cancer [88].

## **1.2. Particulate vaccine/protein delivery systems**

The main reason for the oral administration of particulate vaccine delivery systems, compared to the administration of free protein as vaccine is the encapsulation and therefore protection of a protein from the harsh gastrointestinal condition or enzymatic degradation [89]. Even the selection of an appropriate particulate vaccine delivery system, opens a lot of questions, regarding the selection of suitable polymers, preparation methods, particle sizes, optimal surface properties, drug loadings and release, as well as the different possibilities for passive or active drug targeting. Especially nanoscale vaccine delivery systems promise great potential for protein delivery. Since APCs, like DCs or macrophages, recognize and engulf viruses and bacteria within the same range like NPs of sizes between 20-2000 nm, leading to a better presentation the antigen on the APCs [90]. The term nanoscale is thereby officially used for size ranges between 1-100 nm, but systems in the sub-micrometer range from 1-1000 nm are also often described as nanoscale systems or NPs [91]. Two different types of NPs, depending on the preparation method, are known in literature, the nanospheres and nanocapsule, which are either

characterized by a uniform polymer matrix or a polymeric shell enveloping a fluidic core (Figure 2A) [92].

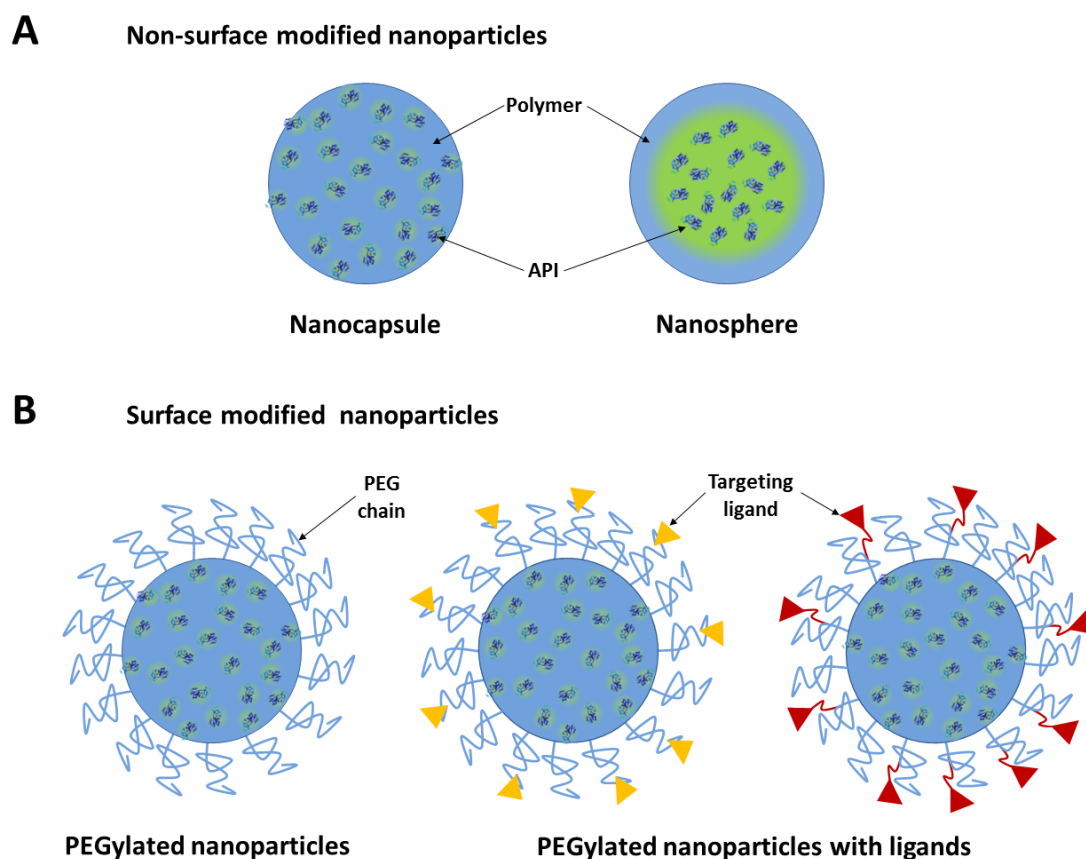


**Figure 2 | Schematic representation of non-targeted and targeted NPs.** A) Two different types of non-targeted NPs; nanocapsule and nanospheres, with distribution of the polymer and the API. B) Targeted NPs with PEG chain and targeting ligands, which are connected at the end (yellow triangle) or in-between (red triangle) of the PEG chain.

For a controlled drug release, improved bioavailability, tissue delivery of antigens or tuning of the overall physical properties, the NPs can be tailor-made on individual needs [93–95]. These include modifications of the polymer molecular weight, different ratios of monomers, drug concentration and possible linkage of ligands or drug targeting molecules on the NP surface. Furthermore, different release kinetics can be established with release over short, but also over long time periods of days, weeks or even month. Requirements for the NPs are good stability, no toxicity, non-immunogenicity, non-inflammatory, biodegradability and especially for intravenous application non-thrombogenicity [89,96–98]. NPs aren't restricted only to oral delivery, because due to their small size, NPs are also able to extravasate intravenously through the epithelium, endothelium, or even penetrate microcapillaries [95,99,100]. If we compare NPs over microparticles (MPs) ( $>1\ \mu\text{m}$ ) the application via intravenous route is another advantages of NPs, because they are small

enough to avoid blocking of the smallest capillaries (5-6  $\mu\text{m}$ ) as it could be for MPs [101,102].

### **1.2.1. Polymers for passive and active drug targeting**

As mentioned before, the selection of a suitable polymer is essential for a successful delivery of the vaccine, because the polymer defines mainly the properties of the prepared cargo. The oldest and most important biopolymers in nature are deoxyribonucleic acid (DNA), ribonucleic acid (RNA) and proteins [103], which consist of multiple polynucleotides and polyamino acids. These polynucleotides and polyamino acids, also called monomers and build blocks, are repeated in large numbers [104]. Nevertheless, monomers of the polymers are not the only target that can be changed in order to modify the characteristics of a polymer. Further modifications can be the use of different polymer or monomer types, different numbers of repeating monomers or the further addition of building blocks for passive or active targeting.

For the administration of nanoparticulate vaccine delivery systems and the application in human, the biocompatibility, biodegradability and the possibility to excrete the polymer/monomers from the body is preferable. Therefore biocompatible and biodegradable polymers contain often, within their structure, a chemical bond, which can be cleaved under basic, acid or even neutral conditions. Focusing on the degradable polymers, these polymers can be divided furthermore in two different groups, first the synthetic polymers, for example, PLGA and poly- $\epsilon$ -lactone (PCL) and second, the natural occurring polymers, like chitosan and starch [105,106]. For our research we focus on the most common synthetic polymer PLGA and further developed and investigated PLGA derivatives. Figure 3 shows the basic structure of PLGA and the new PLGA derivatives, which were used during the studies.

#### **PLGA**

The most common biocompatible and biodegradable polymer, for the encapsulation of hydrophilic substances, like proteins, is the co-block-polymer PLGA [107]. It has been used for more than two decades for biomedical application and is approved by the Food and Drug Administration (FDA) for therapeutic devices for the application in humans [108]. The abbreviation PLGA is an acronym for poly(D,L-lactide-co-glycolide) where usually D- and

L-lactic acid forms can be found in equal ratios. Furthermore, the lactic to glycolic acid ratio is an important characteristic. If the polymer consists of 65% lactic acid and 35% glycolic acid, the PLGA is identified as 65:35 PLGA in literature. PLGA is a polyester that is synthesized by a ring-opening co-polymerization of cyclic dimers of lactic acid and glycolic acid (1,4-dioxane-2,5-diones) [109,110]. The basic PLGA polymer is already used in drug delivery applications, like implants (e.g. Zoladex®) or microparticles (e.g. Trelstar™ Depot®) [111], whereas protein delivery applications with NPs are still under investigation [112]. Independently from the final formulation, the polymer has shown no toxicity and is extremely safe [113].

### **Copolymers of PLGA**

Considering PLGA as a monoblock, different types of copolymers for PLGA were investigated during the last years, in order to overcome the limitations of PLGA, regarding restricted capability of loading and release of proteins. For our purpose, we focused on modified PLGA with the aim to increase its hydrophilic character and to reduce the interactions between the polymer and protein, thus resulting in an increased encapsulation of proteins and a faster release. By addition or linkage of a polyethylene glycol (PEG) group to PLGA, the encapsulation and release properties for hydrophilic APIs of the obtained PEG-*b*-PLGA [114–117] can be improved. PEG is a surface active, hydrophilic and flexible molecule that is also approved by the FDA for the use in humans. Another positive property of PEG in PEG-*b*-PLGA is that the PEG chains orient themselves mainly towards the outer aqueous phase and form a layer of PEG on the NPs surface, when using PEG-*b*-PLGA polymer in NP preparation [118]. This PEG layer can mask the NPs from the host's immune system [119] prolonging the presence of the PEGylated NPs in the human body [120]. It is also believed that PEGylation facilitates the transport through the Peyer's Patches, making it even more interesting for an vaccination approach [121]. As this modification does not have a specific target, but increases the resting time in the human body, it leads to an improved passive drug targeting. Further details on PEG-*b*-PLGA can be found in the chapter 1.2.4 dealing about the surface properties of NPs or in our publication "Impact of hydrophilic-modified PLGA on particle formation, protein loading and release".

## Functionalization of PLGA

Besides the passive drug targeting properties of PEG, the focus is nowadays on active drug targeting strategies. This includes the possibility to link covalently functional groups, like antibodies or receptor ligands to the polymers or on the surface of the NPs (Figure 2B). Efficient and active drug targeting can increase the drug concentration in specific body sites with reduction of total, delivered dose and reduction of associated side effects [122–124]. For our approach an poly(allyl glycidyl ether) (PAGE) group, between the PEG and PLGA building block was added, to form a PEG-*b*-PAGE-*b*-PLGA polymer. This PAGE group gives us the possibility to link receptor agonists. One of this new covalent side-chain functionalization is the Mannose functionalized Mannose-PEG-*b*-PAGE-*b*-PLGA. The Mannose receptor is mainly present on APCs, like DCs or macrophages [125,126] enhancing the uptake of Mannose-PEG-*b*-PAGE-*b*-PLGA. Another approach is an amine functionalized Amine-PEG-*b*-PAGE-*b*-PLGA polymer. The tertiary amine, linked to the PAGE group, will be protonated in neutral to acid conditions and hence influence the surface charge of the resulting NP. The aim was to mimic the cationic surface properties of starch or chitosan NPs to open the tight junctions [35,36] facilitating the uptake of NPs through the intestinal wall.

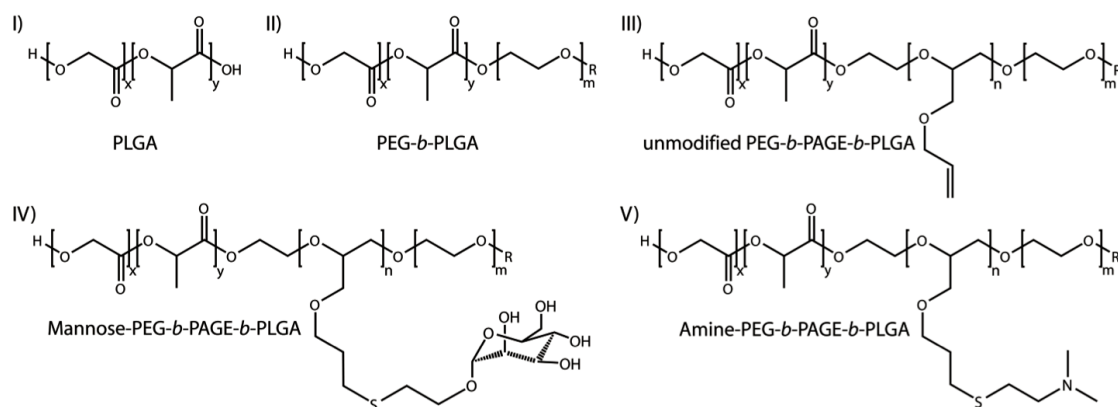


**Figure 3 | Schematic representation of PLGA (I), PEG-*b*-PLGA (II), unmodified PEG-*b*-PAGE-*b*-PLGA (III), Mannose-PEG-*b*-PAGE-*b*-PLGA (IV) and Amine-PEG-*b*-PAGE-*b*-PLGA (V) with x = lactic acid group, y = glycolic acid group, m = polyethylene glycol, n = poly(allyl glycidyl ether) with Amine-/Mannose functionality, R = methyl- or biphenyl-group.**

### 1.2.2. Preparation methods

The selection of appropriate methods for NP preparation depends on the loaded drug and the physicochemical character of the polymer [127]. NPs can be prepared either by direct polymerization of monomers or by preformed polymers. As PLGA and its derivatives are already preformed polymers, the most common methods for the preparation of NPs are the solvent diffusion-emulsion evaporation method, solvent displacement/nanoprecipitation method and further, not so frequent used methods, like salting-out [128] and emulsions-diffusion methods [129]. Every preparation method has its advantages, but also notable disadvantages. Disadvantages for all preparation methods can be (I) unknown toxicity of reagents and solvent, (II) harsh processes, due to mechanical mixing and homogenization (damage of biological macromolecules), (III) low encapsulation and loading efficiencies for different types of drugs, (IV) poor reproducibility [130] and (V) poor scale-up capabilities [130]. The choice and modification of preparation method are influencing the resulting NP properties and drug loading. On the contrary, the prior selection of API limits also the selection of the preparation method. Drug-loaded NPs can be achieved by two ways; first by incorporation of the drug into the NPs or second by adsorption of drug onto the surface of the NPs [93]. The incorporation of drugs is performed during the NP production, whereas the adsorption onto the surface can be realized after the NP preparation. As the adsorption of proteins on the surface of the NPs does not protect the protein, it was not focus of our work.

#### **Solvent diffusion-evaporation method**

The first mentioned and most frequently used method for the preparation of micro- and NPs is the solvent diffusion-evaporation method (Figure 4A) [131–134]. In the first step the polymer is dissolved in a water insoluble organic solvent. In the past most frequently chloroform or dichloromethane (DCM) were used, but today these solvents are replaced by ethyl acetate, due to better handling and lower toxicity [135]. By ultrasonication or high speed homogenization the polymer solution is emulsified into the water phase, to prepare an oil in water (o/w) emulsion. Usually the water phase contains a surfactant, such as polyvinyl alcohol (PVA), to obtain a stable emulsion. The water phase is mostly stabilized by a surfactant, like polyvinyl alcohol or poloxamer, avoiding the formation of agglomerates and coalescence. After evaporation of the organic solvent, the polymer precipitates

and NPs are formed. The biggest disadvantage of this method is the limited capability for encapsulation of hydrophilic drugs, like proteins, because they are not soluble within the organic phase, to be encapsulated within the polymer.

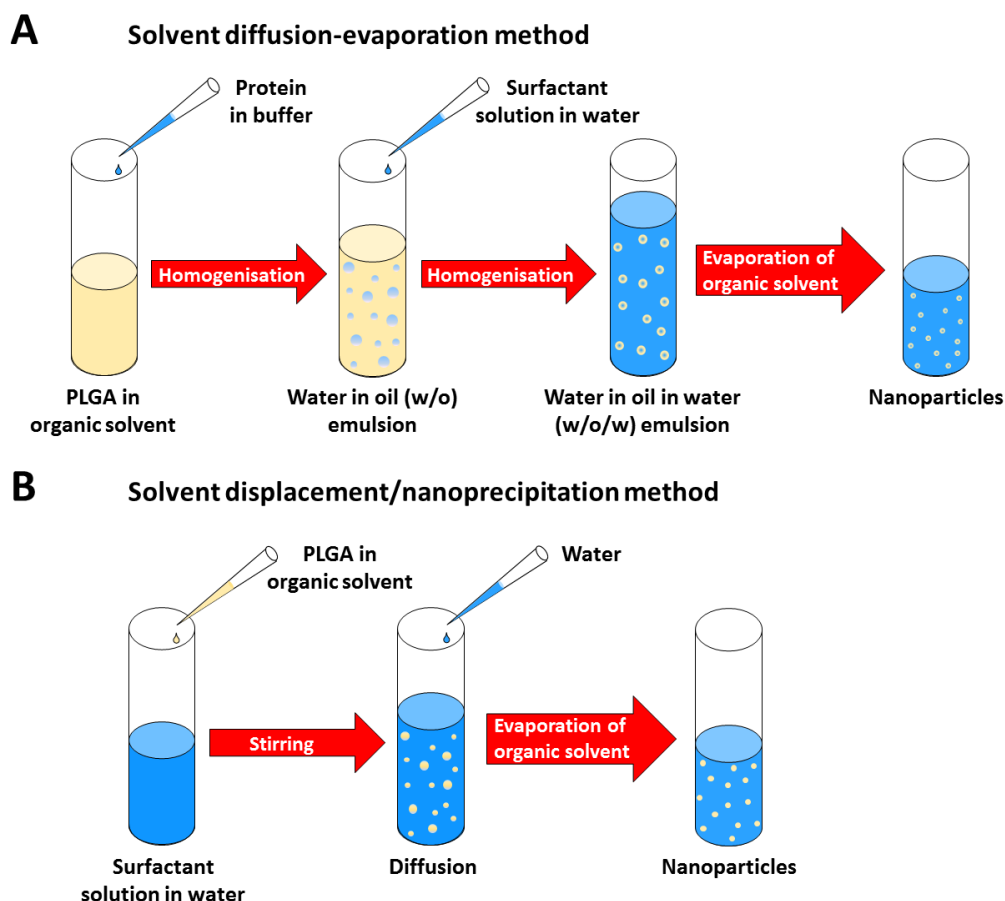


**Figure 4 | Schematic representation of NP preparation methods** A) Solvent diffusion-evaporation method. For the double emulsion diffusion-evaporation method the protein in buffer is added to the organic solvent, containing the polymer, and homogenized, to obtain the w/o emulsion. Within the next step a surfactant solution is added and the solution is again homogenized, to obtain the w/o/w emulsion. After diffusion and evaporation of the organic solvent the NPs are formed. For the single emulsion diffusion-evaporation method the initial step, adding the protein, does not have to be performed B) Solvent displacement/nanoprecipitation method. The polymer dissolved in organic solvent is added under stirring to a surfactant solution. After addition of water, the organic solvent evaporates and the NPs are formed.

To encapsulate proteins a modification of the single emulsion diffusion-evaporation method was investigated - the double emulsion diffusion-evaporation method [132,136,137]. Therefore an aqueous, concentrated protein solution is added to the primary organic polymer solution by ultrasonication or high speed homogenization, to form a water in oil (w/o) emulsion. The protein is now dispersed in nano-droplets within an organic polymer solution. This primary emulsion is then added under continuous stirring to a second aqueous phase, to form a water in oil in water (w/o/w) emulsion. After

evaporation of the organic solvent and precipitation of the polymer the hydrophilic API is trapped inside of the NPs.

### **Solvent displacement/nanoprecipitation method**

The solvent displacement method, or so-called nanoprecipitation method (Figure 4B), was developed from Fessi et al in the 1980<sup>th</sup> [138,139]. For the preparation of NPs a preformed polymer is dissolved in a semipolar, water miscible organic solvent, like Acetone, Acetonitrile or Dimethyl sulfoxide (DMSO) [140]. The polymer is then injected into an aqueous solution, with or without surfactant, and the organic solvent diffuses into the aqueous phase. Small nano-droplets are formed by the rapid diffusion of polymer solvent into non-solvent, which precipitate and form NPs.

Two of the below mentioned disadvantages, poor reproducibility [130] and poor scale-up capabilities [130], were addressed within the thesis published in a research article (Chapter 3). Our aim was the establishment of an operator independent, scalable and size adjustable method for NP preparation.

### **1.2.3. Particle size**

The most important parameters in NP characterization are particle size, particle size distribution and particle morphology. The size can influence the physicochemical properties of the NPs, like hydrophobicity, zeta potential and consequently API loading, API release and stability of the NPs, but also the biological fate, *in vivo* distribution and toxicity. In literature the most appropriate methods for the determination of particle sizes are the dynamic light scattering (DLS) or so-called photon-correlation spectroscopy, scanning electron microscopy (SEM), transmission electron microscopy (TEM), and atomic force microscopy (AFM). The DLS measurements of NPs require a NP suspension in medium with known viscosity and refractive index of the polymer. During the measurement monochromatic light hits the spherical particles within the solution and the light is scattered in all directions (Rayleigh scattering). The Brownian motion of the particles causes additionally an intensity fluctuation (constructive or destructive) of the incoming light, when the moving particles are hit. With the help of these parameters the hydrodynamic diameter of the particle can be determined [141]. In addition to the particle size, also the polydispersity (called the polydispersity index - PDI) can be defined [142]. PDI



values smaller than 0.2 indicate monodisperse size distribution [142], whereas PDI values larger than 0.2 reflect polydisperse distributions. To verify the results from DLS, usually SEM, TEM or AFM measurements are performed, as a visual control and for an evaluation of the particle morphology [143]. TEM and AFM operate on different principles compared to SEM, but result also in evaluable image data, 2D images for SEM and TEM and 3D image for AFM. In detail, SEM produces images of a fixed sample by a scan of a focused beam of electrons. Therefore the fixed sample is generated by a dry powder of NPs that is fixed on a silicon wafer, with a cover of a 3-6 nm gold layer. The electrons within the beam interact with the fixed sample, by random scattering or absorption, generating various signals that create information about the composition and surface topography of the NPs. Comparing the obtained sizes from SEM, TEM or AFM to DLS, the identified sizes by SEM are slightly smaller, because with DLS method the hydrodynamic diameter is determined which is larger due to the connected water molecules.

Various studies demonstrated already *in vitro* and in animal studies *in vivo* the advantages of NPs over MPs and the potential for the application in humans as drug carrier [95]. One example for size dependent uptake of MPs was published by Desai et al [99]. They examined the uptake in Caco-2 cells and found that for 10  $\mu\text{m}$  MPs the uptake was 6-fold lower than for 1  $\mu\text{m}$  MPs, which were furthermore 2.5-fold lower in uptake compared to 100 nm NPs (on weight basis). The human Caco-2 cell line is the first-line *in vitro* model for the intestinal barrier that was obtained from human colon adenocarcinoma. In a similar study Lamprecht et al. studied the bioadhesion of NPs and MPs to inflamed tissue within the intestinal mucosa. They found that the adherence of NP with a size of 100 nm is higher compared to MPs of 1 or 10  $\mu\text{m}$  diameter [144]. Also for specific cell type uptake the size of the particles is essential. The uptake or so-called ingestion of particles in APCs, like DCs or macrophages is size dependent. Macrophages preferentially take up particles with larger, bacterial sizes (500-2000 nm), whereas DCs mainly take up smaller particles of virus sizes (20-300 nm). This size dependent uptake was also part of our research article "Antigen delivery via hydrophilic PEG-*b*-PAGE-*b*-PLGA NPs improves vaccination efficiency". Therefore blank and OVA loaded PLGA and PEG-*b*-PAGE-*b*-PLGA NPs of different sizes (100-450 nm) were incubated with macrophages. From these studies we could conclude that optimal uptake of PLGA and PEG-*b*-PAGE-*b*-PLGA NPs in macrophages is between 250 to 400 nm.

Another aspect is the particle size dependent release, assuming the same API loading. Smaller particles have an increased surface area-to-volume ratio, while the API at or near the surface is released faster. On the other hand bigger particles have the ability to encapsulate higher amounts of API, what can negate the decreased surface area-to-volume ratio [145].

#### **1.2.4. Surface properties of nanoparticles**

The properties of the NP surface, including charge, hydro- or lipophilicity and modification of the surface are important aspects for NP delivery. However, it must be noted that different application routes have different requirements. For example, for intravenous applications the charge of the NP surface has only little impact. This could be explained by the very fast and unspecific uptake by the mononuclear phagocyte system, especially in Kupffer cells of the liver and the spleen macrophages [146–148]. This is why the research is focused on hydrophilic modifications, for example PEGylation of NPs, to avoid recognition and unspecific uptake of NPs and increase the circulation time in the blood. With regard on the oral application, in detail for the uptake through the intestinal wall, possible positive, neutral or negative charges of NPs are of higher relevancy.

The surface charge of NPs is commonly characterized by the zeta potential and is thereby influenced by the dispersing medium and composition of the particle [149]. The surface charge of the NPs should be, independent from polymer, either strongly negative or strongly positive for a good stability of the NPs, because higher absolute charges increase the repulsion between the particles and prevent aggregation [150]. For the uptake of NPs in the intestine, the adherence and mobility within the protecting layer of the intestine - the mucus - is important [151,152]. Usually virulent and bacterial particles, particles or drugs are efficiently trapped and removed in the GIT by mucus clearance [153]. A successful example for the diffusion through the mucus layer and the penetration through the epithelium is a virus. A virus can successfully overcome the intestinal barriers mainly due to its small size of about 20-400 nm and the non-adhesive surface of the virus [151,153]. Mimicking these properties for the development of NPs, would already increase the possibility of successful NP uptake.

First of all, as already mentioned, the mucosal adherence of the particles is an important aspect. The adherence increases the retention time on the mucosal surface, what can be achieved by strong interactions between the particles and the mucus. These interactions can be hydrogen bonds, polymer chain interactions, hydrophobic forces, Van der Waals interactions and ionic interactions [152]. Especially ionic interactions between the mucus and the particle surface are important aspects. High interactions and therefore increased resting time in the intestine can be achieved by the usage of positively charged NPs. This is due to the interaction between the negatively charged glycocalyx of the intestinal mucosa and the positive groups on the surface of the NPs [154]. Examples of polymers with positive surface charges are Chitosan and EUDRAGIT® NPs (for example with Eudragit RL/RS). Polymers with a negative surface charge, like PLGA and its derivatives might have a lower resting time, because of lower ionic interactions [154]. Nevertheless, besides mucoadhesion, good mucus penetration and fast diffusion through the mucus has to be ensured, explaining that too strong interactions with the mucus are also less beneficial. Negatively charged polymers offer significantly higher mucus penetration and diffusion, than positively charged polymers [154]. Another approach to positively influence the mucus penetration and furthermore achieve lower mucus interactions, is the coating of the NP surface masking the surface properties. The most often used surface coating is polyethylene glycol (PEG), which is typically covalently linked to the surface of the NP. The coating minimizes the interactions between the particle and the mucus and makes the particle more hydrophilic, which increases the penetration of the NPs [153,155]. If the PEG coating is only applied via adsorption a fast desorption could be possible, with lose of PEG properties, why in literature the PEG is predominantly covalently linked to the polymer. To sum up, the right balance between mucus penetration and mucoadhesion is important for the efficient delivery and uptake of NPs in the GIT. The NPs must be small enough to avoid steric interactions with the mucus and should diffuse fast through the mucus [152,156]. On the other hand they should have also mucoadhesive properties for a higher retention time in the GIT.

Another NP characteristic is the determination of surface hydrophobicity. Therefore in literature several techniques are established such as hydrophobic interaction chromatography [157], contact angle measurements [158] and adsorption of probes [159,160]. In detail, we focused on the adsorption of hydrophilic and hydrophobic probes in comparison

to the adsorption of the target drug. This was adapted from the Rose Bengel assay and can be read in detail in “Impact of hydrophilic-modified PLGA on particle formation, protein loading and release”.

### **1.2.5. Drug loading**

For a given delivery systems the total dose, the drug load and the encapsulation efficacy are important parameters. The drug load or encapsulation capacity indicates the percentage of the active API relative to the entire delivery system (API + excipients), whereas the encapsulation efficiency refers to the actually loaded drug amount compared to the drug amount needed for the preparation of a given delivery system. Obviously, high encapsulation efficiencies of 80% and more are most desirable but do not necessarily correspond to high loading rates, which can sometimes be 10% or less, but still satisfactorily: If the loading rate/encapsulation capacity is 10% (i.e. 10 mg API are contained in 100 mg of a given formulation, for example NPs), an encapsulation efficiency of 80% would mean that 12.5 mg of the API are needed to produce the aforementioned 10 mg API encapsulated in 100 mg NPs. For drug delivery purposes high loading rates for efficient drug delivery are important, whereas high encapsulation efficiencies are helpful to reduce the production cost of the NPs. As previous described in the chapter 1.2.2 NP preparation, drug loading can be achieved by two ways, either by encapsulation of the drug into the NPs or by adsorption of drug onto the surface of the NPs. The major benefit of protein encapsulation is the protection of the protein from environmental influences and higher achievable loading rates in NPs, compared to the adsorption of the NP surface. Encapsulation capacity and efficiency are also dependent on the solubility of the API within the polymer matrix or dispersion medium. In addition to the solubility, the highest loading of proteins is found when the proteins are loaded close to or at their isoelectric point [161]. This is related to the preparation technique and the selection of polymer, dispersion medium and further excipients. For hydrophobic APIs most often the nanoprecipitation method is used, because the drug can be solved together with the polymer and additionally precipitated together. For hydrophilic drugs, such as protein or vaccines, the method of choice is the double emulsion diffusion-evaporation method. While the protein is encapsulated under liquid conditions, it precipitates inside of the NPs and is stabilized by the polymer matrix. However encapsulation of proteins by the

emulsion technique raises questions, like whether unwanted aggregation or denaturation of the protein happens at the w/o/w solvent interface, because of the usage of organic solvents and high shear forces during the preparation [162]. The best way might be the usage of a hydrophilic polymer, in a hydrophilic nanoparticulate system for a gentle encapsulation of protein in an aqueous encapsulation procedure.

### **1.2.6. Drug release**

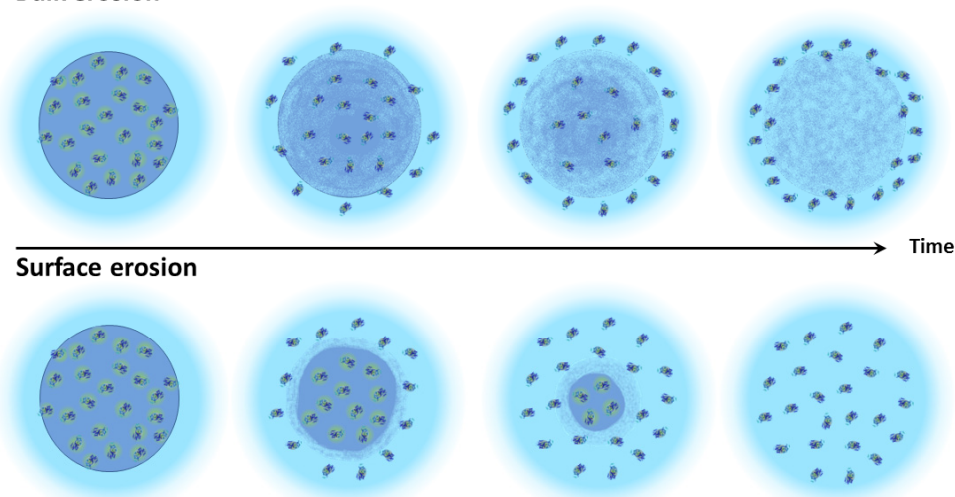
For the release of proteins from nanoparticulate systems the polymer and API itself has to be considered. Certain aspects that need to be examined are solubility and diffusion of the protein through the polymer matrix, differentiation between absorbed and encapsulated protein, polymer matrix degradation, erosion and combination of water diffusion and polymer erosion processes. However the properties of the polymer (chemical structure, molecular weight, crystallinity and hydrophobicity) and prepared NPs (size, distribution, morphology and preparation method) is influencing the release behavior [108]. Different types of degradation or erosion behaviors of the polymer are known from literature, which are characterized by bulk, surface or combined erosion mechanisms. For all erosion mechanisms the extent of water diffusion into the NPs, compared to the rate of degradation, is important.

The bulk erosion (Figure 5A) [163] is defined by the release of protein dependent from diffusion, while during this process the water reaches the matrix very quickly and dissolves the protein for diffusion. The erosion and degradation of the polymer, in comparison to the diffusion, occurs slower. Once water has entered the polymeric matrix all polymeric bonds are cleaved simultaneously. This is one reason why these polymers with bulk erosion characteristics tend to break into smaller units. Surface erosion (Figure 5A) [105] is mainly found for polymers, where the water diffuses only slowly into the polymer matrix and the erosion and degradation via hydrolysis can occur only at the surface. The release of the protein is dependent on the polymer degradation, as the entrapped protein cannot be released until the matrix is degraded and dissolved into polymer monomers.

All polyesters, as well as PLGA, undergo bulk erosion, as the hydration of the whole matrix occurs in minutes, whereas the degradation, by the dissolution or degradation of the polymeric bonds, takes weeks or even month. The degradation of PLGA occurs by

hydrolysis to the monomers lactic and glycolic acid. Both monomers are un-toxic and can be metabolized in the human body via the Krebs cycle, to carbon dioxide (CO<sub>2</sub>) and water (H<sub>2</sub>O) (Figure 5B) [164,165]. As the biocompatibility is favorable, the undesired property of very slow degradation is an important reason, why the basic PLGA polymer shows such a little practical relevance for vaccine delivery systems.

### A Bulk erosion



### B

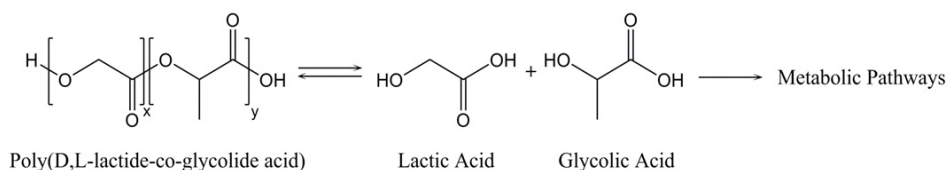


**Figure 5 | Schematic representation of bulk and surface erosion and PLGA degradation.** A) In bulk erosion water enters the polymer matrix very fast, while the whole polymer matrix is degraded at the same time and the drug is dissolved. In surface erosion water cannot enter the polymer matrix and degrades the particle from the surface. B) PLGA degradation to the un-toxic monomers lactic and glycolic acid.

In general, polymeric NPs with encapsulated protein made of PLGA and its derivate, show a biphasic release profile [166–168]. First the initial and fast, so-called burst release, is attributed to the protein, which is located near at the surface or is directly adsorbed on the surface. This process of release is mainly driven by diffusion and solubility of the protein and hydrophilicity of the polymer. The second phase of protein release is the slower, so-called sustained release. This phase is defined by the diffusion of protein through the matrix and hydroxylation/degradation of the polymer to soluble polymer products. Another aspect is the adsorption of pure protein to the surface of the NPs, instead of the incorporation of the protein into the particles. The release is then controlled by the absorption or desorption to the surface and diffusion processes of the protein. As a result the burst release can reach up to 100%, with a negligible sustained release [169].

To modify the release out of PLGA particles, different approaches were investigated in literature during the last years [170,171]. Degradation studies for PLGA show faster degradation of the PLGA with 50% lactic acid and 50% glycolic acid, compared to polymer with higher amounts of lactic acid (75:25%, 65:35%). The higher amount of lactic acid, increases the hydrophobic character of the polymer, absorbs less water and as a consequence degrades more slowly [172]. Additionally the molecular weight of polymer can be decreased, in order to increase the release of the protein, as the degradation occurs faster. However, these modifications in polymer structure for protein release are only visible in long term studies longer than 10 to 20 days [173]. Further modifications of the polymer can be the addition of a surface active molecule, like polyethylene glycol (PEG), which reduces the interaction between the polymer and protein, resulting in higher release rates.

### 1.3. References

1. Gross CP, Sepkowitz KA. The myth of the medical breakthrough: Smallpox, vaccination, and Jenner reconsidered. *Int. J. Infect. Dis.* Elsevier; 1998;3:54–60.
2. Morgan D. Smallpox--The Fight to Eradicate a Global Scourge.: David A Koplow. Berkeley, CA: University of California Press, 2003, pp. 274, ISBN: 0-520-23732-3. *Int. J. Epidemiol.* 2003;32:889–90.
3. Black RE, Cousens S, Johnson HL, Lawn JE, Rudan I, Bassani DG, et al. Global, regional, and national causes of child mortality in 2008: a systematic analysis. *Lancet.* Elsevier; 2010;375:1969–87.
4. Kochhar S, Rath B, Seeber LD, Rundblad G, Khamesipour A, Ali M. Introducing new vaccines in developing countries. *Expert Rev. Vaccines.* Informa HealthcareLondon; 2013;12:1465–78.
5. Kane A, Lloyd J, Zaffran M, Simonsen L, Kane M. Transmission of hepatitis B, hepatitis C and human immunodeficiency viruses through unsafe injections in the developing world: model-based regional estimates. *Bull. World Health Organ.* 1999;77:801–7.
6. Levine MM. Can needle-free administration of vaccines become the norm in global immunization? *Nat. Med.* 2003;9:99–103.
7. Wattigney WA, Mootrey GT, Braun MM, Chen RT. Surveillance for poliovirus vaccine adverse events, 1991 to 1998: impact of a sequential vaccination schedule of inactivated poliovirus vaccine followed by oral poliovirus vaccine. *Pediatrics.* 2001;107:E83.
8. Jagger J, Hunt EH, Brand-Elnaggar J, Pearson RD. Rates of needle-stick injury caused by various devices in a university hospital. *N. Engl. J. Med.* 1988;319:284–8.

9. Kim W-U, Lee W-K, Ryoo J-W, Kim S-H, Kim J, Youn J, et al. Suppression of collagen-induced arthritis by single administration of poly(lactic-co-glycolic acid) nanoparticles entrapping type II collagen: a novel treatment strategy for induction of oral tolerance. *Arthritis Rheum.* 2002;46:1109–20.
10. Liu Z, Guo H, Wu Y, Yu H, Yang H, Li J. Local nasal immunotherapy: efficacy of *Dermatophagoides farinae*-chitosan vaccine in murine asthma. *Int. Arch. Allergy Immunol.* 2009;150:221–8.
11. Da Costa Martins R, Gamazo C, Sánchez-Martínez M, Barberán M, Peñuelas I, Irache JM. Conjunctival vaccination against *Brucella ovis* in mice with mannosylated nanoparticles. *J. Control. Release.* 2012;162:553–60.
12. Seo KY, Han SJ, Cha H-R, Seo S-U, Song J-H, Chung S-H, et al. Eye mucosa: an efficient vaccine delivery route for inducing protective immunity. *J. Immunol.* 2010;185:3610–9.
13. Hopkins WJ, Elkahwaji J, Beierle LM, Levenson GE, Uehling DT. Vaginal mucosal vaccine for recurrent urinary tract infections in women: results of a phase 2 clinical trial. *J. Urol.* 2007;177:1349–53; quiz 1591.
14. Karpenko LI, Danilenko A V, Bazhan SI, Danilenko ED, Sysoeva GM, Kaplina ON, et al. Attenuated *Salmonella enteritidis* E23 as a vehicle for the rectal delivery of DNA vaccine coding for HIV-1 polyepitope CTL immunogen. *Microb. Biotechnol.* 2012;5:241–50.
15. Petrovsky N, Aguilar JC. Vaccine adjuvants: current state and future trends. *Immunol. Cell Biol.* 2004;82:488–96.
16. Charles A Janeway J, Travers P, Walport M, Shlomchik MJ. *Immunobiology*. Garland Science; 2001.
17. Silin DS, Lyubomska O V, Jirathitikal V, Bourinbaiar AS. Oral vaccination: where we are? *Expert Opin. Drug Deliv.* Informa UK Ltd London, UK; 2007;4:323–40.
18. Barratt G. Colloidal drug carriers: achievements and perspectives. *Cell. Mol. Life Sci.* 2003;60:21–37.
19. Bramwell VW, Perrie Y. Particulate delivery systems for vaccines. *Crit. Rev. Ther. Drug Carrier Syst.* 2005;22:151–214.
20. Csaba N, Garcia-Fuentes M, Alonso MJ. The performance of nanocarriers for transmucosal drug delivery. *Expert Opin. Drug Deliv.* 2006;3:463–78.
21. Santander-Ortega MJ, Stauner T, Loretz B, Ortega-Vinuesa JL, Bastos-González D, Wenz G, et al. Nanoparticles made from novel starch derivatives for transdermal drug delivery. *J. Control. Release.* 2010;141:85–92.
22. Weiner HL, Friedman A, Miller A, Khoury SJ, al-Sabbagh A, Santos L, et al. Oral tolerance: immunologic mechanisms and treatment of animal and human organ-specific autoimmune diseases by oral administration of autoantigens. *Annu. Rev. Immunol.* 1994;12:809–37.



23. Garside P, Mowat AM, Khoruts A. Oral tolerance in disease. *Gut*. 1999;44:137–42.
24. Mowat AM. Anatomical basis of tolerance and immunity to intestinal antigens. *Nat. Rev. Immunol.* 2003;3:331–41.
25. Takahashi I, Kiyono H. Gut as the largest immunologic tissue. *JPEN. J. Parenter. Enteral Nutr.* 23:S7–12.
26. Brandtzaeg P, Berstad AE, Farstad IN, Haraldsen G, Helgeland L, Jahnsen FL, et al. Mucosal immunity--a major adaptive defence mechanism. *Behring Inst. Mitt.* 1997;1–23.
27. Charles A. Janeway J. *Immunobiology: the immune system in health and disease*. New York: Garland Science; 2005.
28. Nagler-Anderson C. Man the barrier! Strategic defences in the intestinal mucosa. *Nat. Rev. Immunol.* 2001;1:59–67.
29. Holmgren J, Czerkinsky C, Lycke N, Svennerholm AM. Mucosal immunity: implications for vaccine development. *Immunobiology.* 1992;184:157–79.
30. Raychaudhuri S, Rock KL. Fully mobilizing host defense: building better vaccines. *Nat. Biotechnol.* Nature America Inc.; 1998;16:1025–31.
31. Roth KA, Hertz JM, Gordon JI. Mapping enteroendocrine cell populations in transgenic mice reveals an unexpected degree of complexity in cellular differentiation within the gastrointestinal tract. *J. Cell Biol.* 1990;110:1791–801.
32. Falk P, Roth KA, Gordon JI. Lectins are sensitive tools for defining the differentiation programs of mouse gut epithelial cell lineages. *Am. J. Physiol. - Gastrointest. Liver Physiol.* 1994;266.
33. Snoeck V, Goddeeris B, Cox E. The role of enterocytes in the intestinal barrier function and antigen uptake. *Microbes Infect.* 2005;7:997–1004.
34. Cheng H, Leblond CP. Origin, differentiation and renewal of the four main epithelial cell types in the mouse small intestine. V. Unitarian Theory of the origin of the four epithelial cell types. *Am. J. Anat.* 1974;141:537–61.
35. Björk E, Isaksson U, Edman P, Artursson P. Starch microspheres induce pulsatile delivery of drugs and peptides across the epithelial barrier by reversible separation of the tight junctions. *J. Drug Target.* 1995;2:501–7.
36. Schipper NG, Olsson S, Hoogstraate JA, deBoer AG, Vårum KM, Artursson P. Chitosans as absorption enhancers for poorly absorbable drugs 2: mechanism of absorption enhancement. *Pharm. Res.* 1997;14:923–9.
37. Gebert A, Rothkötter H-J, Pabst R. M Cells in Peyer's Patches of the Intestine. *Int. Rev. Cytol.* 1996;167:91–159.

38. Corr SC, Gahan CCGM, Hill C. M-cells: origin, morphology and role in mucosal immunity and microbial pathogenesis. *FEMS Immunol. Med. Microbiol.* 2008;52:2–12.
39. Brayden DJ, Jepson MA, Baird AW. Keynote review: intestinal Peyer's patch M cells and oral vaccine targeting. *Drug Discov. Today.* 2005;10:1145–57.
40. Mantis NJ, Frey A, Neutra MR. Accessibility of glycolipid and oligosaccharide epitopes on rabbit villus and follicle-associated epithelium. *Am. J. Physiol. Gastrointest. Liver Physiol.* 2000;278:G915–23.
41. Frey A, Giannasca KT, Weltzin R, Giannasca PJ, Reggio H, Lencer WI, et al. Role of the glycocalyx in regulating access of microparticles to apical plasma membranes of intestinal epithelial cells: implications for microbial attachment and oral vaccine targeting. *J. Exp. Med.* 1996;184:1045–59.
42. Jani P, Halbert GW, Langridge J, Florence AT. The Uptake and Translocation of Latex Nanospheres and Microspheres after Oral Administration to Rats. *J. Pharm. Pharmacol.* 1989;41:809–12.
43. Ruedl C, Rieser C, Böck G, Wick G, Wolf H. Phenotypic and functional characterization of CD11c+ dendritic cell population in mouse Peyer's patches. *Eur. J. Immunol.* 1996;26:1801–6.
44. Kelsall BL, Strober W. Peyer's patch dendritic cells and the induction of mucosal immune responses. *Res. Immunol.* 1997;148:490–8.
45. Jondal M, Schirmbeck R, Reimann J. MHC Class I-Restricted CTL Responses to Exogenous Antigens. *Immunity.* 1996;5:295–302.
46. Ramachandra L, Chu RS, Askew D, Noss EH, Canaday DH, Potter NS, et al. Phagocytic antigen processing and effects of microbial products on antigen processing and T-cell responses. *Immunol. Rev.* 1999;168:217–39.
47. Mayer L. Mucosal immunity and gastrointestinal antigen processing. *J. Pediatr. Gastroenterol. Nutr.* 2000;30 Suppl:S4–12.
48. Charles A Janeway J, Travers P, Walport M, Shlomchik MJ. The mucosal immune system. Garland Science; 2001.
49. Alberts B, Johnson A, Lewis J, Raff M, Roberts K, Walter P. The Adaptive Immune System. Garland Science; 2002.
50. Engelhard VH. Structure of peptides associated with MHC class I molecules. *Curr. Opin. Immunol.* 1994;6:13–23.
51. Howard JC. Supply and transport of peptides presented by class I MHC molecules. *Curr. Opin. Immunol.* 1995;7:69–76.
52. Cresswell P. Antigen Presentation: Getting peptides into MHC class II molecules. *Curr. Biol.* Elsevier; 1994;4:541–3.

53. Germain RN. MHC-dependent antigen processing and peptide presentation: providing ligands for T lymphocyte activation. *Cell*. 1994;76:287–99.
54. Karlsson L, Péléraux A, Lindstedt R, Liljedahl M, Peterson PA. Reconstitution of an operational MHC class II compartment in nonantigen-presenting cells. *Science*. 1994;266:1569–73.
55. Brocker C, Thompson D, Matsumoto A, Nebert DW, Vasiliou V. Evolutionary divergence and functions of the human interleukin (IL) gene family. *Hum. Genomics*. BioMed Central Ltd; 2010;5:30.
56. Farber DL, Yudanin NA, Restifo NP. Human memory T cells: generation, compartmentalization and homeostasis. *Nat. Rev. Immunol.* Nature Publishing Group, a division of Macmillan Publishers Limited. All Rights Reserved.; 2014;14:24–35.
57. Kurosaki T, Kometani K, Ise W. Memory B cells. *Nat. Rev. Immunol.* Nature Publishing Group, a division of Macmillan Publishers Limited. All Rights Reserved.; 2015;15:149–59.
58. Panariti A, Miserocchi G, Rivolta I. The effect of nanoparticle uptake on cellular behavior: disrupting or enabling functions? *Nanotechnol. Sci. Appl.* 2012;5:87–100.
59. Unanue ER. Antigen-presenting function of the macrophage. *Annu. Rev. Immunol.* 1984;2:395–428.
60. Cella M, Sallusto F, Lanzavecchia A. Origin, maturation and antigen presenting function of dendritic cells. *Curr. Opin. Immunol.* 1997;9:10–6.
61. Banchereau J, Steinman RM. Dendritic cells and the control of immunity. *Nature*. 1998;392:245–52.
62. Bluestone JA. New perspectives of CD28-B7-mediated T cell costimulation. *Immunity*. 1995;2:555–9.
63. Janeway CA. The immune system evolved to discriminate infectious nonself from noninfectious self. *Immunol. Today*. 1992;13:11–6.
64. Medzhitov R. Toll-like receptors and innate immunity. *Nat. Rev. Immunol.* 2001;1:135–45.
65. Pulendran B, Ahmed R. Immunological mechanisms of vaccination. *Nat. Immunol.* 2011;12:509–17.
66. Committee for Medicinal Products for Human Use (CHMP). Guideline on adjuvants in vaccines for human use. *Reproduction*. 2005.
67. Sasaki S, Okuda K. The use of conventional immunologic adjuvants in DNA vaccine preparations. *Methods Mol. Med.* 2000;29:241–9.
68. Leroux-Roels G. Unmet needs in modern vaccinology: adjuvants to improve the immune response. *Vaccine*. 2010;28 Suppl 3:C25–36.

- 
69. Hemmi H, Takeuchi O, Kawai T, Kaisho T, Sato S, Sanjo H, et al. A Toll-like receptor recognizes bacterial DNA. *Nature*. Macmillan Magazines Ltd.; 2000;408:740–5.
70. Dunn LA, McMillan DJ, Batzloff M, Zeng W, Jackson DCJ, Upcroft JA, et al. Parenteral and mucosal delivery of a novel multi-epitope M protein-based group A streptococcal vaccine construct: investigation of immunogenicity in mice. *Vaccine*. 2002;20:2635–40.
71. Song H, Wang Z, Zheng D, Fang W, Li Y, Liu Y, et al. A novel mucosal vaccine against foot-and-mouth disease virus induces protection in mice and swine. *Biotechnol. Lett.* 2005;27:1669–74.
72. Zuercher AW, Horn MP, Wu H, Song Z, Bundgaard CJ, Johansen HK, et al. Intranasal immunisation with conjugate vaccine protects mice from systemic and respiratory tract infection with *Pseudomonas aeruginosa*. *Vaccine*. 2006;24:4333–42.
73. Abe N, Kodama S, Hirano T, Eto M, Suzuki M. Nasal vaccination with CpG oligodeoxynucleotide induces protective immunity against non-typeable *Haemophilus influenzae* in the nasopharynx. *Laryngoscope*. 2006;116:407–12.
74. Haan L de, Hirst TR. Cholera toxin: A paradigm for multi-functional engagement of cellular mechanisms (Review). *Mol. Membr. Biol.* Taylor & Francis; 2009;
75. Diwan M, Elamanchili P, Lane H, Gainer A, Samuel J. Biodegradable nanoparticle mediated antigen delivery to human cord blood derived dendritic cells for induction of primary T cell responses. *J. Drug Target*. 2003;11:495–507.
76. Ramachandra L, Chu RS, Askew D, Noss EH, Canaday DH, Potter NS, et al. Phagocytic antigen processing and effects of microbial products on antigen processing and T-cell responses. *Immunol. Rev.* 1999;168:217–39.
77. Gupta RK, Siber GR. Adjuvants for human vaccines—current status, problems and future prospects. *Vaccine*. 1995;13:1263–76.
78. Neutra MR, Kozlowski PA. Mucosal vaccines: the promise and the challenge. *Nat. Rev. Immunol.* 2006;6:148–58.
79. Lee VHL, Yamamoto A. Penetration and enzymatic barriers to peptide and protein absorption. *Adv. Drug Deliv. Rev.* 1989;4:171–207.
80. JM S. Physical biochemistry of peptide drugs: Structure, properties, and stabilities of peptide compared with proteins. In: VHL L, editor. *Pept. protein drug Deliv.* New York: Marcel Dekker; 1991. p. 137–66.
81. Bilati U, Allémann E, Doelker E. Strategic approaches for overcoming peptide and protein instability within biodegradable nano- and microparticles. *Eur. J. Pharm. Biopharm.* 2005;59:375–88.
82. Bummer PM KS. Chemical and physical considerations in protein stability. In: EJ M, editor. *Protein Formul. Deliv.* New York: Marcel Dekker; 2000. p. 5–69.

83. Berg JM, Tymoczko JL, Stryer L. Protein Structure and Function. W H Freeman; 2002.
84. Berg JM, Tymoczko JL, Stryer L. Quaternary Structure: Polypeptide Chains Can Assemble Into Multisubunit Structures. W H Freeman; 2002.
85. Huntington JA, Stein PE. Structure and properties of ovalbumin. *J. Chromatogr. B Biomed. Sci. Appl.* 2001;756:189–98.
86. O'Hagan DT, Jeffery H, Davis SS. Long-term antibody responses in mice following subcutaneous immunization with ovalbumin entrapped in biodegradable microparticles. *Vaccine.* 1993;11:965–9.
87. Zhang X-Y, Liu X-G, Wang W, Wang W-C, Gao X-M. Anti-T-cell humoral and cellular responses in healthy BALB/c mice following immunization with ovalbumin or ovalbumin-specific T cells. *Immunology.* 2003;108:465–73.
88. Mitri Z, Constantine T, O'Regan R. The HER2 Receptor in Breast Cancer: Pathophysiology, Clinical Use, and New Advances in Therapy. *Chemother. Res. Pract.* 2012;2012:743193.
89. Des Rieux A, Fievez V, Garinot M, Schneider Y-J, Préat V. Nanoparticles as potential oral delivery systems of proteins and vaccines: a mechanistic approach. *J. Control. Release.* 2006;116:1–27.
90. Manolova V, Flace A, Bauer M, Schwarz K, Saudan P, Bachmann MF. Nanoparticles target distinct dendritic cell populations according to their size. *Eur. J. Immunol.* 2008;38:1404–13.
91. Kreuter J. Nanoparticles. *Encycl. Pharm. Technol. M. Dekker.* New York; 1994. p. 165–90.
92. Rekha, M.R., Sharma CP. Nanoparticle Mediated Oral Delivery of Peptides and Proteins: Challenges and Perspectives. *Pept. Protein Deliv.* 1. Edition. London: Elsevier; 2011.
93. Kreuter J. Nanoparticles. *Colloid. Drug Deliv. Syst. M. Dekker.* New York; 1994. p. 219–342.
94. Moghimi SM, Hunter AC, Murray JC. Long-circulating and target-specific nanoparticles: theory to practice. *Pharmacol. Rev.* 2001;53:283–318.
95. Panyam J, Labhasetwar V. Biodegradable nanoparticles for drug and gene delivery to cells and tissue. *Adv. Drug Deliv. Rev.* 2003;55:329–47.
96. Singh R, Lillard JW. Nanoparticle-based targeted drug delivery. *Exp. Mol. Pathol. Elsevier Inc.;* 2009;86:215–23.
97. Farokhzad OC, Langer R. Impact of nanotechnology on drug delivery. *ACS Nano. American Chemical Society;* 2009;3:16–20.
98. Hall JB, Dobrovolskaia MA, Patri AK, McNeil SE. Characterization of nanoparticles for therapeutics. *Nanomedicine (Lond).* 2007;2:789–803.
99. Desai MP, Labhasetwar V, Walter E, Levy RJ, Amidon GL. The mechanism of uptake of biodegradable microparticles in Caco-2 cells is size dependent. *Pharm. Res.* 1997;14:1568–73.

100. Panyam J, Sahoo SK, Prabha S, Bargar T, Labhasetwar V. Fluorescence and electron microscopy probes for cellular and tissue uptake of poly(d,l-lactide-co-glycolide) nanoparticles. *Int. J. Pharm.* 2003;262:1–11.
101. Gelperina S, Kisich K, Iseman MD, Heifets L. The potential advantages of nanoparticle drug delivery systems in chemotherapy of tuberculosis. *Am. J. Respir. Crit. Care Med.* 2005;172:1487–90.
102. Mews A. *Nanomaterials Handbook*. Edited by Yury Gogotsi. *Angew. Chemie Int. Ed.* 2007;46:2143–2143.
103. Alberts B, Johnson A, Lewis J, Raff M, Roberts K, Walter P. *Molecular Biology of the Cell*. Garland Science; 2002.
104. Rudin A, Choi P. *The Elements of Polymer Science & Engineering*. *Elem. Polym. Sci. Eng.* Elsevier; 2013.
105. Uhrich KE, Cannizzaro SM, Langer RS, Shakesheff KM. Polymeric Systems for Controlled Drug Release. *Chem. Rev. American Chemical Society*; 1999;99:3181–98.
106. Nair LS, Laurencin CT. Biodegradable polymers as biomaterials. *Prog. Polym. Sci.* 2007;32:762–98.
107. Makadia HK, Siegel SJ. Poly Lactic-co-Glycolic Acid (PLGA) as Biodegradable Controlled Drug Delivery Carrier. *Polymers (Basel)*. 2011;3:1377–97.
108. Jain RA. The manufacturing techniques of various drug loaded biodegradable poly(lactide-co-glycolide) (PLGA) devices. *Biomaterials*. 2000;21:2475–90.
109. Kiremitci-Gumusderelioglu M, Deniz G. Synthesis, characterization and in vitro degradation of poly(dl-lactide)/poly(dl-lactide-co-glycolide) films. *TURKISH J. Chem. SCIENTIFIC TECHNICAL RESEARCH COUNCIL TURKEY, PO BOX 605 YENISEHIR, 06445 ANKARA, TURKEY*; 1999;23:153–61.
110. Ogawa Y, Yamamoto M, Okada H, Yashiki T, Shimamoto T. A new technique to efficiently entrap leuprolide acetate into microcapsules of polylactic acid or copoly(lactic/glycolic) acid. *Chem. Pharm. Bull. (Tokyo)*. 1988;36:1095–103.
111. Bala I, Hariharan S, Kumar MNVR. PLGA nanoparticles in drug delivery: the state of the art. *Crit. Rev. Ther. Drug Carrier Syst.* 2004;21:387–422.
112. Danhier F, Ansorena E, Silva JM, Coco R, Le Breton A, Préat V. PLGA-based nanoparticles: an overview of biomedical applications. *J. Control. Release*. 2012;161:505–22.
113. Kumari A, Yadav SK, Yadav SC. Biodegradable polymeric nanoparticles based drug delivery systems. *Colloids Surf. B. Biointerfaces*. 2010;75:1–18.
114. Cheng J, Teply BA, Sherifi I, Sung J, Luther G, Gu FX, et al. Formulation of functionalized PLGA-PEG nanoparticles for in vivo targeted drug delivery. *Biomaterials*. 2007;28:869–76.

- 
115. Li Y, Pei Y, Zhang X, Gu Z, Zhou Z, Yuan W, et al. PEGylated PLGA nanoparticles as protein carriers: synthesis, preparation and biodistribution in rats. *J. Control. Release.* 2001;71:203–11.
116. Gref R, Lück M, Quellec P, Marchand M, Dellacherie E, Harnisch S, et al. “Stealth” corona-core nanoparticles surface modified by polyethylene glycol (PEG): influences of the corona (PEG chain length and surface density) and of the core composition on phagocytic uptake and plasma protein adsorption. *Colloids Surfaces B Biointerfaces.* 2000;18:301–13.
117. Liu Y, Li K, Liu B, Feng S-S. A strategy for precision engineering of nanoparticles of biodegradable copolymers for quantitative control of targeted drug delivery. *Biomaterials.* 2010;31:9145–55.
118. Tobío M, Gref R, Sánchez A, Langer R, Alonso MJ. Stealth PLA-PEG Nanoparticles as Protein Carriers for Nasal Administration. *Pharm. Res. Kluwer Academic Publishers-Plenum Publishers;* 1998;15:270–5.
119. Bazile D, Prud’homme C, Bassoullet MT, Marlard M, Spenlehauer G, Veillard M. Stealth Me.PEG-PLA nanoparticles avoid uptake by the mononuclear phagocytes system. *J. Pharm. Sci.* 1995;84:493–8.
120. Solaro R, Chiellini F, Battisti A. Targeted Delivery of Protein Drugs by Nanocarriers. *Materials (Basel). Molecular Diversity Preservation International;* 2010;3:1928–80.
121. Vila A, Sánchez A, Tobío M, Calvo P, Alonso MJ. Design of biodegradable particles for protein delivery. *J. Control. Release.* 2002;78:15–24.
122. Leroux J-C, Allémann E, De Jaeghere F, Doelker E, Gurny R. Biodegradable nanoparticles — From sustained release formulations to improved site specific drug delivery. *J. Control. Release.* 1996;39:339–50.
123. Couvreur P, Fattal E, Andreumont A. Liposomes and nanoparticles in the treatment of intracellular bacterial infections. *Pharm. Res.* 1991;8:1079–86.
124. Couvreur P, Fattal E, Alphandary H, Puisieux F, Andreumont A. Intracellular targeting of antibiotics by means of biodegradable nanoparticles. *J. Control. Release.* 1992;19:259–67.
125. Stahl PD. The mannose receptor and other macrophage lectins. *Curr. Opin. Immunol.* 1992;4:49–52.
126. Stahl PD, Ezekowitz RAB. The mannose receptor is a pattern recognition receptor involved in host defense. *Curr. Opin. Immunol.* 1998;10:50–5.
127. Sovan Lal Pal, Utpal Jana, P. K. Manna, G. P. Mohanta RM. Nanoparticle: An overview of preparation and characterization. *J. Applied Pharm. Sci.* 2011;228–34.
128. Pinto Reis C, Neufeld RJ, Ribeiro AJ, Veiga F. Nanoencapsulation I. Methods for preparation of drug-loaded polymeric nanoparticles. *Nanomedicine.* 2006;2:8–21.
129. Takeuchi H, Yamamoto H, Kawashima Y. Mucoadhesive nanoparticulate systems for peptide drug delivery. *Adv. Drug Deliv. Rev.* 2001;47:39–54.

- 
130. Davis ME, Chen ZG, Shin DM. Nanoparticle therapeutics: an emerging treatment modality for cancer. *Nat. Rev. Drug Discov.* Nature Publishing Group; 2008;7:771–82.
131. Arshady R. Preparation of biodegradable microspheres and microcapsules: 2. Polyactides and related polyesters. *J. Control. Release.* 1991;17:1–21.
132. King TW, Patrick CW. Development and in vitro characterization of vascular endothelial growth factor (VEGF)-loaded poly(DL-lactic-co-glycolic acid)/poly(ethylene glycol) microspheres using a solid encapsulation/single emulsion/solvent extraction technique. *J. Biomed. Mater. Res.* 2000;51:383–90.
133. Rosca ID, Watari F, Uo M. Microparticle formation and its mechanism in single and double emulsion solvent evaporation. *J. Control. Release.* 2004;99:271–80.
134. Sah H. Microencapsulation techniques using ethyl acetate as a dispersed solvent: effects of its extraction rate on the characteristics of PLGA microspheres. *J. Control. Release.* 1997;47:233–45.
135. Sah H, Smith MS, Chern RT. A novel method of preparing PLGA microcapsules utilizing methylethyl ketone. *Pharm. Res.* 1996;13:360–7.
136. Mao S, Xu J, Cai C, Germershaus O, Schaper A, Kissel T. Effect of WOW process parameters on morphology and burst release of FITC-dextran loaded PLGA microspheres. *Int. J. Pharm.* 2007;334:137–48.
137. Lamprecht A, Ubrich N, Hombreiro Pérez M, Lehr C-M, Hoffman M, Maincent P. Influences of process parameters on nanoparticle preparation performed by a double emulsion pressure homogenization technique. *Int. J. Pharm.* 2000;196:177–82.
138. Fessi H, Puisieux F, Devissaguet JP, Ammoury N, Benita S. Nanocapsule formation by interfacial polymer deposition following solvent displacement. *Int. J. Pharm.* 1989;55:R1–4.
139. Govender T, Stolnik S, Garnett MC, Illum L, Davis SS. PLGA nanoparticles prepared by nanoprecipitation: drug loading and release studies of a water soluble drug. *J. Control. Release.* 1999;57:171–85.
140. Schubert S, Delaney, Jr JT, Schubert US. Nanoprecipitation and nanoformulation of polymers: from history to powerful possibilities beyond poly(lactic acid). *Soft Matter.* 2011;7:1581–8.
141. Swarbrick, J., Boylan J. *Encyclopedia of Pharmaceutical Technology*. 2nd editio. Dekker M, editor. New York; 2002.
142. Keck, C.M., Müller RH. Photonenkorrelationsspektroskopie. *Mod. Pharm. Technol.* 2009. p. 56–60.
143. Jores K, Mehnert W, Drechsler M, Bunjes H, Johann C, Mäder K. Investigations on the structure of solid lipid nanoparticles (SLN) and oil-loaded solid lipid nanoparticles by photon correlation spectroscopy, field-flow fractionation and transmission electron microscopy. *J. Control. Release.* 2004;95:217–27.



- 
144. Lamprecht A, Schäfer U, Lehr CM. Size-dependent bioadhesion of micro- and nanoparticulate carriers to the inflamed colonic mucosa. *Pharm. Res.* 2001;18:788–93.
145. Redhead HM, Davis SS, Illum L. Drug delivery in poly(lactide-co-glycolide) nanoparticles surface modified with poloxamer 407 and poloxamine 908: in vitro characterisation and in vivo evaluation. *J. Control. Release.* 2001;70:353–63.
146. Hans M., Lowman A. Biodegradable nanoparticles for drug delivery and targeting. *Curr. Opin. Solid State Mater. Sci.* PERGAMON-ELSEVIER SCIENCE LTD, THE BOULEVARD, LANGFORD LANE, KIDLINGTON, OXFORD OX5 1GB, ENGLAND; 2002;6:319–27.
147. Stolnik S, Dunn SE, Garnett MC, Davies MC, Coombes AG, Taylor DC, et al. Surface modification of poly(lactide-co-glycolide) nanospheres by biodegradable poly(lactide)-poly(ethylene glycol) copolymers. *Pharm. Res.* 1994;11:1800–8.
148. Gref R, Minamitake Y, Peracchia MT, Trubetskoy V, Torchilin V, Langer R. Biodegradable long-circulating polymeric nanospheres. *Science.* 1994;263:1600–3.
149. Couvreur P, Dubernet C, Puisieux F. Controlled drug-delivery with nanoparticles - current possibilities and future-trends. *Eur. J. Pharm. Biopharm.* 1995;41:2–13.
150. Müller R., Jacobs C, Kayser O. Nanosuspensions as particulate drug formulations in therapy. *Adv. Drug Deliv. Rev.* 2001;47:3–19.
151. Cone RA. Barrier properties of mucus. *Adv. Drug Deliv. Rev.* 2009;61:75–85.
152. Lai SK, Wang Y-Y, Hanes J. Mucus-penetrating nanoparticles for drug and gene delivery to mucosal tissues. *Adv. Drug Deliv. Rev.* 2009;61:158–71.
153. Tang BC, Dawson M, Lai SK, Wang Y-Y, Suk JS, Yang M, et al. Biodegradable polymer nanoparticles that rapidly penetrate the human mucus barrier. *Proc. Natl. Acad. Sci. U. S. A.* 2009;106:19268–73.
154. Crater JS, Carrier RL. Barrier properties of gastrointestinal mucus to nanoparticle transport. *Macromol. Biosci.* 2010;10:1473–83.
155. Wang Y-Y, Lai SK, Suk JS, Pace A, Cone R, Hanes J. Addressing the PEG mucoadhesivity paradox to engineer nanoparticles that “slip” through the human mucus barrier. *Angew. Chem. Int. Ed. Engl.* 2008;47:9726–9.
156. Primard C, Rochereau N, Luciani E, Genin C, Delair T, Paul S, et al. Traffic of poly(lactic acid) nanoparticulate vaccine vehicle from intestinal mucus to sub-epithelial immune competent cells. *Biomaterials.* 2010;31:6060–8.
157. Carstensen H, Müller BW, Müller RH. Adsorption of ethoxylated surfactants on nanoparticles. I. Characterization by hydrophobic interaction chromatography. *Int. J. Pharm.* 1991;67:29–37.
158. Metin CO, Baran JR, Nguyen QP. Adsorption of surface functionalized silica nanoparticles onto mineral surfaces and decane/water interface. *J. Nanopart. Res.* 2012;14:1246.

159. Müller RH, Rühl D, Lück M, Paulke B-R. Influence of Fluorescent Labelling of Polystyrene Particles on Phagocytic Uptake, Surface Hydrophobicity, and Plasma Protein Adsorption. *Pharm. Res.* Kluwer Academic Publishers-Plenum Publishers; 1997;14:18–24.
160. Tobio M, Gref R, Sanchez A, Langer R, Alonso M. Stealth PLA-PEG nanoparticles as protein carriers for nasal administration. *Pharm. Res.* 1998;15:270–5.
161. Calvo P, Remuñan-López C, Vila-Jato JL, Alonso MJ. Chitosan and chitosan/ethylene oxide-propylene oxide block copolymer nanoparticles as novel carriers for proteins and vaccines. *Pharm. Res.* 1997;14:1431–6.
162. Wang W. Instability, stabilization, and formulation of liquid protein pharmaceuticals. *Int. J. Pharm.* 1999;185:129–88.
163. Ulery BD, Nair LS, Laurencin CT. Biomedical Applications of Biodegradable Polymers. *J. Polym. Sci. B. Polym. Phys.* 2011;49:832–64.
164. Bazile DV, Ropert C, Huve P, Verrecchia T, Mariard M, Frydman A, et al. Body distribution of fully biodegradable [14C]-poly(lactic acid) nanoparticles coated with albumin after parenteral administration to rats. *Biomaterials.* 1992;13:1093–102.
165. Crotts G, Park TG. Protein delivery from poly(lactic-co-glycolic acid) biodegradable microspheres: release kinetics and stability issues. *J. Microencapsul.* 15:699–713.
166. Ramchandani M, Robinson D. In vitro and in vivo release of ciprofloxacin from PLGA 50:50 implants. *J. Control. Release.* 1998;54:167–75.
167. Amann LC, Gandai MJ, Lin R, Liang Y, Siegel SJ. In vitro-in vivo correlations of scalable PLGA-risperidone implants for the treatment of schizophrenia. *Pharm. Res.* 2010;27:1730–7.
168. Faisant N, Siepmann J, Benoit JP. PLGA-based microparticles: elucidation of mechanisms and a new, simple mathematical model quantifying drug release. *Eur. J. Pharm. Sci.* 2002;15:355–66.
169. Fresta M, Puglisi G, Giammona G, Cavallaro G, Micali N, Furneri PM. Pefloxacin mesilate- and ofloxacin-loaded polyethylcyanoacrylate nanoparticles: characterization of the colloidal drug carrier formulation. *J. Pharm. Sci.* 1995;84:895–902.
170. Lu L, Peter SJ, D. Lyman M, Lai H-L, Leite SM, Tamada JA, et al. In vitro and in vivo degradation of porous poly(DL-lactic-co-glycolic acid) foams. *Biomaterials.* 2000;21:1837–45.
171. Lu L, Garcia CA, Mikos AG. In vitro degradation of thin poly(DL-lactic-co-glycolic acid) films. *J. Biomed. Mater. Res.* John Wiley & Sons, Inc.; 1999;46:236–44.
172. Park TG. Degradation of poly(lactic-co-glycolic acid) microspheres: effect of copolymer composition. *Biomaterials.* 1995;16:1123–30.
173. Park TG. Degradation of poly(D,L-lactic acid) microspheres: effect of molecular weight. *J. Control. Release.* 1994;30:161–73.

## 2. Research Objectives

From the general introduction chapter of the thesis it can be concluded that oral vaccination is the preferred route of vaccination, compared to sc or im injections of vaccines. However the oral route of vaccine administration promises lots of obstacles, which could be solved by the delivery of vaccines encapsulated in nanoparticulate delivery systems. Since NPs suffer from their inefficient uptake or low immune response, novel polymers for the preparation of vaccine delivery systems were investigated. These novel polymers were made of different polymers compositions from PLGA, polyethylene glycol (PEG) and poly(allyl glycidyl ether) (PAGE) building blocks.

On the one hand, these building blocks were introduced to increase, *in vitro* and *in vivo*, the protein load and release. On the other hand passive and active drug targeting abilities were introduced. For the above mentioned points the thesis has focused on several aspects which are reflected by the different chapters:

- Chapter I.      Systematic study of polymer parameters for the preparation of model protein loaded NPs (loading, release and activity of the protein), with induction of a passive or active drug targeting building blocks.
- Chapter II.     Selected polymers were used for the preparation of NPs with different sizes, protein loading efficiencies and release kinetics to investigate time dependent antigen release and uptake efficiencies in APCs (*in vitro*). Furthermore an adjuvant effect of the novel polymers *in vivo* was shown.
- Chapter III.    For the preparation of NPs with different sizes an operator independent, reproducible and scalable semi-automated system was investigated.

### **3. Impact of hydrophilic-modified PLGA on particle formation, protein loading and release**

The author of the thesis made the following contribution to this chapter: Planned, designed and performed all experiments, analyzed data from the mentioned studies, interpreted all experimental data and wrote the manuscript.

The synthesis of the polymers, for the preparation of nanoparticles, was kindly performed by Justyna A. Czaplewska and Tobias Majdanski at Laboratory of Organic and Macromolecular Chemistry (IOMC) and Jena Center for Soft Matter (JCSM) in Jena. The author thanks the IOMC and JCSM for the support.

### 3.1. Introduction

It is well-known that larger, complex and hydrophilic active pharmaceutical ingredients (API) such as proteins, administered without any protection/vehicle, are prone to degradation and suffer from a low capability to cross biological barriers [1]. To overcome this problem the incorporation of proteins in the polymeric matrix of nanoparticles (NPs) appears to be a promising strategy [2–5]. Numerous advanced drug delivery systems, such as NPs, microparticles and liposomes were developed in the last decades [6,7]. Among those, NPs show high potential to control the delivery of various APIs [8,9]. Many polymeric matrix materials have been intensively investigated in this context, including poly(D,L-lactic-co-glycolide) (PLGA) [10–14], chitosan [15–17], poly- $\epsilon$ -caprolactone (PCL) [18,19], starch [20,21], alginate [22,23], and gelatin [24–26]. One of the most common biodegradable and biocompatible polymers [27] used to prepare NPs for the encapsulation of proteins, via the water-in-oil-in-water (w/o/w) double emulsion method, is PLGA. The major disadvantages of using a hydrophobic polymer such as PLGA are however a limited capability of both protein loading and release over time. There has been an increasing interest in the past years to overcome this problem through the development of more hydrophilic PLGA derivatives, as an increased hydrophilic character is expected to improve interaction with and facilitate encapsulation of hydrophilic substances such as proteins. In this respect, the covalent linkage of polyethylene glycol (PEG) as a flexible, hydrophilic, and FDA-approved molecule to PLGA [28] has been extensively described in literature [29,30]. The PEGylation of PLGA, in order to produce PEG-*b*-PLGA, also creates the potential for improved passive drug targeting properties; this is due to a longer circulation time, as a consequence of passively masking the NPs from the host immune system [31]. The next step in the development of a superior PLGA is considered to be the addition of a functional block to PEG-*b*-PLGA, allowing for the covalent linkage of targeting ligands for active drug targeting/delivery. This is a new approach based on the insertion of a poly(allyl glycidyl ether) (PAGE) group between PEG and PLGA units of PEG-*b*-PLGA (PEG-*b*-PAGE-*b*-PLGA) (Figure 1). This PAGE group can then act as a linker for drug targeting ligands. In the current study the influence of hydrophilic PEG building blocks and different subtypes of PLGA on the properties of various PEG-*b*-PLGA and non-functionalized, novel PEG-*b*-PAGE-*b*-PLGA polymers was systematically investigated, while keeping all other method parameters fixed – an approach which has

not been extensively explored in literature to date. The produced PEG-*b*-PLGA and PEG-*b*-PAGE-*b*-PLGA polymer subtypes had different lactic-to-glycolic acid ratios, different molar masses ( $M_n$ ) of PLGA and different degrees of PEGylation. The evaluation of the effect of various building blocks on NP characteristics was based on measurements of protein encapsulation efficiency, loading and release. For this purpose, the model protein ovalbumin (OVA), found in egg white, was used for all experiments. OVA is commonly used as a model antigen/protein in murine animal studies investigating protein drug delivery with hydrophobic micro- or nanoparticles; its use in the current work therefore allowed for comparison of the obtained data to literature [32,33]. Further to the evaluation of encapsulation, loading and release, the native structure of the protein within the different PLGA polymer NPs was studied. For a meaningful comparison of polymer effects it was important to identify a standard NP preparation procedure and to keep all other preparation parameters identical. The optimization of such a preparation procedure was performed for the PEG-*b*-PAGE-*b*-PLGA polymer and adapted to the other polymers. Protein release was investigated over the course of 7 days, in order to allow for evaluation of both short and long-term release kinetics.

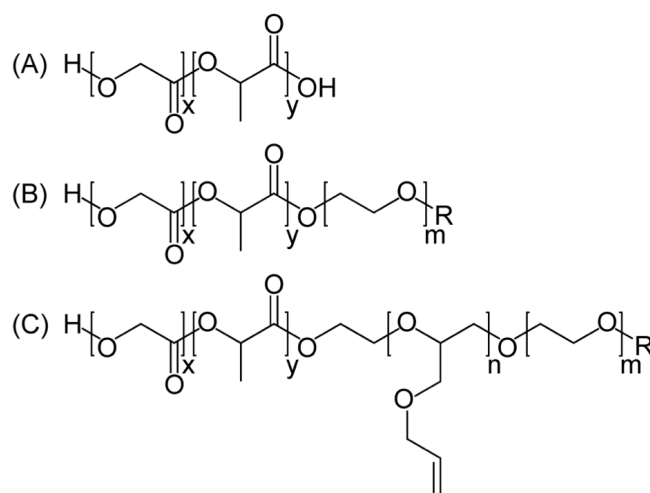


**Figure 1 | Schematic representation of PLGA (A), PEG-*b*-PLGA (B) and PEG-*b*-PAGE-*b*-PLGA (C);** in detail number of x = lactic acid, y = glycolic acid, m = polyethylene glycol, n = poly(allyl glycidyl ether), R = methyl- or biphenyl group.

## 3.2. Materials and methods

### 3.2.1. Materials

Different types of PLGA (Resomer®, Table 1) were supplied by Evonik Industries AG (Darmstadt, Germany). Various PEG-*b*-PLGA and PEG-*b*-PAGE-*b*-PLGA polymers were synthesized in the Laboratory of Organic and Macromolecular Chemistry (IOMC) and Jena Center for Soft Matter (JCSM), at the Friedrich Schiller University of Jena (Table 1) [34]. The number average molar mass ( $M_n$ ) of the different polymers was given as a mean average, determined by size exclusion chromatography (SEC) and nuclear magnetic resonance (NMR).

**Table 1 | Composition of PLGA-Resomer types and synthesized PEG-*b*-PLGA/PEG-*b*-PAGE-*b*-PLGA polymers; PLGA as a co-polymer was considered as a monoblock.**

Number	Polymer	Polymer Type	Lactic-to-glycolic acid ratio	PEG [Da]	PAGE [Da]	PLGA [Da]	Ratio (PEG:PLGA)
P 1	Resomer RG 502 H	Monoblock-	50:50	-	-	10 800	-
P 2	Resomer RG 503 H	Monoblock	50:50	-	-	23 200	-
P 3	Resomer RG 653 H	Monoblock	65:35	-	-	23 900	-
P 4	Resomer RG 753 H	Monoblock	75:25	-	-	24 400	-
P 5	Resomer RG 504 H	Monoblock	50:50	-	-	38 800	-
PP 1	PEG <sub>34</sub> - <i>b</i> -PLGA <sub>833</sub>	Diblock	50:50	1 500	-	54 500	1 : 36
PP 2	PEG <sub>45</sub> - <i>b</i> -PLGA <sub>694</sub>	Diblock	50:50	2 000	-	45 000	1 : 22.5
PP 3	PEG <sub>72</sub> - <i>b</i> -PLGA <sub>718</sub>	Diblock	50:50	3 200	-	46 700	1 : 14.5
PPP 1	PEG <sub>45</sub> - <i>b</i> -PAGE <sub>8</sub> - <i>b</i> -PLGA <sub>294</sub>	Triblock	50:50	2 000	850	19 150	1 : 9.6
PPP 2	PEG <sub>45</sub> - <i>b</i> -PAGE <sub>9</sub> - <i>b</i> -PLGA <sub>458</sub>	Triblock	50:50	2 000	1 000	29 700	1 : 15
PPP 3	PEG <sub>42</sub> - <i>b</i> -PAGE <sub>9</sub> - <i>b</i> -PLGA <sub>833</sub>	Triblock	50:50	2 000	1 000	54 250	1 : 27
PPP 4	PEG <sub>54</sub> - <i>b</i> -PAGE <sub>8</sub> - <i>b</i> -PLGA <sub>840</sub>	Triblock	50:50	2 400	900	54 630	1 : 23
PPP 5	PEG <sub>66</sub> - <i>b</i> -PAGE <sub>9</sub> - <i>b</i> -PLGA <sub>754</sub>	Triblock	50:50	2 900	1 000	49 050	1 : 17
PPP 6	PEG <sub>98</sub> - <i>b</i> -PAGE <sub>9</sub> - <i>b</i> -PLGA <sub>786</sub>	Triblock	50:50	4 300	1 000	51 100	1 : 12
PPP 7	PEG <sub>125</sub> - <i>b</i> -PAGE <sub>13</sub> - <i>b</i> -PLGA <sub>687</sub>	Triblock	50:50	5 550	1 500	44 750	1 : 8

Albumin from chicken egg white (ovalbumin, type Grade V, purity  $\geq 98\%$ , 44 kDa), the QuantiPro™ BCA Assay Kit (for 0.5-30  $\mu\text{g}/\text{ml}$  protein), and D-(+)-trehalose dihydrate (from *Saccharomyces cerevisiae*, purity  $\geq 99\%$ ), dichloromethane (DCM, HPLC grade) were purchased from Sigma-Aldrich Chemie GmbH (Steinheim, Germany), as were sodium chloride (NaCl, BioXtra, purity  $\geq 99.5\%$ ), potassium chloride (KCl, BioXtra, purity  $\geq 99.0\%$ ), sodium phosphate dibasic heptahydrate ( $\text{Na}_2\text{HPO}_4 \cdot 7\text{H}_2\text{O}$ , meets USP testing specifications) and monobasic potassium phosphate ( $\text{KH}_2\text{PO}_4$ , for molecular biology, purity  $\geq 98.0\%$ ), which were used to prepare phosphate buffer (PB Buffer) and phosphate buffered saline (PBS buffer). Polyvinyl alcohol (PVA) was purchased from Kuraray Europe

GmbH (Hattersheim, Germany). Water used for all preparations and investigations was produced by a Millipore Q-Gard 2 purification system (Merck Millipore, Billerica, United States). All other used chemicals were of analytical grade.

### 3.2.2. Preparation of nanoparticles

OVA-loaded NPs based on PLGA, PEG-*b*-PLGA and PEG-*b*-PAGE-*b*-PLGA were prepared using a double emulsion solvent evaporation technique. Briefly, 50 mg of polymer was dissolved in 2.5 ml DCM (20 mg/ml) and emulsified with 0.5 ml OVA solution (in PBS pH 7.4, OVA concentration 20 mg/ml) by sonication with 35% amplitude (energy introduced 280 J) at room temperature (Branson digital sonifier 250, Danbury, United States). Subsequently 5 ml of a 2% PVA solution (w/v) was added to the first emulsion and sonicated again with 35% amplitude (energy introduced 595 J), at room temperature, to obtain the w/o/w emulsion. The same procedure was carried out with only 0.5 ml PBS in the absence of OVA solution to prepare blank, unloaded polymer NPs. The double emulsion was diluted by adding water dropwise followed by stirring at 1,000 rpm overnight at room temperature, to evaporate the DCM. To produce NPs surface coated with OVA, unwashed blank NPs after overnight DCM evaporation were incubated for 1 h with 0.5 ml OVA solution (in PBS pH 7.4, OVA concentration 20 mg/ml). Finally, unloaded, OVA-loaded and OVA surface-coated NPs were purified, by centrifugation at 15,000 g for 11 min (Rotina 420 R, Hettich Lab Technology, Tuttlingen, Germany) and washed twice with water. After purification trehalose and PVA were added to NPs as a cryoprotectant and stabilizer for lyophilization respectively. For lyophilization the NP suspension was frozen for 3 h at -80 °C and lyophilized for 3 days under vacuum (Alpha 2-4 LSC, Christ GmbH, Osterrode, Germany). Four batches of every formulation were prepared.

### 3.2.3. Characterization of nanoparticles

The average size (in nm), size distribution (polydispersity index - PDI) and  $\zeta$ -potential (in mV) of the polymeric NPs were measured using dynamic light scattering (DLS) and electrophoretic mobility (Zetasizer Nano ZSP, Malvern Instruments, Herrenberg, Germany) at 25 °C. The measurements were performed with aqueous dispersions of NPs (~ 0.1 mg/ml) prior to lyophilization. The surface morphology of NPs was determined by scanning electron microscopy (SEM - Zeiss EVO HD15, Jena, Germany). NPs were coated



with a gold layer of approximately 10 nm under vacuum before SEM examination (accelerating voltage 5 kV, focal distance 10 mm).

#### **3.2.4. Determination of Encapsulation efficiency and loading**

A bicinchoninic acid protein (BCA) assay kit (QuantiPro™ BCA Assay Kit) was used for the determination of encapsulation efficiency (% EE = encapsulated OVA [mg]/initial drug in formulation [mg] \* 100) and loading (% L = encapsulated OVA [mg]/weight prepared NPs [mg] \* 100) of OVA in NPs, according to the manufacturer's instructions. Accordingly, 1 mg of lyophilized NPs was dissolved in 1 ml of 1 M NaOH solution (1 mg/ml). After overnight incubation and neutralization with 1 M HCl at 20 °C, the protein concentration within dissolved NP samples was determined using the QuantiPro™ BCA Assay Kit and the Tecan Infinite M200 Pro (Männedorf, Switzerland) plate reader at  $\lambda = 562$  nm. Blank NPs were used as control. Each batch was analyzed in triplicate.

#### **3.2.5. In vitro release of protein**

Approximately 10 mg of lyophilized NPs were incubated with 10 ml of PBS buffer (100 mM and pH 7.4) in glass vials, over 7 days under continuous stirring at 150 rpm at 37 °C. At appropriate time intervals (1 h, 2 h, 4 h, 8 h, 1 d, 3 d, 5 d, 7 d) the samples were collected and centrifuged for 15 min at 20,000 g. The clear supernatant was used to determine the amount of OVA released from the formulation using the QuantiPro™ BCA Assay Kit. Each batch was analyzed in triplicate.

#### **3.2.6. Activity of OVA**

Quantification of the activity of OVA encapsulated or coated on the surface of the NPs was performed using an ELISA assay, in order to determine whether the native state of the protein was maintained. The prepared NP dispersion (1 mg/ml) was incubated for 24 h in PBS buffer pH 7.4 at 37 °C under continuous stirring at 150 rpm. The dispersion was centrifuged at 20,000 g for 15 min and the total amount of protein in the supernatant was determined using the QuantiPro™ BCA Assay Kit. To determine the amount of active OVA in the same supernatant an ELISA assay (Serazym® Ovalbumin ELISA, Seramun Diagnostica GmbH, Heidesee, Germany, range 0.625-20 ng/ml, lower limit of detection (LLOD) = 0.125 ng/ml), which was performed according to the instructions provided by the

manufacturer, was used. Consequently, the amount of OVA quantified with the ELISA assay was divided by the total amount of OVA within the supernatant to determine the percentage of active or so-called native protein ( $\% \text{ Activity} = (\text{amount of native OVA [mg]} / \text{total amount of OVA in the supernatant [mg]}) * 100$ ). As negative control supernatant from blank particles was employed, and a freshly prepared OVA solution in PBS was used as positive control.

### 3.2.7. Determination of surface hydrophobicity

The surface hydrophobicity was determined by the adsorption of the hydrophobic dye Rose Bengal (RB) on NPs. The hydrophobic dye (with a constant  $c_{\text{RB}} = 40 \mu\text{g/ml}$ ) was incubated with an increasing NP concentration (0.3125-5 mg/ml) for 1 h at room temperature [35]. After the incubation time the suspensions were centrifuged at 20,000 g for 15 min and the absorption of the supernatants was measured at  $\lambda = 542 \text{ nm}$ . An RB calibration curve (40-0.625  $\mu\text{g/ml}$ ) was prepared to determine the RB concentration in the supernatant. The partitioning coefficient (PQ) of RB for each NP concentration was then calculated by dividing the adsorbed amount of RB on NP surface by the free amount of RB in the dispersion medium. This PQ was plotted versus the increasing NP surface area. The obtained plots were used as a measure for the degree of NP surface hydrophobicity.

### 3.2.8. Statistical analysis

Statistical analysis of loading and encapsulation efficiencies was performed via one way analysis of variance (ANOVA) followed by Tukey's multiple comparisons test using GraphPad Prism 6 software (GraphPad Software, Inc, La Jolla, CA). The confidence interval was set at 95%, a p value of  $> 0.05$  was taken as not significant (n.s.) and a p value of  $< 0.05$  was accepted as significant (\*);  $p < 0.01$  (\*\*),  $p < 0.001$  (\*\*\*)

## 3.3. Results and discussion

In many studies to date, the influence of changing numerous process parameters - such as the amount of polymer and drug used, the time for preparation, and the selected excipients (different emulsifier or release modifier) - on particles produced via the double emulsion method has been described [36–40]. However, for comparison of the potential of a polymer to act as an encapsulation material it is of utmost importance to keep the

majority of process parameters unchanged. As a consequence, only the Mw of the different polymer building blocks, and hence the fraction of its influence on the polymers' properties, was varied.

### 3.3.1. Characterization of nanoparticles

Blank and OVA-loaded NPs of all PLGA subtypes were prepared using the same conditions by a double-emulsion method. The results yielded narrowly distributed ( $PDI < 0.15$ ) sub-micron particles with a mean size of OVA-loaded PLGA, PEG-*b*-PLGA and PEG-*b*-PAGE-*b*-PLGA particles in the range of 170-220 nm (Figure 2). Blank particles were roughly 15-25 nm smaller than the OVA-loaded particles, which is not surprising taking into consideration the size of the encapsulated protein (mean size of a single OVA molecule determined by DLS is 2-3 nm). No substantial influence of PLGA, PEG or PAGE Mn or of lactic:glycolic acid ratio was found on NP physiochemical characteristics for any of the tested polymer derivatives (PLGA, PEG-*b*-PLGA and PEG-*b*-PAGE-*b*-PLGA). It should however be noted that NP could not be prepared from PEGylated PLGAs with molecular weight ratios of PEG to PLGA  $< 1:5$  using the double emulsion method.

All types of PLGA (Figure 2) were found to form particles with a negative surface charge of  $-29.1 \pm 2.2$  mV. Protein incorporation led to a reduction in magnitude of surface charge, to  $-20.1 \pm 3.6$  mV. No major difference in surface charge was observed for blank particles prepared from PLGA (-30 mV), PEG-*b*-PLGA (-29 mV) to PEG-*b*-PAGE-*b*-PLGA (-27 mV); this is due to the use of PVA, both as an emulsifier in the preparation method and most importantly, as a stabilizer for our final lyophilized product. The stabilization of the freeze-dried formulation with PVA was necessary to prevent particle aggregation. Therefore, the remaining PVA in the preparation acts to shield the NP interface and thus maintain a consistent zeta potential. The SEM images in Figure 2 show smooth, spherical NPs with sizes approximately 20 nm smaller (determined by Image J) than those measured by DLS. These differences are most likely due to conduction of SEM imaging in vacuum in contrast to DLS measurement of the hydrodynamic radius in suspension.

Nanoparticle	Size [nm]	PDI	Zeta potential [mV]
PLGA - Blank NPs	199.7 ± 6.2	0.06 ± 0.02	-30.4 ± 1.4
PLGA - OVA loaded NPs	218.4 ± 9.7	0.11 ± 0.03	-23.8 ± 3.8
PEG- <i>b</i> -PLGA - Blank NPs	173.1 ± 7.8	0.07 ± 0.02	-29.5 ± 3.1
PEG- <i>b</i> -PLGA - OVA loaded NPs	188.4 ± 12.9	0.11 ± 0.02	-18.7 ± 2.2
PEG- <i>b</i> -PAGE- <i>b</i> -PLGA - Blank NPs	178.5 ± 11.0	0.07 ± 0.04	-27.5 ± 3.1
PEG- <i>b</i> -PAGE- <i>b</i> -PLGA - OVA loaded NPs	192.5 ± 5.3	0.11 ± 0.03	-17.7 ± 2.8

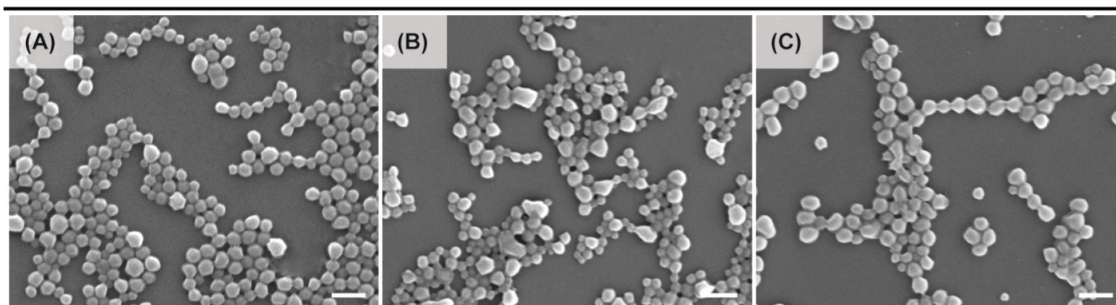


**Figure 2 | Characteristics of blank and OVA-loaded NPs using PLGA, PEG-*b*-PLGA and PEG-*b*-PAGE-*b*-PLGA polymer;** Data in the table represent mean ± SD (n=6); SEM images of OVA-loaded NPs made of (A) P 5, (B) PP 2 and (C) PPP 3. Size of the scale bar = 500 nm.

### 3.3.2. Loading and of Encapsulation efficiency

As mentioned, all NPs were prepared using the same conditions, with an initial fixed OVA concentration (20 mg/ml). Consequently, the encapsulation efficiency is a function of loading and qualitatively behaves the same way. Encapsulation efficiency will therefore not be mentioned additionally during the results and discussion, with a focus placed instead on loading. It should be noted however that a maximum loading of 20% would correspond to 100% encapsulation efficiency.

First the loadings of five commercially available PLGA types from Evonik (Table 2) were determined. Three different Mn of PLGA (P 1 - 10,800 Da, P 2 - 23,200 Da and P 5 - 38,800 Da) were used to investigate the effect of different Mn on the loading while keeping the lactic:glycolic acid ratio of 50:50 constant. Furthermore, three PLGA types were used to show the influence of the lactic:glycolic acid ratio (P 2 - 50:50, P 3 - 65:35, P 4 - 75:25) on produced NPs, using the same Mn for PLGA of approximately 24,000 Da. For all PLGA polymers an average load of  $8.2 \pm 1.0\%$ , independent of the  $Mn_{PLGA}$ , lactic:glycolic acid ratio and particle size was found.

For all three available PEG-*b*-PLGA polymers (PP 1-3) the total Mn of approximately 50,000 Da and the lactic:glycolic acid ratio of 50:50 were kept constant. The degree of PEGylation of polymers however increased, from 2.8% (PP 1) to 4.4% (PP 2) to 6.8% (PP 3).

For the available PEG-*b*-PLGAs an overall average loading of  $8.7 \pm 1.0\%$  was determined. Ultimately no significant increase of loading was encountered from lower to higher degree of PEG-*b*-PLGA PEGylation. Comparing PEG-*b*-PLGA NPs with the unmodified PLGA NPs a slight increase of the mean values for loading and encapsulation was observed, however this was not significant - an observation which has already been described in literature [41,42].

The major group of interest for investigation was the triblock polymer, PEG-*b*-PAGE-*b*-PLGA, assuming PLGA as a monoblock. For this polymer different combinations of PEGylation and Mn of PLGA were used, while maintaining a low variation of incorporated PAGE groups and keeping the lactic:glycolic acid ratio constant (Table 1). Overall an average loading for PEG-*b*-PAGE-*b*-PLGA NPs of  $10.1 \pm 3.0\%$  was observed. This is a first hint that a combination of PEG and PAGE with PLGA acts to increase protein encapsulation, compared to PLGA and PEG-*b*-PLGA. We will first focus on the polymers PPP 1, PPP 2 and PPP 3 (Table 2) with a constant PEG and PAGE fraction, but increasing Mn of PLGA from approximately 20,000 Da to 55,000 Da. The data show a significant increase of loading from  $7.7 \pm 0.5\%$  (PPP 1) up to  $11.4 \pm 0.7\%$  (PPP 3). From this group we can conclude that the loading increases with increasing Mn of PLGA in PEG-*b*-PAGE-*b*-PLGA NPs. With this knowledge the Mn of PLGA was fixed at a higher molecular weight (Mn = 50,000 Da, Mn of PAGE was kept as before at approximately 1,000 Da) and the Mn of the PEG-block was increased from 2,000 Da to 4,300 Da (PPP 3-6). The influence of the varying PEG block length was the same as observed for the PEG-*b*-PLGA: no significant increase in loading (10-11.4%) with increasing PEGylation was obtained. However, a significantly higher load of PEG-*b*-PAGE-*b*-PLGA polymers was determined compared to both PLGA alone and the PEG-polymers with the same degree of PEGylation. In contrast, the PEG-*b*-PAGE-*b*-PLGA polymer (PPP 7, loading  $12.5 \pm 0.5\%$ ) with the largest PAGE (1,500 Da) and PEG (5,550 Da) blocks provided a 35% and 30% higher loading compared to PLGA and PEG-*b*-PLGA NPs respectively. Excluding PPP 1 and PPP 2 with their lower Mn of PLGA (resulting in a significantly lower loading), an average loading for PEG-*b*-PAGE-*b*-PLGA NPs of  $11.0 \pm 1.8\%$  was determined, which is overall 25% higher than the loading of the other polymers. From these loading studies, we conclude that the PEG-block in the PEGylated PLGAs has no significant influence on protein encapsulation, in contrast to the insertion of the PAGE building block which is determined to have a significant impact [41,42].

**Table 2 | Loading and encapsulation efficiency for OVA-loaded PLGA, PEG-*b*-PLGA and PEG-*b*-PAGE-*b*-PLGA particles with their specific polymer composition; Data in the table represent mean  $\pm$  SD (n=6).**

Nanoparticle	PEG [Da]	PAGE [Da]	PLGA [Da]	Loading efficiency [%] <sup>a</sup>	Encapsulation efficiency [%] <sup>a</sup>
P 1	-	-	10 800	8.8 $\pm$ 1.8	44.0 $\pm$ 9.0
P 2	-	-	23 200	8.6 $\pm$ 0.5	43.0 $\pm$ 2.5
P 3	-	-	23 900	7.8 $\pm$ 0.6	39.0 $\pm$ 3.0
P 4	-	-	24 400	8.7 $\pm$ 0.3	43.5 $\pm$ 1.5
P 5	-	-	38 800	7.9 $\pm$ 0.4	39.5 $\pm$ 2.0
PP 1	1 500	-	54 500	8.5 $\pm$ 0.2	42.5 $\pm$ 1.0
PP 2	2 000	-	45 000	8.5 $\pm$ 0.9	42.5 $\pm$ 4.5
PP 3	3 200	-	46 700	9.2 $\pm$ 0.6	46.0 $\pm$ 3.0
PPP 1	2 000	850	19 150	7.7 $\pm$ 0.5	38.5 $\pm$ 2.5
PPP 2	2 000	1 000	29 700	8.2 $\pm$ 0.5	41.0 $\pm$ 2.5
PPP 3	2 000	1 000	54 250	11.4 $\pm$ 0.7	57.0 $\pm$ 3.5
PPP 4	2 400	900	54 630	10.1 $\pm$ 0.3	50.5 $\pm$ 1.5
PPP 5	2 900	1 000	49 050	10.0 $\pm$ 0.6	50.0 $\pm$ 3.0
PPP 6	4 300	1 000	51 100	11.0 $\pm$ 1.0	55.0 $\pm$ 5.0
PPP 7	5 550	1 500	44 750	12.5 $\pm$ 0.5	62.5 $\pm$ 2.5

<sup>a</sup> p value > 0.05 not significant (n.s), p values < 0.05 significant

### 3.3.3. Adsorption and activity studies

To evaluate the loading of various NP formulations in more detail, an adsorption and activity study with 3 representative polymers of PLGA, PEG-*b*-PLGA and PEG-*b*-PAGE-*b*-PLGA was performed. The aim of this study was to understand the influence of protein adsorption on the NP surface in contrast to protein encapsulation into the NPs, using different polymers. Additionally, the structural stability of the protein during encapsulation and after release was under investigation.

We compared the PLGA NP formulation with the highest Mn of 38,800 Da (P 5) with the PEGylated PLGA with having a PEG-block of 2,000 Da and the smallest PLGA block (PP 2). Furthermore, a PEG-*b*-PAGE-*b*-PLGA with the same PEG block Mn and the closest Mn<sub>PLGA</sub> was used (PPP 3). Three additional particle batches were prepared using these polymers (Table 3). Blank and OVA-loaded NPs prepared from each polymer were found to show comparable size, PDI, zeta potential and loading. As a control purely surface-loaded NPs were also prepared in the case of each polymer, by incubation of blank NPs in OVA solution.

For correlating the adsorption of the hydrophilic model protein OVA to the surface polarity of the particles, the surface hydrophobicity of produced NPs with surface-adsorbed OVA

was determined using the hydrophobic RB dye as a reference system [35,43]. Plotting the PQ of RB against the surface area of the NPs should result in a straight line. The slope of each plot is then taken as a measure for the surface hydrophobicity, with a steeper the slope indicating a more hydrophobic surface [35]. The RB Assay allows for a comparison of the surface properties of the different produced NPs. The larger slope for PLGA NP PQ vs. surface area profiles (P 5) indicates a relatively more hydrophobic NP surface compared to PEG-*b*-PLGA (PP 2) and PEG-*b*-PAGE-*b*-PLGA NPs (PPP 3), for which profiles with more shallow gradients were determined (Figure 3).

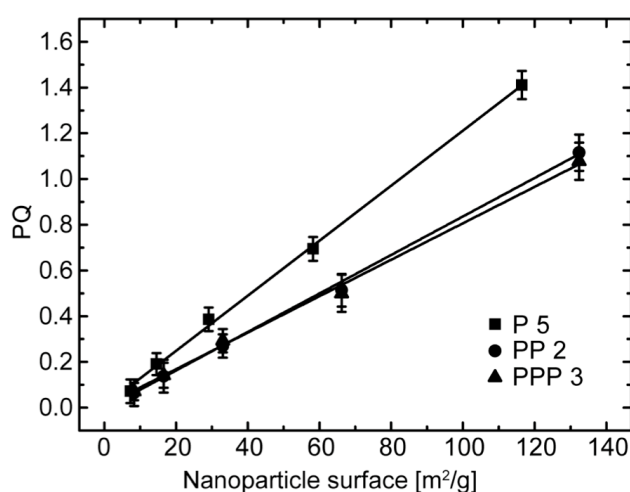


Figure 3 | Plot of partitioning coefficient (PQ) of RB at increasing nanoparticle surface of P 5, PP 3 and PPP 3.

The amount of OVA adsorbed to the same surface-loaded NPs from the RB assay was also quantified, in order to determine the surface loading of such formulations. In accordance with the higher degree of surface hydrophobicity as determined in the RB assay, PLGA NPs showed the lowest OVA surface loading of  $0.16 \pm 0.01\%$ . In contrast, surface loading of PEGylated PLGA NPs and PEG-*b*-PAGE-*b*-PLGA NPs was found to be  $0.47 \pm 0.04\%$  and  $0.5 \pm 0.03\%$ , respectively. The difference between the PLGA and PEGylated PLGAs polymers is of course the presence of the hydrophilic PEG-chains, which are located on the surface of the NPs. The adsorption of hydrophilic substances to such a surface is therefore reported to be better than to the more hydrophobic PLGA surface [44], in agreement with the current observations. The PAGE group seems not to impact on surface loading; this is also reflected in the RB assay, which revealed the same surface polarity for NPs prepared from PEG-*b*-PLGA and PEG-*b*-PAGE-*b*-PLGA. Although the PEGylated PLGAs show an increased protein adsorption this had no strong consequence on the comparative overall loading efficiency. Therefore it can be concluded that the higher overall loading observed

for the PEG-*b*-PAGE-*b*-PLGA polymers is the result of a matrix effect of the polymer building block. The adsorption studies (Table 3) further revealed, as already described previously with respect to NP characterization (Figure 2), a load dependent decrease of the zeta potential of the NPs, regardless of whether OVA was loaded into or adsorbed onto the NPs. The zeta potential of the surface-loaded NPs lies between the zeta potential of the loaded and the unloaded NPs in the case of each polymer, which is particularly interesting with respect to the difference in zeta potential of OVA-loaded particles as compared to the surface coated NPs. From this experiment we can conclude that the lower zeta potential of the OVA-loaded NPs is not only caused by the presence of adsorbed protein. Surface loaded NPs were prepared by incubating blank NPs for only 1 h with 20 mg of OVA, which led to a surface adsorption but no encapsulation of OVA into the NPs. Compared to the surface loaded NPs, the zeta potential of the protein loaded NPs is of a lower magnitude, due not only to the protein which is obviously adsorbed at the surface, but also in some way to the encapsulated protein itself.

In addition to the adsorption measurements an ELISA was performed to check the activity of OVA following its release from NPs of the different polymers. The NP encapsulation of the protein offers a potential protection from environmental influences, preventing aggregation or cleavage and allowing for retention of biological activity [45]. However, the encapsulation procedure utilizes both organic and aqueous solvents, which, in addition to the final freeze drying of the NPs, could decrease the amount of native OVA. For all NPs the amount of OVA released within 24 h was determined, and the activity of released OVA was quantified. For the surface loaded NPs an activity of approximately 40% was found, which is not unexpected, as the protein was not completely protected from degrading environmental influences. In the case of NPs where OVA was encapsulated, a higher activity of OVA was found; activity was further seen to increase in the order of PLGA (~ 60%) < PEG-*b*-PLGA (~ 65%) < PEG-*b*-PAGE-*b*-PLGA (~ 75%). This leads to the conclusion that (1) the encapsulation of proteins confers protection from negative environmental influences to a greater extent than surface adsorption and (2) the PEGylated PLGA polymers and, to an even greater degree, the PEG-*b*-PAGE-*b*-PLGA polymers are able to preserve the activity of encapsulated protein.



**Table 3 | Results for loading and adsorption studies of PLGA (P 5), PEG-*b*-PLGA (PP 2) and PEG-*b*-PAGE-*b*-PLGA NPs (PPP 3); Data in the table represent mean  $\pm$  SD (n=3).**

Nanoparticle	Size [nm]	PDI	Zeta potential [mV]	Loading [%]	Activity [%]
P 5 - Blank NPs	192.3 $\pm$ 2.3	0.03 $\pm$ 0.02	-27.5 $\pm$ 1.1	0	0
P 5 - Surface loaded NPs	198.6 $\pm$ 17.3	0.10 $\pm$ 0.06	-25.9 $\pm$ 1.9	0.16 $\pm$ 0.01	38.86 $\pm$ 4.66
P 5 - OVA loaded NPs	195.0 $\pm$ 1.1	0.06 $\pm$ 0.02	-20.9 $\pm$ 1.6	7.73 $\pm$ 0.38	59.14 $\pm$ 12.31
PP 2 - Blank NPs	178.4 $\pm$ 1.9	0.05 $\pm$ 0.02	-28.8 $\pm$ 1.4	0	0
PP 2 - Surface loaded NPs	176.8 $\pm$ 1.2	0.07 $\pm$ 0.02	-23.1 $\pm$ 1.1	0.47 $\pm$ 0.04	43.5 $\pm$ 1.00
PP 2 - OVA loaded NPs	190.3 $\pm$ 1.4	0.06 $\pm$ 0.02	-18.1 $\pm$ 2.5	8.66 $\pm$ 0.87	64.89 $\pm$ 6.34
PPP 3 - Blank NPs	178.4 $\pm$ 2.3	0.06 $\pm$ 0.02	-30.9 $\pm$ 0.7	0	0
PPP 3 - Surface loaded NPs	186.5 $\pm$ 9.9	0.10 $\pm$ 0.05	-24.7 $\pm$ 2.6	0.50 $\pm$ 0.03	36.59 $\pm$ 2.82
PPP 3 - OVA loaded NPs	189.1 $\pm$ 1.8	0.08 $\pm$ 0.02	-13.0 $\pm$ 1.5	11.0 $\pm$ 0.85	74.32 $\pm$ 13.11

### 3.3.4. OVA release from the particles

The OVA release from three batches of NPs made of the different polymer types was determined at definite time intervals up to 7 days (1, 2, 4, 8, 24, 48, 72, 144 and 168 h) in PBS buffer pH 7.4 at 37 °C. Generally, NPs made of PLGA show a biphasic release profile, with an initial burst release followed by a sustained release phase [46]. The fast initial burst release is induced by the fast release of protein at or near to the surface of the NP, whereas the sustained release is caused by additional and slower release of protein from the NP polymer matrix through channels. The water inside the matrix hydrolyzes the polymer into soluble polymer products, which forms a passage for protein to be released by diffusion and erosion until complete polymer solubilization has occurred [46]. The aim of determining relative protein release kinetics was to compare and evaluate the effects of the various compositions of polymer subtypes, possessing different Mns for PEG, PAGE and PLGA as well as different lactic:glycolic acid ratios. For every PLGA polymer type respective release studies were performed, to determine the impact of both overall polymer composition as well as individual polymer building block character. Considerable differences in release behavior between the particles made from different polymers - PLGA, PEG-*b*-PLGA and PEG-*b*-PAGE-*b*-PLGA - were observed.

Different Mn of PLGA, PEG, PAGE or lactic:glycolic acid ratios within a polymer type had no major influence. However, when comparing between the polymer types, a total release of  $8.8 \pm 0.4\%$  for PLGA,  $11.1 \pm 0.2\%$  for PEG-*b*-PLGA and  $16.9 \pm 1.1\%$  for PEG-*b*-PAGE-*b*-PLGA over 168 h was found (Figure 4A). This correlates to a 25% higher release of OVA from PEG-*b*-PLGA in comparison to PLGA, and a nearly 100% or 50% higher release of OVA from

PEG-*b*-PAGE-*b*-PLGA compared to PLGA or PEG-*b*-PLGA. The lack of influence of the different Mn of PLGA or the lactic:glycolic acid ratio on protein release within a particular polymer group could be due to the degradation behavior of the polymers. Systematic studies of the degradation of the well-known PLGA with different lactic:glycolic acid ratios over 70 days or longer, show a faster degradation for a PLGA lactic:glycolic acid ratio of 50:50 and slower degradation for PLGA with a lactic:glycolic acid ratio of 75:25 [47,48]. However, the difference in release between these PLGAs is typically visible only after 10 to 20 days and is almost negligible for the first days. Besides the lactic:glycolic acid ratio, the Mn of the PLGA backbone structure is important. From literature it can be concluded that with higher molecular weight slower degradation of the polymer is expected, and therefore a slower release of drugs can be hypothesized [46]. This lower degradation and as a consequence slower release, is also however not visible in the first 10 to 20 days.

Looking at Figure 4A one might get the impression that the difference in release noted between NPs of the three polymer groups is mainly due to the different extent of burst release. That is not the case however, as can be clearly seen when the burst release (Figure 4B) is depicted separately from the sustained release phase (Figure 4C). The burst release is defined, as mentioned before, as the fast release of the cargo located either at or near to the particle surface; this burst release is then followed by a slower, sustained release phase. The decrease in release and transition from the burst to the sustained release phase can be seen as a gradual transition in the release profile, determined to be between 8 h to 24 h for our polymers. Therefore, the release within 24 h (burst release) and the release from 24 h until 168 h (sustained release) were plotted separately. For PLGA and PEG-*b*-PLGA a lower extent of burst release of 8 to 10% was found, while a greater burst release of 14% for PEG-*b*-PAGE-*b*-PLGA was noted (Figure 4B). This corresponds to an increase of 4-6% in protein release from PEG-*b*-PAGE-*b*-PLGA polymer NPs in comparison to PLGA and PEG-*b*-PLGA within the first 24 h. Taking the adsorption studies into consideration, where an additional 0.3 to 0.4% of protein adsorbed to the surface of the PEGylated polymer NPs was found, the additional release of PEG-*b*-PLGA as compared to PLGA may be explained; however, this does not account for the significantly higher burst release of protein noted to occur from the PEG-*b*-PAGE-*b*-PLGA NPs. For a better comparison of the sustained release curves, the differences in release were displayed from the 24 h value onwards and the error bars excluded for clarity (Figure 4C). A slower

sustained release level of 0.7% for PLGA NPs and 1.2% for PEG-*b*-PLGA NPs was observed, compared to a higher sustained release of 2.7% for PEG-*b*-PAGE-*b*-PLGA NPs.

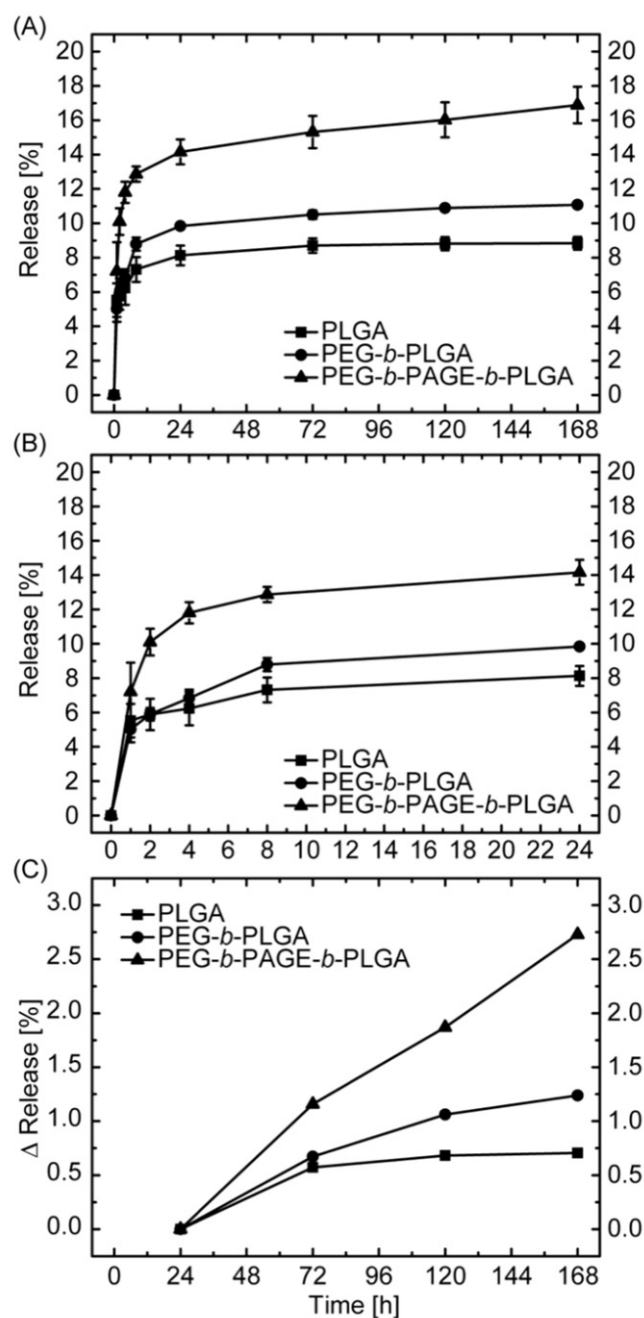


**Figure 4 | Results for release of PLGA, PEG-*b*-PLGA and PEG-*b*-PAGE-*b*-PLGA NPs;** A) Release of all polymers in percent over 168 h. B) Release of all polymers in percent over 24 h. C) Δ Release of all polymers in percent from 24 h to 168 h. Data in the figure represent mean ± SD (n=3).

Considering the burst and sustained release phases together, it can be seen that the PEGylation of PLGA led to an increase in the extent of protein release, which can be explained by the properties of PEG in the polymer. It is known that PLGA polymers interact with tensioactive proteins such as OVA [49]; this provided the possibility to form uniform

NPs by a double emulsion method, but led also to the formation of compact NPs exhibiting a slow and low release of protein. By addition of another surface active molecule such as PEG, which is covalently linked to the parent polymer, the interaction between polymer and protein is reduced – this was reflected in the higher release rates observed from PEG-*b*-PLGA NPs [50].

However the presence of the PEG building block cannot account for the significantly higher burst and prolonged protein release over 168 h seen for the PEG-*b*-PAGE-*b*-PLGA polymer. This could however be explained empirically by the properties of the PAGE building block in the polymer. The PAGE group adds a branched functionality to the typically linear polymer that could reduce the occurrence of steric interactions between polymer side chains. This could lead to the formation of voids or channels in the NP or a modified degradation behavior of the polymer, and therefore higher burst and sustained release of the protein. The differences in the release curves can therefore be clearly attributed to the composition of the NPs.

### 3.4. Conclusion

In this work, the effect of different PLGA and PEGylated PLGA polymers on the preparation of OVA-loaded NPs was studied, with the major objective being to achieve an improved protein loading. Based on PLGA, PEGylated PLGA NPs with a PEG shell for passive targeting and PEGylated PAGE-PLGA NPs with an active group for potential drug targeting - the PAGE building block - were prepared. Morphological characterization demonstrated a spherical shape of the NPs produced from all polymers with an average diameter of approximately 200 nm, as determined by DLS and SEM. PEGylation of PLGA alone had no major impact on OVA loading (PLGA NPs 8.2%; PEG-*b*-PLGA NPs 8.7%), but the addition of the PAGE building block between PEG and PLGA resulted in an increase in OVA loading (PEG-*b*-PAGE-*b*-PLGA 10.1-11%). In contrast to protein loading, the PEGylation of PLGA alone had an effect on the release of protein from formed NPs. After 168 h PEG-*b*-PLGA showed a slightly higher release of 11.1% of originally incorporated OVA, as compared to PLGA NPs, which released 8.8% of incorporated protein. This difference can be attributed to the PEG building block. For PEG-*b*-PAGE-*b*-PLGA NPs (16.9% total protein released), a nearly 100% greater extent of release was found compared to PLGA NPs. The different polymer building blocks were observed to influence not only the released

fraction of protein, but also the release behavior. An increased sustained release over 168 h could be shown for PLGA, PEG-*b*-PLGA and PEG-*b*-PAGE-*b*-PLGA, with values of 0.7%, 1.2% and 2.7% respectively. This modified release behavior can also be attributed to the different polymer compositions, rather than to different burst release profiles or adsorption effect of protein on the NP surface. Ultimately, the improved loading and the modified release of OVA from NPs prepared from modified PLGA was seen to be accompanied by a higher stability of the OVA, demonstrated by a higher fraction of intact and active protein. As the impact of the protein on the delivery system differs from protein to protein, the data presented in the current work cannot be directly transferred to other protein payloads. However, our evaluation of the different polymer NPs using OVA is a valuable start and has already been successfully adapted for another protein [51]. Finally, the PEGylation of PLGA and especially the insertion of the PAGE group led to higher loading and release rates for OVA loaded PEG-*b*-PAGE-*b*-PLGA NPs, demonstrating the potential of such a delivery system for many application routes.

### 3.5. References

1. Zhu KJ, Xiangzhou L, Shilin Y. Preparation, characterization, and properties of polylactide (PLA)–poly(ethylene glycol) (PEG) copolymers: A potential drug carrier. *J. Appl. Polym. Sci.* 1990;39:1–9.
2. Barratt G. Colloidal drug carriers: achievements and perspectives. *Cell. Mol. Life Sci.* 2003;60:21–37.
3. Bramwell VW, Perrie Y. Particulate delivery systems for vaccines. *Crit. Rev. Ther. Drug Carrier Syst.* 2005;22:151–214.
4. Csaba N, Garcia-Fuentes M, Alonso MJ. The performance of nanocarriers for transmucosal drug delivery. *Expert Opin. Drug Deliv.* 2006;3:463–78.
5. Santander-Ortega MJ, Stauner T, Loretz B, Ortega-Vinuesa JL, Bastos-González D, Wenz G, et al. Nanoparticles made from novel starch derivatives for transdermal drug delivery. *J. Control. Release.* 2010;141:85–92.
6. Yadav SC, Kumari A, Yadav R. Development of peptide and protein nanotherapeutics by nanoencapsulation and nanobioconjugation. *Peptides.* 2011;32:173–87.
7. Soppimath KS, Aminabhavi TM, Kulkarni AR, Rudzinski WE. Biodegradable polymeric nanoparticles as drug delivery devices. *J. Control. Release.* 2001;70:1–20.
8. Conti B, Pavanetto F, Genta I. Use of polylactic acid for the preparation of microparticulate drug delivery systems. *J. Microencapsul.* 1991;9:153–66.

9. Sanders LM, Kent JS, McRae GI, Vickery BH, Tice TR, Lewis DH. Controlled release of a luteinizing hormone-releasing hormone analogue from poly(d,l-lactide—co-glycolide) microspheres. *J. Pharm. Sci.* 1984;73:1294–7.
10. Dillen K, Vandervoort J, Van den Mooter G, Verheyden L, Ludwig A. Factorial design, physicochemical characterisation and activity of ciprofloxacin-PLGA nanoparticles. *Int. J. Pharm.* 2004;275:171–87.
11. Fonseca C, Simões S, Gaspar R. Paclitaxel-loaded PLGA nanoparticles: preparation, physicochemical characterization and in vitro anti-tumoral activity. *J. Control. Release.* 2002;83:273–86.
12. Govender T, Stolnik S, Garnett MC, Illum L, Davis SS. PLGA nanoparticles prepared by nanoprecipitation: drug loading and release studies of a water soluble drug. *J. Control. Release.* 1999;57:171–85.
13. Lemoine D, Pr  at V. Polymeric nanoparticles as delivery system for influenza virus glycoproteins. *J. Control. Release.* 1998;54:15–27.
14. Nafee N, Taetz S, Schneider M, Schaefer UF, Lehr C-M. Chitosan-coated PLGA nanoparticles for DNA/RNA delivery: effect of the formulation parameters on complexation and transfection of antisense oligonucleotides. *Nanomedicine.* 2007;3:173–83.
15. Rhim J-W, Hong S-I, Park H-M, Ng PKW. Preparation and characterization of chitosan-based nanocomposite films with antimicrobial activity. *J. Agric. Food Chem.*; 2006;54:5814–22.
16. Janes KA, Fresneau MP, Marazuela A, Fabra A, Alonso MJ. Chitosan nanoparticles as delivery systems for doxorubicin. *J. Control.*; 2001;73:255–67.
17. Prabha S, Zhou W-Z, Panyam J, Labhasetwar V. Size-dependency of nanoparticle-mediated gene transfection: studies with fractionated nanoparticles. *Int. J. Pharm.*; 2002;244:105–15.
18. Gan Z, Yu D, Zhong Z, Liang Q, Jing X. Enzymatic degradation of poly( $\epsilon$ -caprolactone)/poly(dl-lactide) blends in phosphate buffer solution. *Polymer (Guildf).* 1999;40:2859–62.
19. Leroueil-Le Verger M, Fluckiger L, Kim Y-I, Hoffman M, Maincent P. Preparation and characterization of nanoparticles containing an antihypertensive agent. *Eur. J. Pharm. Biopharm.* 1998;46:137–43.
20. Le Corre D, Bras J, Dufresne A. Starch nanoparticles: a review. *Biomacromolecules.*; 2010;11:1139–53.
21. Kreuter J. Peroral administration of nanoparticles. *Adv. Drug Deliv. Rev.*; 1991;7:71–86.
22. Johnson FA, Craig DQ, Mercer AD. Characterization of the block structure and molecular weight of sodium alginates. *J. Pharm. Pharmacol.* 1997;49:639–43.
23. Sarmiento B, Ferreira D, Veiga F, Ribeiro A. Characterization of insulin-loaded alginate nanoparticles produced by ionotropic pre-gelation through DSC and FTIR studies. *Carbohydr. Polym.*; 2006;66:1–7.

24. Khan SA, Schneider M. Improvement of nanoprecipitation technique for preparation of gelatin nanoparticles and potential macromolecular drug loading. *Macromol. Biosci.*; 2013;13:455–63.
25. Truong-Le VL, Walsh SM, Schweibert E, Mao HQ, Guggino WB, August JT, et al. Gene transfer by DNA-gelatin nanospheres. *Arch. Biochem. Biophys.*; 1999;361:47–56.
26. Balthasar S, Michaelis K, Dinauer N, von Briesen H, Kreuter J, Langer K. Preparation and characterisation of antibody modified gelatin nanoparticles as drug carrier system for uptake in lymphocytes. *Biomaterials*. 2005;26:2723–32.
27. Langer R, Peppas N. Present and future applications of biomaterials in controlled drug delivery systems. *Biomaterials*. 1981;2:201–14.
28. Dumitriu S, Popa VI. *Polymeric Nanoparticles for Drug Delivery*. Polym. Biomater. Vol. 1. CRC Press; 2013.
29. Gref R, Lück M, Quellec P, Marchand M, Dellacherie E, Harnisch S, et al. “Stealth” corona-core nanoparticles surface modified by polyethylene glycol (PEG): influences of the corona (PEG chain length and surface density) and of the core composition on phagocytic uptake and plasma protein adsorption. *Colloids Surfaces B Biointerfaces*. 2000;18:301–13.
30. Liu Y, Li K, Liu B, Feng S-S. A strategy for precision engineering of nanoparticles of biodegradable copolymers for quantitative control of targeted drug delivery. *Biomaterials*. 2010;31:9145–55.
31. Bazile D, Prud’homme C, Bassoullet MT, Marlard M, Spenlehauer G, Veillard M. Stealth Me.PEG-PLA nanoparticles avoid uptake by the mononuclear phagocytes system. *J. Pharm. Sci.* 1995;84:493–8.
32. Slütter B, Plapied L, Fievez V, Sande MA, des Rieux A, Schneider Y-J, et al. Mechanistic study of the adjuvant effect of biodegradable nanoparticles in mucosal vaccination. *J. Control. Release*. Elsevier B.V.; 2009;138:113–21.
33. Reddy ST, van der Vlies AJ, Simeoni E, Angeli V, Randolph GJ, O’Neil CP, et al. Exploiting lymphatic transport and complement activation in nanoparticle vaccines. *Nat. Biotechnol.* Nature Publishing Group; 2007;25:1159–64.
34. Justyna A. Czaplewska, Tobias C. Majdanski, Markus J. Barthel, Michael Gottschaldt USS. Functionalized PEG-b-PAGE-b-PLGA Triblock Terpolymers as Materials for Nanoparticle Preparation. *J. Polym. Sci. Part A Polym. Chem.* 2015;
35. Müller RH, Rühl D, Lück M, Paulke B-R. Influence of Fluorescent Labelling of Polystyrene Particles on Phagocytic Uptake, Surface Hydrophobicity, and Plasma Protein Adsorption. *Pharm. Res.* Kluwer Academic Publishers-Plenum Publishers; 1997;14:18–24.
36. Mundargi RC, Babu VR, Rangaswamy V, Patel P, Aminabhavi TM. Nano/micro technologies for delivering macromolecular therapeutics using poly(D,L-lactide-co-glycolide) and its derivatives. *J. Control. Release*. 2008;125:193–209.
37. Feczko T, Tóth J, Dósa G, Gyenis J. Optimization of protein encapsulation in PLGA nanoparticles. *Chem. Eng. Process. Process Intensif.* 2011;50:757–65.

38. Cruz LJ, Tacke PJ, Fokkink R, Figdor CG. The influence of PEG chain length and targeting moiety on antibody-mediated delivery of nanoparticle vaccines to human dendritic cells. *Biomaterials*. Elsevier Ltd; 2011;32:6791–803.
39. Buske J, König C, Bassarab S, Lamprecht a, Mühlau S, Wagner KG. Influence of PEG in PEG-PLGA microspheres on particle properties and protein release. *Eur. J. Pharm. Biopharm.* Elsevier B.V.; 2012;81:57–63.
40. Corrigan OI, Li X. Quantifying drug release from PLGA nanoparticulates. *Eur. J. Pharm. Sci.* 2009;37:477–85.
41. Li Y, Pei Y, Zhang X, Gu Z, Zhou Z, Yuan W, et al. PEGylated PLGA nanoparticles as protein carriers: synthesis, preparation and biodistribution in rats. *J. Control. Release*. 2001;71:203–11.
42. Tobío M, Gref R, Sánchez A, Langer R, Alonso MJ. Stealth PLA-PEG Nanoparticles as Protein Carriers for Nasal Administration. *Pharm. Res.* Kluwer Academic Publishers-Plenum Publishers; 1998;15:270–5.
43. Doktorovova S, Shegokar R, Martins-Lopes P, Silva AM, Lopes CM, Müller RH, et al. Modified Rose Bengal assay for surface hydrophobicity evaluation of cationic solid lipid nanoparticles (cSLN). *Eur. J. Pharm. Sci.* 2012;45:606–12.
44. Jeyachandran YL, Mielczarski E, Rai B, Mielczarski J a. Quantitative and qualitative evaluation of adsorption/desorption of bovine serum albumin on hydrophilic and hydrophobic surfaces. *Langmuir*. 2009;25:11614–20.
45. Weert M van de, Hennink WE, Jiskoot W. Protein Instability in Poly(Lactic-co-Glycolic Acid) Microparticles. *Pharm. Res.* Kluwer Academic Publishers-Plenum Publishers; 2000;17:1159–67.
46. Makadia HK, Siegel SJ. Poly Lactic-co-Glycolic Acid (PLGA) as Biodegradable Controlled Drug Delivery Carrier. *Polymers (Basel)*. 2011;3:1377–97.
47. Lu L, Garcia CA, Mikos AG. In vitro degradation of thin poly(DL-lactic-co-glycolic acid) films. *J. Biomed. Mater. Res.* John Wiley & Sons, Inc.; 1999;46:236–44.
48. Lu L, Peter SJ, D. Lyman M, Lai H-L, Leite SM, Tamada JA, et al. In vitro and in vivo degradation of porous poly(DL-lactic-co-glycolic acid) foams. *Biomaterials*. 2000;21:1837–45.
49. De Feijter, J. A., & Benjamins J. Adsorption kinetics of proteins at the air–water interface. *Food Emuls. Foam*. 1987. p. 72–85.
50. Blanco D, Alonso MJ. Protein encapsulation and release from poly(lactide-co-glycolide) microspheres: effect of the protein and polymer properties and of the co-encapsulation of surfactants. *Eur. J. Pharm. Biopharm.* 1998;45:285–94.
51. Baleeiro RB, Rietscher R, Diedrich A, Czaplewska JA, Lehr C-M, Scherließ R, et al. Spatial separation of the processing and MHC class I loading compartments for cross-presentation of the tumor-associated antigen HER2/ neu by human dendritic cells. *Oncoimmunology*. Taylor & Francis; 2015



## **4. Antigen delivery via hydrophilic PEG-*b*-PAGE-*b*-PLGA nanoparticles improves vaccination efficiency**

The author of the thesis made the following contribution to this chapter: Planned, designed and performed experiments related to particle preparation and characterization, release studies, cytotoxicity assays and stability tests, analyzed data from the mentioned studies, interpreted the experimental data and wrote the manuscript.

The in vitro and in vivo mice studies were performed by Matthias Schröder at the University of Bonn. He analyzed data from the mentioned studies and interpreted the experimental data. The author thanks Matthias Schröder for the great collaboration.

The synthesis of the polymers, for the preparation of nanoparticles, was kindly performed by Justyna A. Czaplewska and Tobias Majdanski at Laboratory of Organic and Macromolecular Chemistry (IOMC) and Jena Center for Soft Matter (JCSM) in Jena. The author thanks the IOMC and JCSM for the support.

## 4.1. Introduction

Prophylactic vaccination, a method to activate the immune system with live attenuated or dead pathogens or recombinant protein/peptides, in combination with an adjuvant, is one of the landmark discoveries of the last century. It is based on the generation of a pool of long-lived memory T and B cells that can quickly respond upon re-encounter with the infectious microorganism to mount protective immunity [1]. Vaccination formulations typically consist of an antigen together with an adjuvant to initiate an antigen-specific immune response against the pathogen/protein that leads to generation of immune effector cells but also long-lived memory cells [1]. Essential to the success of vaccination is uptake and appropriate presentation of antigens by antigen-presenting-cells (APC), such as dendritic cells or macrophages. The use of adjuvants, e.g. aluminum hydroxide or Toll-Like-Receptor (TLR) agonists, is necessary to induce an innate immune response that leads to functional maturation of APCs for delivery of co-stimulatory signals that are required for the generation of a memory cell generation [1]. One of the major problems in delivering vaccine formulations via the oral, intravenous, subcutaneous or other routes is the fast degradation and elimination of the delivered antigens. Therefore the use of advanced drug delivery systems (DDSs), like nanoparticles (NPs), liposomes, nano-emulsions and micelles have been studied to protect the antigen from degradation and allow for protracted release [2]. Zhu et al. showed that EUDRAGIT®-coated PLGA-NPs can be used as an oral carrier for a protein-TLR formulation for oral application, that protects the protein from degradation in the gastrointestinal tract and thereby facilitates prophylactic vaccination [3]. For other vaccination routes, e.g. inhalative or nasal, chitosan-coated PLGA-NPs or chitosan-NPs were used successfully as protective carriers for a vaccine DDSs [4–6]. The most often used polymer for such nanoparticulate carriers is poly(D,L-lactide-co-glycolide) (PLGA) due to its biodegradable and biocompatible character, followed by or in combination with, chitosan, poly-ε-caprolactone (PCL), gelatin, alginate and many others [7–11]. PLGAs and their capability to encapsulate hydrophilic proteins, by using the double emulsion solvent evaporation technique, is of high interest despite its hydrophobicity [12–15]. To improve vaccination success, however, the encapsulation and kinetics of antigen release needs to be controlled. In consequence, internalized NPs must release sufficient high antigen concentrations inside the APCs within a short period of time, to allow for optimal antigen presentation [16,17]. Slow release of

antigens in the absence of inflammation over a long period of time, however, leads to failure to induce antigen-specific immunity and immune tolerance [18,19]. One interesting concept to improve the antigen release and the limited antigen loading capability is the linkage of the hydrophilic molecule polyethylene glycol (PEG) to the hydrophobic PLGA, resulting in a PEG-*b*-PLGA copolymer (PP) [20]. The covalent linkage with PEG increases the hydrophilic character of PLGA thus alleviating the capability to load and to release higher amounts of the antigen. Additionally, PEGylation, if used for intravenous application, could lead to further pharmacological and immunological advantages, like reduced renal clearance [21,22] and a protection from innate immune responses [23]. NP uptake and presentation of antigen by APCs is essential for activation of adaptive immunity. Specificity can be increased by targeting using active groups. To introduce such active targeting, a poly(allyl glycidyl ether) (PAGE) group between PEG and PLGA can be implemented resulting in a functionalizable PEG-*b*-PAGE-*b*-PLGA (PPP) copolymer. The PAGE group works as a possible donor for the covalent linkage of functional groups [24–26] for active drug targeting.

Here, we report the synthesis and characterization of PLGA-, PP- and PPP-NPs for their use in vaccination. We investigated the antigen release kinetics and the uptake of NPs in myeloid APCs depending on size, polymer type and concentration. To address the immune response in a mouse model, NPs were loaded with the model protein/antigen ovalbumin (OVA), to assess the ability of such modified NPs to increase antigen presentation and CD8 T cell activation. We analyzed CD69 expression and IL-2 release by CD8 T cells and evaluated the cross-talk with APCs leading to their activation and CD80 expression. We found that PPP-OVA-NPs were superior to PLGA-OVA-NPs or free OVA with respect to antigen-specific T cell activation by antigen-presenting cells. We further evaluated these NPs in an in vivo approach for a prophylactic vaccination against OVA. In the absence of an adjuvant, PPP-OVA-NPs were able to induce a significant specific cytotoxic activity against OVA-loaded target cells. When we used TLR-agonists as adjuvant, antigen-specific cytotoxicity induced by application of free OVA was increased to similar levels as that observed after application of PPP-OVA-NPs without TLR-agonists. Our data suggest that PPP-NPs are a suitable platform for future vaccination formulations as it efficiently delivers antigen to APCs and already contains adjuvant-function.

## 4.2. Materials and methods

### 4.2.1. Materials

PLGA - RESOMER® RG 504 H was supplied by Evonik Industries AG (Darmstadt, Germany) and PEG-*b*-PLGA (PP) and PEG-*b*-PAGE-*b*-PLGA (PPP) were synthesized by the Laboratory of Organic and Macromolecular Chemistry (IOMC) in Jena (Figure 1) following a published procedure [27]. The number average molar mass ( $M_n$ ) was determined by nuclear magnetic resonance and size exclusion chromatography. Phosphate buffered saline (PBS) was prepared by dissolving 10 mM disodium phosphate ( $\text{Na}_2\text{HPO}_4$ , Sigma Aldrich, Taufkirchen, Germany), 1.8 mM monopotassium phosphate ( $\text{KH}_2\text{PO}_4$ , Sigma Aldrich, Taufkirchen, Germany), 2.7 mM potassium chloride (KCl, Sigma Aldrich, Taufkirchen, Germany) and 137 mM sodium chloride (NaCl, Sigma Aldrich, Taufkirchen, Germany) in water. For all preparations and investigations water generated with Millipore Q-Gard 2 (Merck Millipore, Billerica, United States) was used and all other chemicals utilized were of analytical grade.

Polymer	Polymer Type	Lactic-to-glycolic acid ratio	PEG [Da]	PAGE [Da]	PLGA [Da]	Total weight [Da]	PEG : PLGA ratio [%]
I. PLGA	Monoblock	50:50	-	-	38 800	38 800	-
II. PP	Diblock	50:50	3 200	-	46 700	49 900	1 : 14.5
III. PPP	Triblock	50:50	2 900	1 000	49 050	52 950	1 : 17

I.

II.

III.

**Figure 1 | Illustration and composition of PLGA, PP and PPP polymer;** with x = lactic acid, y = glycolic acid, m = polyethylene glycol, n = poly(allyl glycidyl ether), R = methyl- or biphenyl group; PLGA is a block-co-polymer considered as one block for simplicity.

### 4.2.2. Fluoresceineamine labeling of PLGA

Fluoresceineamine (FA) labeled PLGA polymer (FA-PLGA) was prepared according to the literature [28,29]. Briefly, 0.35 mM PLGA, 0.7 mM FA, isomer I (Sigma Aldrich, Taufkirchen, Germany) and 1.4 mM 4-Dimethylaminopyridine (Sigma Aldrich, Taufkirchen, Germany), as nucleophilic catalyst, were dissolved in acetonitrile (Sigma Aldrich, Taufkirchen, Germany) and stirred for 24 h overnight, at room temperature protected from light. The resulting

polymer was precipitated with equal amounts of water compared to acetonitrile and separated by centrifugation at 5,000 g (Rotina 420 R, Hettich Lab Technology, Tuttlingen, Germany) for 40 min. The supernatant was discarded and the polymer was solved in acetone (Sigma Aldrich) and precipitated again with pure ethanol (Sigma Aldrich, Taufkirchen, Germany). This procedure was repeated three times to get rid of excessive reagents and finally lyophilized (Alpha 2-4 LSC, Christ GmbH, Osterrode, Germany).

#### **4.2.3. Preparation of NPs**

Plain and OVA-loaded (Grade V, purity  $\geq 98\%$ , MW = 44 kDa) NPs were prepared, using a double emulsion solvent evaporation technique. The polymer was dissolved in dichloromethane (DCM, 2.5 mL, 20 mg/mL) and emulsified at room temperature (RT) with PBS pH 7.4 solution or OVA in PBS pH 7.4 (0.5 mL, 20 mg/mL) by sonication with 35% amplitude (energy introduced 280 J, Branson digital sonifier 250, Danbury, United States). Afterwards an aqueous polyvinyl alcohol solution (PVA, 5 mL, 20 mg/mL, Mowiol® 4-88, Mn  $\sim 31\,000$  Da, Kuraray Europe GmbH, Hattersheim, Germany) was added to the first emulsion and sonicated at RT with 35% amplitude (energy introduced 595 J), to obtain the double emulsion. The resulting emulsion was diluted by the addition of water, and stirred for 3 h at 1,000 rpm at RT, to evaporate DCM. Finally, the NPs were washed twice with water after centrifugation at 15,000 g for 11 min. After the second washing step trehalose (ratio NP:trehalose 2:1 (w/w)(Sigma Aldrich, Taufkirchen, Germany) and 0.3% PVA were added as cryoprotectants and stabilizer for the subsequent lyophilization process.

NPs with different sizes and fluorescent dyes were prepared as following (Tab. 1): For 6-coumarin loaded PPP-NPs using the double emulsion evaporation method, 50  $\mu\text{g}$  of 6-coumarin was added to different amounts of polymer, dissolved in DCM (2.5 mL, 20-40 mg/mL) and emulsified at RT with a PVA solution (5 mL, 1-20 mg/mL) by sonication, to obtain the final emulsion. Besides the polymer concentration, different times (20-60 s) and amplitudes (15-40%) were used to generate NPs covering a relevant size range.

**Table 1 | Preparation of NPs with different sizes using PLGA and PPP polymer.** (a) PPP-NPs loaded with 6-coumarin using the double emulsion evaporation method. (b) FA-PLGA-NPs using double emulsion evaporation method. (c) FA-PLGA-NPs using nanoprecipitation method. Data in the table represent mean  $\pm$  SD (n=1).

(a) Nanoparticle and preparation method	Time [s]	Amplitude [%]	Polymer [mg]	PVA [%]	Size [nm]	PDI
6-coumarin loaded PPP-NPs Double emulsion evaporation method	30	30	50	2	184.1 $\pm$ 0.7	0.07 $\pm$ 0.01
	30	15	100	2	243.6 $\pm$ 1.4	0.09 $\pm$ 0.01
	60	40	50	2	277.4 $\pm$ 4.7	0.21 $\pm$ 0.01
	30	15	100	1	315.1 $\pm$ 2.7	0.14 $\pm$ 0.05
	20	20	100	0.5	385.8 $\pm$ 7.6	0.27 $\pm$ 0.01
(b) Nanoparticle and preparation method	Time [min]	Rotation [rpm]	Polymer [mg]	PVA [%]	Size [nm]	PDI
FA-PLGA-NPs Double emulsion evaporation method	15	15,000	100	4	200.2 $\pm$ 6.4	0.03 $\pm$ 0.01
	15	10,000	100	0.4	250.1 $\pm$ 3.9	0.13 $\pm$ 0.02
	10	8,000	100	2	341.6 $\pm$ 5.4	0.17 $\pm$ 0.01
	20	6,000	100	1	426.0 $\pm$ 8.7	0.19 $\pm$ 0.02
(c) Nanoparticle and preparation method	Time [min]	Stirring speed [rpm]	Polymer [mg]	PVA [%]	Size [nm]	PDI
FA-PLGA-NPs Nanoprecipitation method	5	1,400	100	1.25	99.6 $\pm$ 4.5	0.06 $\pm$ 0.01
	5	1,000	100	2	130.4 $\pm$ 3.4	0.06 $\pm$ 0.01

For FA-PLGA-NPs and double emulsion evaporation method, a high shear homogenizer was used to form the NPs. Briefly, the polymer was dissolved in ethyl acetate (2.5 mL, 20 mg/mL) and emulsified at RT with a PVA solution (5 mL, 5-20 mg/mL) by a high shear homogenizer (POLYTRON® PT 2500 E with a PT-DA 20/2 EC-E170 attachment), to obtain the final emulsion. Various homogenization times (10-20 min) and speeds (6-15k rpm) were used to generate NPs with different sizes. To produce smaller FA-PLGA-NPs nanoprecipitation was applied. The polymer was dissolved in acetone (2.5 mL, 40 mg/mL). The polymeric solution was then slowly injected (5 min) via a syringe into a PVA solution (10 mL, 10.25 and 20 mg/mL) (w/v) and the resulting dispersion was stirred at 1,000 or 1,400 rpm. The resulting NPs were washed and dialyzed (molecular weight cut-off 300,000 Da, Dialysis membrane Spectra/Por®, Roth, Karlsruhe, Germany) three times for 2 h in water, to remove residual amounts of acetone and PVA. The NP suspension was concentrated with Vivaspin® 20 mL centrifugal concentrators (molecular weight cut-off 300,000 Da, Sartorius, City, Country) at 5,000 g for 5 min and resuspended in water. After washing, trehalose was added as a cryoprotectant, for the subsequent lyophilization process.

#### 4.2.4. Characterization of NPs

The average size (in nm), size distribution (polydispersity index - PDI) and  $\zeta$ -potential (in mV) of the NPs was determined at 25 °C, using dynamic light scattering (DLS) and laser Doppler anemometry (Zetasizer Nano ZSP, Malvern Instruments, Herrenberg, Germany). The measurements were performed with an aqueous dispersion of NPs (~ 0.1 mg/mL) after lyophilization. The morphology of the NPs was determined by scanning electron microscopy (SEM - Zeiss EVO HD15, Jena, Germany). The NPs were first covered with a ~10 nm gold layer under vacuum and then scanned by SEM (accelerating voltage 5 kV, focal distance 10 mm). To determine OVA-loading (% L = encapsulated OVA [mg]/ weight prepared NPs [mg]  $\times$  100) and –encapsulation efficiency (% EE = encapsulated OVA [mg]/ initial drug in formulation [mg]  $\times$  100) inside the NPs we used a bicinchoninic acid protein (BCA) assay kit (QuantiPro™ BCA Assay Kit for 0.5-30  $\mu$ g/mL protein), according to the manufacturer's instructions in 96 micro-well plates. In detail, the lyophilized NPs were dissolved and incubated overnight at RT in 1 M NaOH solution (10 mL, 1 mg/mL). After the incubation, the solution was neutralized with 1 M HCl and the antigen concentration, with the BCA assay solution was determined using the Tecan Infinite M200 Pro (Männedorf, Switzerland) plate reader at  $\lambda$  = 562 nm. As a control unloaded NPs were used and analyzed in triplicate. To determine what percentage of NP-loaded OVA is still in native form, OVA-loaded NPs were stirred at 150 rpm during incubation for 24 h in PBS buffer (1 mg/mL, pH 7.4 at 37 °C). After centrifugation at 20,000 g for 15 min the total amount of protein in the supernatant, containing native OVA and unfolded, degraded parts of OVA, was determined using the BCA Assay Kit. The amount of native OVA that was released from the NPs was quantified using an OVA-specific ELISA that does not detect unfolded, degraded OVA (Serazym® Ovalbumin ELISA, Seramun Diagnostica GmbH, Heidesee, Germany). The percentage of native OVA was then calculated (% native OVA = (amount of native OVA [mg]/ total amount of protein in the supernatant [mg])  $\times$  100). Supernatant from unloaded NPs and freshly prepared OVA solution in PBS were used as negative and positive control respectively.

#### **4.2.5. In vitro release of antigen**

The lyophilized NPs were incubated with 100 mM PBS buffer (1 mg/mL, pH 7.4) in glass vials, over 7 days stirred at 150 rpm. The samples were collected at appropriate time intervals (1 h, 2 h, 4 h, 8 h, 1 d, 3 d, 5 d, 7 d, respectively) after centrifugation at 20,000 g for 15 min. To analyze the amount of OVA released from the NPs the clear supernatant was used for the BCA Assay and analyzed in triplicate.

#### **4.2.6. Determination of endotoxin concentrations**

The Pierce LAL Chromogenic Endotoxin Quantitation Kit (sensitivity range 0.1-50.0 EU/mL) was used to determine endotoxin concentrations. Pure polymer, pure OVA, as well as plain and OVA NPs (20 mg/mL) were dissolved or suspended in endotoxin free water, to release the endotoxins in water. The sample pH was set to pH 7 and incubated at 37 °C for 4 h. After incubation the solutions or suspensions were centrifuged at 15,000 g for 11 min and the clear endotoxin containing supernatant was used for the further assay. Four endotoxin standard concentrations (0.1-1 EU/mL) were prepared to create a corresponding calibration curve. The test was performed according to the manufacturer's instructions. Briefly, 50 µL of standard or sample and 50 µL of limulus amoebocyte lysate (LAL) was added to each 96-well plate and incubated at 37 °C for 10 min. After 10 min 100 µL of substrate was added to each well and incubated at 37 °C for 6 min. 10 s after adding 50 µL of stop reagent (25% acetic acid) the absorbance at 405 nm was measured using the Tecan Infinite M200 Pro.

#### **4.2.7. Cytotoxicity assay for NPs**

The cytotoxicity of plain and loaded NPs was evaluated using an MTT assay. Caco-2 cells (stem C2Bbe1, passage 66) were cultured in Dulbecco's Modified Eagle Medium (DMEM) supplemented with 10% fetal calf serum (FCS) and 1% non-essential amino acids (NEAA) with 5% CO<sub>2</sub> at 37 °C. Caco-2 cells were seeded in a 96-well plate in 200 µL medium per well at a density of 1 × 10<sup>4</sup> cells/well for 4 days. After removing the supernatant the cells were washed twice in HBSS buffer and then cultivated with 200 µL of medium-containing NPs of different concentrations (0.01, 0.1, 0.5 and 1.0 mg/mL) for 4 h in triplicate. Hank's Balanced Salt Solution (HBSS) or HBSS + 1% Triton X was used as negative or positive



control respectively. The 96-well plate was then incubated at 37 °C for 4 h. After removing the NPs-containing media the cells were washed twice with HBSS buffer and cultivated in 100 µL HBSS buffer with 10 µL MTT solution (5 mg/mL) for additional 4 h at 37 °C. Finally the cells were washed with HBSS and lysed with 100 µL DMSO for 15 min at 37 °C. MTT absorbance was measured at 550 nm using the Tecan Infinite M200Pro.

#### **4.2.8. Stability of NP formulations in different media**

The resulting freeze-dried, antigen-loaded NPs were incubated in different media used for in vitro and in vivo evaluation. Plain and loaded NPs were dispersed in water pH 7.4, PBS pH 7.4, HBSS pH 7.4, DMEM - FCS, and incubated at 25 °C for 7 days. The size and zeta-potential of the NPs were measured to evaluate the tendency of the NPs to aggregate in the respective media.

#### **4.2.9. Mice**

C57BL/6J and OTI transgenic mice, bearing a T cell receptor recognizing the OVA-derived peptide SIINFEKL in the context of the murine MHC I molecule H2Kb, were maintained under specific pathogen-free conditions in the animal facility of the University of Bonn. All animal experiments were done in accordance with German legislation governing animal studies (reference number: 84-02.04.2013.A265) and the Principles of Laboratory Animal Care guidelines (US National Institutes of Health publication 85-23, 1996 revision).

#### **4.2.10. Isolation and Differentiation of myeloid antigen presenting cells**

Myeloid antigen presenting cells (mAPC) used in this study have all been generated from bone marrow of C57BL/6J mice. The bone marrow isolation protocol was performed as published previously [30]. Briefly, bone marrow cells were isolated from the hind legs of the mice and cultured in Roswell Park Memorial Institute medium (RPMI) medium supplemented with 10% FCS, 100 IU/mL penicillin, 100 µg/mL streptomycin, 50 µM β-mercaptoethanol and either 100 nM macrophage colony-stimulating factor (M-CSF), for differentiation, in a humidified incubator (5% CO<sub>2</sub> and 37 °C) at a cell concentration of  $0.8 \times 10^6$  cells/mL in an untreated petri dish. For differentiation of bone-marrow derived APCs we used supernatant of the M-CSF-producing cell line R1. After four days, the cells

were split 1:2 on additional petri dishes and cultivated for additional three days with freshly added culture medium and growth factors. At day 7 the adherent cells were used for our in vitro experiments, fluorescence-activated cell sorting (FACS) analysis and microscopic experiments.

#### **4.2.11. Isolation of CD8<sup>+</sup> cells (CTLs)**

Naive CD8 $\alpha$ <sup>+</sup> T cells were isolated from spleen of OTI mice and purified by autoMACS (Miltenyi Biotec). After counting the cells they were directly used for in vitro co-culture with myeloid antigen presenting cells.

#### **4.2.12. Flow cytometry**

Antibody staining was done in presence of Fc receptor blockade (monoclonal antibody 2.4G2 to mouse CD16/CD32 (10  $\mu$ g/mL); prepared in-house) in flow cytometry buffer. Hoechst 33258 (10  $\mu$ g/mL; Sigma-Aldrich) was used for exclusion of dead cells. Antibodies used for flow cytometry were as follows (all from eBioscience unless indicated otherwise): phycoerythrin (PE)-conjugated anti-CD69 (H1.2F3), allophycocyanin (APC)-conjugated anti-CD80 (16-10A1). A FACSCanto II or Fortessa (BD Biosciences) and FlowJo software (TreeStar) were used for acquisition and data analysis.

#### **4.2.13. NP-uptake studies**

For the NP-uptake studies we used  $5 \times 10^4$  myeloid antigen presenting cells seeded in a 96-well cell-culture-treated plate in a volume of 100  $\mu$ L (DMEM, 10% FCS, 100 IU/mL penicillin, 100  $\mu$ g/mL streptomycin). We then added 1 mg/mL labelled or non-labelled PLGA- or PPP-NPs of different sizes for 24 h in 100  $\mu$ L cell culture medium. After the incubation phase the cells were scraped, washed twice with phosphate buffered saline (PBS) and prepared for flow cytometry.

#### **4.2.14. Evaluation of ovalbumin-NPs**

For the in vitro evaluation of OVA-loaded NPs we used  $5 \times 10^4$  myeloid APC in a cell-culture-treated 96-well plate in a volume of 100  $\mu$ L (DMEM, 10% FCS, 100 IU/mL penicillin, 100  $\mu$ g/mL streptomycin). We then added  $1 \times 10^5$  freshly isolated CD8 $\alpha$ <sup>+</sup> OTI T cells in 50  $\mu$ L medium and OVA-loaded NPs (PLGA or PPP polymer) or free, unloaded OVA of the

same concentration in 50  $\mu$ L medium. After 24 h we isolated the supernatant, which was stored at -20 °C for subsequent ELISA measurements, and used the remaining cells for flow cytometry analysis.

#### 4.2.15. In vivo experiments

C57BL/6J mice were immunized subcutaneously in the back with 150  $\mu$ L PBS or 150  $\mu$ L PBS containing 75  $\mu$ g OVA, 75  $\mu$ g OVA with soluble 100  $\mu$ g ODN CpG1826 or 100  $\mu$ g Cholera Toxin Subunit B (CTB), PLGA-OVA-NPs, PPP-OVA-NPs or PPP-OVA-NPs with soluble 100  $\mu$ g ODN CpG1826 or 100  $\mu$ g CTB (all NPs formulations contained equal amounts of 75  $\mu$ g OVA) at day 0 and boosted at day 7. At day 13 we isolated splenocytes to prepare them as target cells. The splenocytes either got incubated with PBS or 1  $\mu$ M SIINFEKL peptide in PBS for 15 min at 37 °C to produce unspecific and specific target cells. To identify these two populations after transfer into the mice we incubated them with 0.25  $\mu$ M carboxyfluorescein succinimidyl ester (CFSE) (low) or 2.5  $\mu$ M CFSE (high) respectively for 15 min at 37 °C. After vigorous washing of the cells, unspecific and specific target cells were mixed 1:1 and injected in 150  $\mu$ L PBS intravenously (iv) in the tail vein of the mice ( $1 \times 10^7$ ). After 4 h or 24 h the spleen of the mice were isolated and prepared for FACS analysis. The ratio of recovered CFSE low and high iv injected splenocytes was analyzed. Specific cytotoxicity was measured using the FACS data and the following formula:

$$\% \text{ specific kill} = 100 - \{(\text{ratio}(\text{high}/\text{low}) \text{ sample} / \text{ratio}(\text{high}/\text{low}) \text{ control group}) \times 100\}.$$

#### 4.2.16. Statistical analysis

Statistical analysis of loading and encapsulation efficiencies were performed via one way analysis of variance (ANOVA) followed by Tukey's multiple comparisons test using GraphPad Prism 6 software (GraphPad Software, Inc, La Jolla, CA). The confidence interval was set at 95%, a p-value of > 0.05 was accepted as not significant (n.s.) and a p-value of < 0.05 was accepted as significant (\*);  $p < 0.01$  (\*\*),  $p < 0.001$  (\*\*\*)

### 4.3. Results and discussion

The aim of this study was to synthesize and to evaluate different PLGA-based NPs in vitro as well as in vivo for their potential use as vaccine carriers. The same PLGA (Mn of 40-50 kDa) backbone structure was used for all synthesized copolymers. First, PEG (Mn of ~3 kDa) was covalently linked to yield PP, as already published elsewhere [20]. Secondly, as a new functionality, an additional PAGE group (Mn of 1 kDa) was inserted between the PEG and the PLGA group, yielding PPP as a polymer. We thus could use three different polymers for NP formation, i.e. PLGA, PP, and PPP. To evaluate the proof of principle of using those NP formulations for vaccination we used the model antigen ovalbumin, as several in vitro and in vivo systems are established to investigate NP-uptake, antigen-processing, -presentation and T cell activation, which are the most important aspects that we wanted to address.

#### 4.3.1. Characterization of antigen-loaded NPs

Independent of the polymer, the manufactured NPs prepared by the double emulsion evaporation technique, had a narrow size distribution ( $PDI < 0.15$ ) and the mean sizes of blank particles were in the range of 170 nm to 200 nm (Figure 2). OVA-loaded particles were approximately 10-20 nm larger, due to the influence of the encapsulated protein (hydrodynamic diameter of OVA = 2-3 nm). All types of PLGA form particles with a negative surface charge. The incorporation of OVA in the NPs leads to a higher surface charge of  $-20.4 \pm 3.5$  mV compared to blank NPs with  $-28.7 \pm 2.9$  mV. The higher surface charge of the OVA loaded NPs is related to the absorbed and released OVA during zeta-potential measurement. An significant increase of surface charge by addition of the PEGylation as described in literature [31,32] was not observed for PEGylated PLGA-NPs. This might be due to the use of PVA, which was used in the primary emulsion, and final formulation, as a stabilizer, to prevent particle aggregation. PVA is coating the surface of the NPs and consequently unifying the surface charge. Ultrastructural analysis revealed that all three PLGA-based NPs formulations generated smooth and spherical particles (Figure 2). The antigen loading capacity of PLGA-OVA-NPs was maximal at  $7.8 \pm 0.6\%$ . The covalent linkage of PEG increased this capacity to  $9.2 \pm 0.6\%$  and the insertion of a PAGE group between the aforementioned PEG and PLGA groups further increased the antigen loading capacity by 0.8% to a total of  $10.0 \pm 0.6\%$  compared with PLGA-OVA-NPs (+2.2%).

Name	Size [nm]	PDI	Zeta potential [mV]	Loading [%]	Encapsulation efficiency [%]	Activity [%]
Blank PLGA NPs	201.3 ± 1.7	0.05 ± 0.01	-29.2 ± 0.5	-	-	-
OVA-loaded PLGA NPs	218.3 ± 3.9	0.10 ± 0.02	-24.7 ± 1.4	7.8 ± 0.6	39.0 ± 3.0	58.0 ± 9.2
Blank PP NPs	168.1 ± 1.1	0.10 ± 0.01	-32.5 ± 0.8	-	-	-
OVA-loaded PP NPs	187.7 ± 1.5	0.11 ± 0.02	-20.7 ± 1.6	9.2 ± 0.6	46.0 ± 3.0	66.0 ± 3.0
Blank PPP NPs	187.7 ± 1.6	0.05 ± 0.03	-24.7 ± 0.3	-	-	-
OVA-loaded PPP NPs	196.5 ± 3.8	0.10 ± 0.01	-16.0 ± 1.2	10.0 ± 0.6	50.0 ± 3.0	74.1 ± 11.4

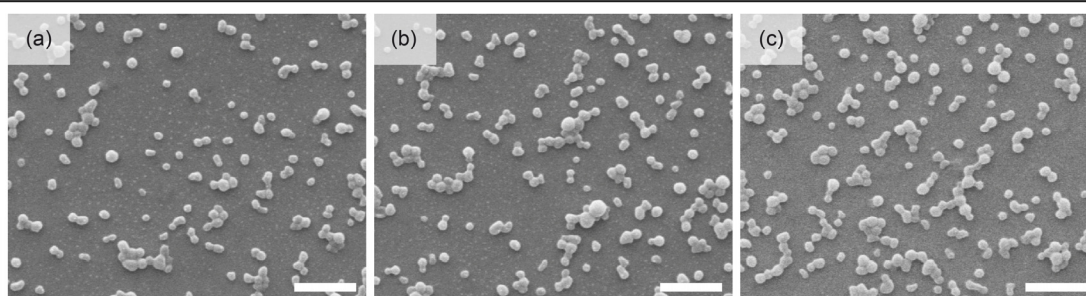


**Figure 2 | Characteristics of blank and OVA-loaded NPs using PLGA, PP and PPP polymer.** Data in the table represent mean ± SD (n=6); SEM images of OVA-loaded a) PLGA-NPs, b) PP-NPs and c) PPP-NPs from 3 independent replicates. Size of the scale bar = 1000 nm.

As indicated in the introduction the amount of antigen that reaches the cytosol is important for the triggered immune response. Although the mechanism by which PLGA-based NP do reach the cytosol to release its payload is not 100% elucidated, several experiments with fluorescently labeled PLGA-NP were performed already, showing that the NP do reach the cytosol. Labhasetwar et al. [33] postulated a mechanism that is based on surface charge as PLGA-NP, usually with a negative zeta-potential, become positively charged in the acidic environment of the endolysosomes (pH ~4) which in turn might trigger the escape mechanism that is known for cationic polymers. Altschuler et al. [34] show similar endosomal escape properties for PEGylated PLGA NPs, indicating that the delivery of antigen to the cytosol is very likely taking place in our case, although we did not investigate this topic. Assuming that the target cells do not differentiate between PLGA- or PPP-NPs of the same size and take up the same amount of NPs per min, the increase of the antigen load by 28% (PLGA- vs. PPP-NPs) already indicates that this may enhance antigen-specific immunity. For a successful vaccination the stability of the secondary/tertiary/quaternary protein structure is not essential as only a short peptide sequence is generated via proteasomal processing for loading on MHC class I within the endoplasmic reticulum (e.g. the OVA-derived peptide SIINFEKL and the MHC class I molecule H2Kb). Nevertheless, as the process of the NP formation could also be transferred for loading of more sensitive antigens or cancer drugs that need to be in a native, folded form, we

investigated the percentage of native OVA released from NPs in PBS (activity of OVA). In principle the antigen should be protected from cleavage or aggregation, when encapsulated and protected from external influences. The OVA-activity was determined to be 58% for PLGA-OVA-NPs, 66% for PP-OVA-NPs and 74% for PPP-OVA-NPs, in comparison to 98% for the pure, solved OVA in PBS. For all types of NPs, the embedding of the antigen and therefore the protection from external environmental influences is similar. It is known, that PLGA itself interacts with surface tension-active antigens like OVA, an interaction that could lead to more compact particles and may induce unwanted folding of the antigen [35]. An explanation for the slightly higher activity of PP-OVA-NPs could be the properties of the PEG group, as the addition of PEG as an additional surface active molecule in PEGylated PLGA polymer is reducing the interaction of PLGA polymer with OVA. The addition of the PAGE group shows another slight increase of activity. This can be explained by the additional hydrophilic properties of the PAGE group and the subsequently higher hydrophilic character of the polymer, making it more suitable for encapsulating hydrophilic drugs.

#### **4.3.2. OVA release from antigen-loaded NPs**

One of the most important factors for vaccination and drug delivery applications, besides the loading and activity, is the release of antigen. The kinetics of the release of the encapsulated antigen, as well as the time until a certain amount of antigen is released, is a very important aspect that needs to be addressed before using these NPs in biological in vitro assays. Thus we investigated the total amount of OVA that is released over time for the three different polymer NPs. In vitro release studies were performed in PBS with pH 7.4, to visualize a differentiation between the different polymers. When the pH of the solvent reaches the isoelectric point of OVA, which is 4.5 in water [36], the solubility decreases significantly and an unfavorable and uncontrolled release behavior occurs. Therefore release studies at lower pH, mimicking the lower pH values (pH 4.5-5.5) of endosomal/lysosomal conditions [37] were not conclusive, due to the low isoelectric point of OVA. Release kinetics are depicted as absolute amount of the ultimately released antigen (Figure 3a) and as a relative release (Figure 3b), normalized to the loading efficiencies described before. Antigen release from biodegradable PLGA polymers occurred in two phases: first, the initial burst release of antigen, which is located at or near

to the surface of the NPs ( $\leq 8$  h), and secondly the sustained and slow release of antigen from the NPs polymer matrix. For the subsequent vaccination studies the antigen release of the first hour is rather unimportant because it occurs already during reconstitution, dilution and application of the NPs in vitro and in vivo. In consequence, the release curves are corrected by subtracting the antigen amount released within the first hour. A corrected total release of 392  $\mu\text{g}$  (4.6%), 610  $\mu\text{g}$  (6.6%) and 1032  $\mu\text{g}$  (10.3%) was observed for PLGA-, PP- and PPP-OVA-NPs over 167 h respectively (Figure 3). Assuming that APCs like macrophages and dendritic cells take up NPs at the site of injection and then migrate to secondary lymphoid tissue for presentation of the antigen to CD8 T cells, it is unlikely that remaining unreleased antigen will be a problem. APCs migrating to secondary lymphoid tissues after uptake of NPs in the periphery typically have a short half-life [38]. Our data reveal an increased release of 150% for PP-OVA-NPs and 250% for PPP-OVA-NPs, compared to PLGA-OVA-NPs. This behavior can also be observed during the burst release time ( $\sim 8$  h). The PEGylated PLGA-NPs did not only release more of the antigen but did so it much faster. This might be attributed to the PEGylation reducing the attractive interaction between OVA and PLGA polymer. Both, the higher burst release and the accelerated sustained release of PEG-modified PLGA-NPs may be explained by such a reduced interaction [39]. Focusing on the PPP polymer, the properties of PEG alone cannot explain the significant increased sustained/burst release, which indicates that the insertion of the PAGE group is essential for this result. How the PAGE group is influencing the more pronounced encapsulation efficiency and significant higher release of the antigen, however, is still unclear and needs further investigation. In conclusion the PPP-OVA-NP formulation shows the highest loading capacity in combination with the fastest cargo-antigen release, compared to PLGA- and PP-OVA-NPs. Regarding biological experiments we focused only on PPP-OVA-NPs due to the superiority of the NP formulation from this polymer in loading, encapsulation efficiency, and release of OVA compared with the PP-OVA-NPs. PLGA-OVA-NPs were considered as reference.

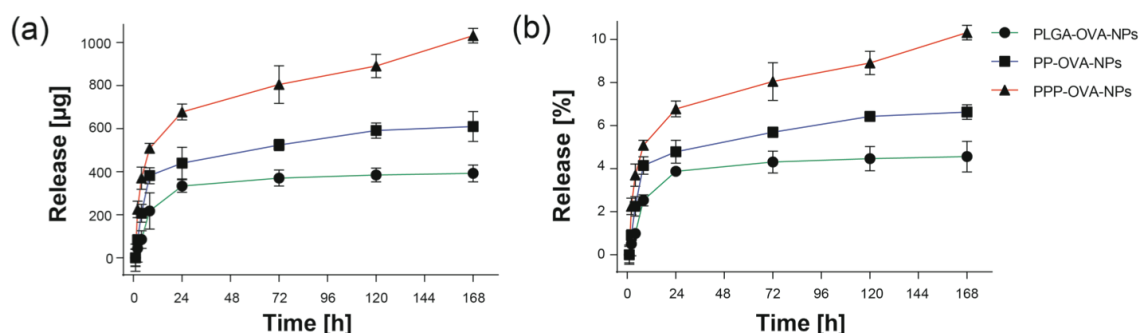


**Figure 3 | OVA release from OVA-loaded PLGA-, PP- and PPP-NPs.** PLGA-, PP- and PPP-NPs were incubated in PBS pH 7.4 for 0-168 h and the released protein content was determined with a BCA assay; the amount of release (% or μg) within the first hour were subtracted from the other time points (308 mg/3.6% for PLGA-OVA-NPs, 476 mg/5.2% for PP-OVA-NPs and 770 mg/7.7% for PPP-OVA-NPs). (a) Release of OVA in microgram, normalized to 100 mg polymer. (b) Release of OVA in percent, independent from loading; mean ± SD is shown for 3 independent replicates.

### 4.3.3. Endotoxin levels, cytotoxicity and stability of the formulations

An important factor for the use of NPs in immunological settings is the evaluation of the polymer and NP formulations regarding endotoxin levels, direct cellular toxicity and its stability in different media. The maximal endotoxin dose of pharmaceutical products should not exceed 5 EU/kg of body weight for intravenous applications [40], to avoid undefined immune responses and erroneously positive results. For the ex vivo/in vivo studies the polymers PLGA and PPP, OVA, PVA and the loaded and unloaded NPs were shown to be free of endotoxin within the aforementioned limits (Figure 4a).

To test any direct toxicity of the NP-formulations we incubated Caco-2 cells with different NP concentrations and assessed the cell viability with a MTT assay. In a concentration range from 0.001 to 1 mg/mL plain or antigen loaded PLGA-/PPP-NPs showed no detectable toxicity (Figure 4b). Additionally the NP formulations were incubated for 7 days in different dispersion media or buffers to study the stability of the final NP formulation. Within 7 days in medium (water pH 7.4, PBS pH 7.4, HBSS pH 7.4, DMEM) no or only a slight increase of size was observed (Figure 4c). The size of the NPs did not increase significantly for all tested experimental settings. Neither the medium used for redispersing the NPs nor the time NPs remained in medium significantly influenced the size of the NPs. For buffers without FCS the size of NPs increased to 400 nm, which was still acceptable for further experiments.



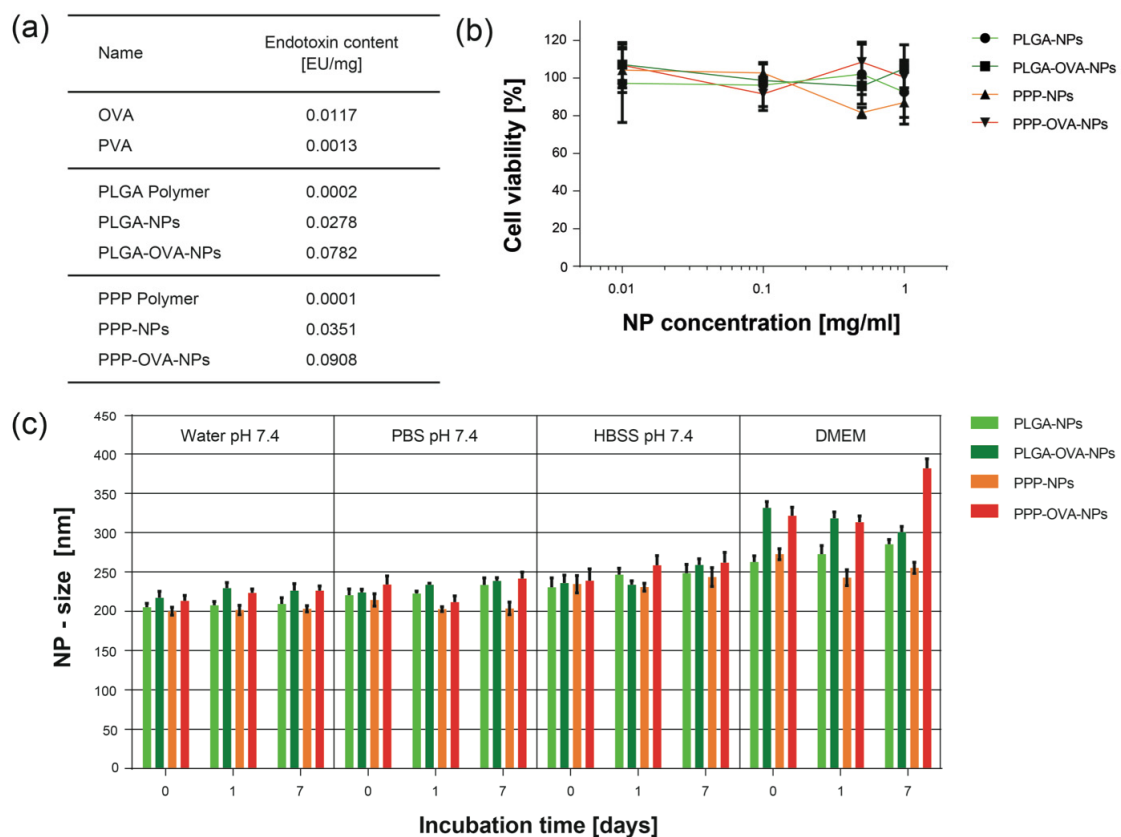


**Figure 4 | NP evaluation for blank and OVA-loaded PLGA- and PPP-NPs.** (a) Endotoxin content of raw/starting material and final formulations, data represent mean values of 3 replicates. (b) Caco-2 cells incubated with different NP-formulations. Cell viability was determined with MTT assay and represent mean  $\pm$  SD (n=3). (c) NP formulations incubated in different media for 0-7 days; the bars represent mean  $\pm$  SD (n=3).

#### 4.3.4. Determination of a size-uptake relationship in APCs for NPs

After showing that NPs can be loaded with protein, release protein in significant amounts and absence of toxicity, we next addressed, if NPs were taken up in vitro by myeloid APCs. Using NPs to deliver antigens, the efficiency of uptake into DCs can be significantly increased up to 30-fold increase in uptake compared with soluble antigen alone [41,42]. This uptake is essential for APCs to process OVA and present SIINFEKL, the peptide cleaved from the protein OVA, to CD8 T cells in vitro and in vivo [1,43]. The amount of antigen presented in the context of MHC I molecules, as well as the amount of co-stimulatory molecules expressed on the APC determine the level of activation of CD8 T cells. To investigate which NP size is taken up most efficiently, as this is supposed to directly correlate with increased antigen presentation and subsequent T cell activation, we co-incubated APCs with fluorescent PPP-NPs of different sizes for 2 h and 24 h and analyzed the mean fluorescence intensity (MFI) of the population as an indicator for the amount of

NPs taken up. We chose NP sizes between 100 nm and 426 nm, because synthesis of NPs below 100 nm is not feasible and above 500 nm the mean diameter of the NPs varies too much with  $\pm 200$  nm. Figure 5a/b shows the data for the 24 h incubation experiments for PLGA- and PPP-NPs and two different concentrations. The uptake pattern for the 2 h incubation looked similar but with lower mean uptake levels and was therefore not included in the figure. None of the NPs tested influenced cell viability of the myeloid APCs (based on Hoechst 33258 viability staining in flow cytometry, data not shown). To exclude a polymer-specific effect on the uptake process we compared the PPP-NP uptake pattern with fluorescently labeled PLGA-NPs. FA was covalently linked to PLGA, whereas 6-coumarin was encapsulated into PPP-NP. The 6-coumarin loading in PPP-NPs was necessary, because a linkage of FA to the PPP polymer was not possible. For 0.1 mg/mL With NPs with sizes between 100-180 nm we observed a slightly increased uptake reaching maximal uptake with NPs ranging between 250-390 nm for PLGA- as well as PPP-NPs. NPs of this size showed 7-11-fold more uptake compared to smaller (<240 nm) or bigger (426 nm) NPC sizes (Figure 5c). Notably uptake further decreased with PLGA-NPs of 426 nm in size, indicating that the NP uptake efficiency was reduced when the size is increased above 400 nm. When the concentration of NPs applied to APCs was increased 10-fold the uptake increased significantly but the preferential uptake of 250-390 nm sized NP remained (Figure 5c). Our results indicate that the efficiency of uptake of NPs in APCs is size-dependent and polymer/concentration independent with an optimal range between 250-400 nm, which is in agreement with recent publications [44]. For all following experiments we therefore used NPs of  $250 \pm 30$  nm in diameter.

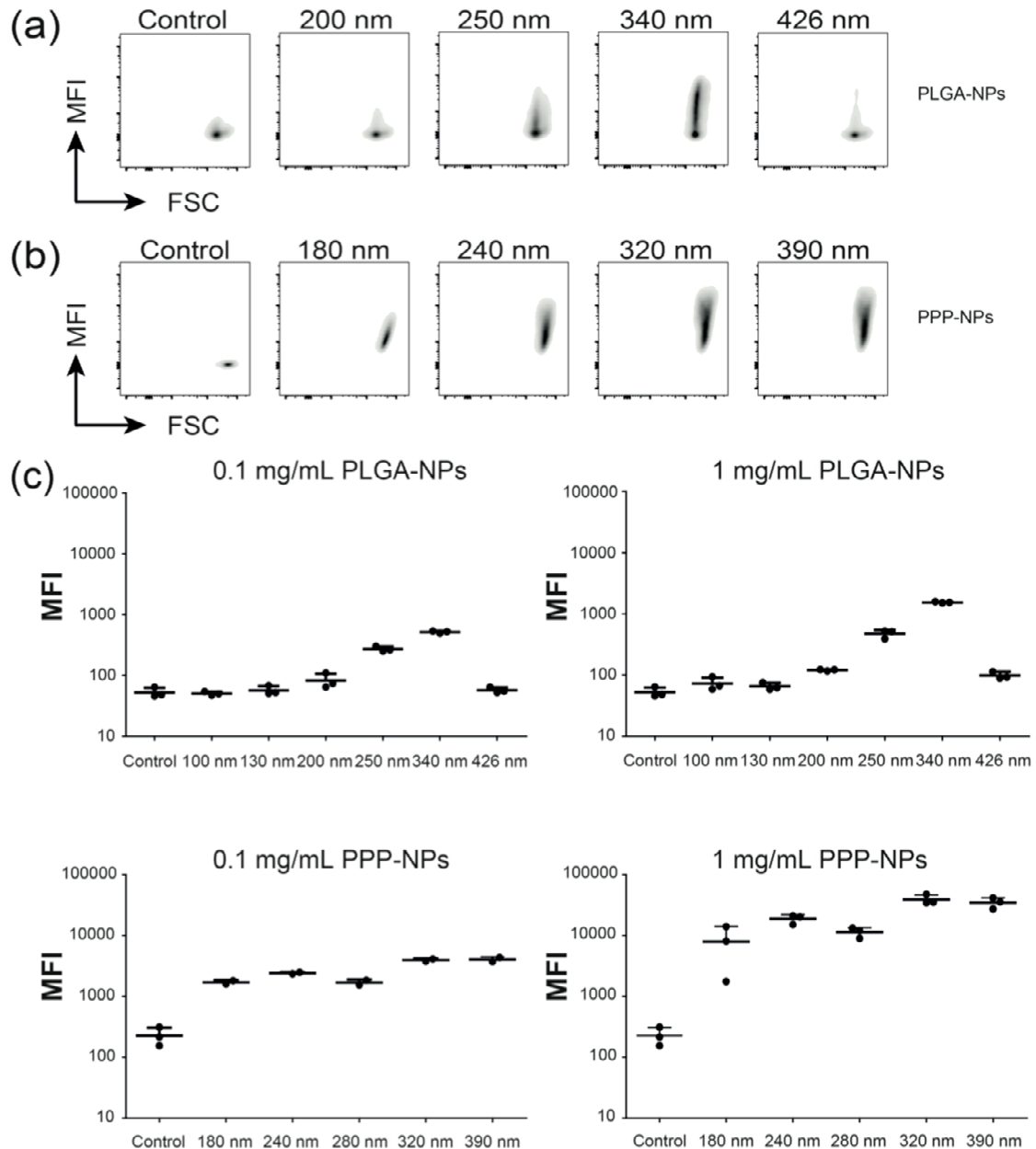


**Figure 5 | NP uptake is size and concentration dependent.** APCs were incubated for 24 h with 0.1 mg/mL or 1 mg/mL FA-labeled or 6-coumarin-loaded NPs of the indicated sizes and polymer types and prepared for FACS analyses. (a-b) Size dependent uptake of FA-labeled PLGA-NPs, 6-coumarin-loaded PPP-NPs or control NPs without fluorophore-loading by APCs. NPs used for this experiment were made of different compounds and different sizes (as indicated). Representative FACS blots for specific NP-sizes are shown. (c) Size and concentration dependent uptake of FA-labeled PLGA-NPs (upper panel), 6-coumarin-loaded PPP-NPs (lower panel) and corresponding control NPs without fluorophore-loading by myeloid APCs ( $n=4$  as triplicates) from (a) and (b). The mean  $\pm$  SD of all tested NP-sizes is shown for PLGA and PPP for 0.1 mg/mL and 1 mg/mL.

#### 4.3.5. In vitro effect of OVA-loaded NPs on T cells and NPs

NPs are commonly used to increase drug solubility, stability and specificity. To investigate if the loading of NPs with OVA-antigen is beneficial for the antigen-specific activation of CD8 T cells we incubated APCs together with naïve CD8 T cells bearing a transgenic T cell

receptor recognizing OVA-derived SIINFEKL-peptide in the context of MHC I molecules (OT-1 T cells) and free OVA at different concentrations and compared this with PLGA-/PPP-NPs loaded with the same amount of OVA. 24 hours later we analyzed the expression of activation markers on the surface of T cells (CD69) and APCs (CD80) and measured T cell-released IL-2 as a further indicator for T cell activation following antigen presentation by APCs (Figure 6a). With increasing OVA concentrations the CD69-expression on T cells was increased, reaching maximal expression levels at 125  $\mu\text{g/mL}$  free, unbound OVA. The half maximal CD69-expression on T cells was reached at 26.5  $\mu\text{g/mL}$ , 4.35  $\mu\text{g/mL}$  or 1.62  $\mu\text{g/mL}$  for soluble OVA, PLGA-OVA-NPs and PPP-OVA-NPs respectively (marked by dotted lines). Incubation with untreated NPs did not affect APC-induced T cell activation and the use of NPs together with unbound OVA did not alter the pattern of the curve compared with free OVA alone. These results indicate that loading of OVA into PLGA- or PPP-NPs increases the efficiency with which APCs can activate CD8 T cells in antigen-specific fashion. Coupling of OVA to NPs leads to a significant decrease of the amount of antigen required for T cell activation, which might be important to increase the efficacy of vaccination. T cell activation is determined by the amount of presented antigen as processed peptides on MHC I molecules by the APCs (signal 1), co-stimulatory signals from the APCs via CD80/86 (signal 2) and co-stimulatory cytokines [1]. We investigated if uptake of NPs affected the expression of the co-stimulatory molecule CD80 on APCs in co-culture with OVA-specific T cells. Incubation with blank NPs did not alter CD80 expression while incubation with unbound OVA increased the percentage of CD80-expressing APCs to more than 80%. The amount of OVA and consequent T cell activation that was needed to reach the half maximal CD80 expression (marked by the dotted lines) was significantly higher for free OVA (39.9  $\mu\text{g/mL}$ ) compared with PLGA-OVA-NPs (6.2  $\mu\text{g/mL}$ ) and PPP-OVA-NPs (1.15  $\mu\text{g/mL}$ ).

Our results demonstrate that NPs alone do not cause functional maturation of APCs, but that the antigen-specific interaction of APCs with T cells led to up regulation of co-stimulatory molecules. The significant difference in T cell and APC activation between OVA-loaded PLGA- and PPP-NPs may be explained by their different properties for antigen-loading and antigen-release over time (pH 7.4) as PPP-NPs have a 2% higher loading efficiency, in combination with an almost doubled antigen release over time. As the antigen-release studies with pH 4.5-5.5, mimicking the phagolysosome conditions, were

not conclusive we cannot prove or disprove that the acidification in the lysosome does have an impact on this antigen release from the different NPs. On the other hand it is reported that PEGylation leads to ~50% reduced phagocytosis of macrophages in vitro compared to non-PEGylated NPs [45,46]. An aspect that alters NPs uptake is the zeta-potential, which was published to negatively correlate with the ability of macrophages to phagocytose NP [47]. As PPP-OVA-NPs do have an 8.7 mV higher zeta potential (-16 mV) than PLGA-OVA-NPs (-24.7 mV) one could assume that the uptake of PLGA-NPs is increased even further compared with PPP-OVA-NPs. Assuming that the PEGylation and the surface charge in our PPP-NPs decreases in vitro uptake, the 16- and 35-fold increase in CD69 and CD80 expression respectively, gets even more distinct, although the same amount of OVA was used. Based on the previous findings of stronger CD69/CD80 expression it is no surprise that these differences are even more pronounced for the production of IL-2. IL-2 is produced by the activated T cells and induces proliferation via an autocrine feedback loop. The amount of free OVA necessary to induce T cell release of 5 ng/mL IL-2 was 38 µg/mL. A 6-fold reduced amount was needed with PLGA-OVA-NP (6.1 µg/mL) and a 30-fold reduced amount with PPP-OVA-NP (1.26 µg/mL) (Figure 5a). Taken together, the NPs from PLGA derivatives incorporating OVA were superior with respect to antigen-presentation and antigen-specific activation of T cells although the uptake speed of PPP-Ova-NPs might be affected by PEGylation and surface charge.

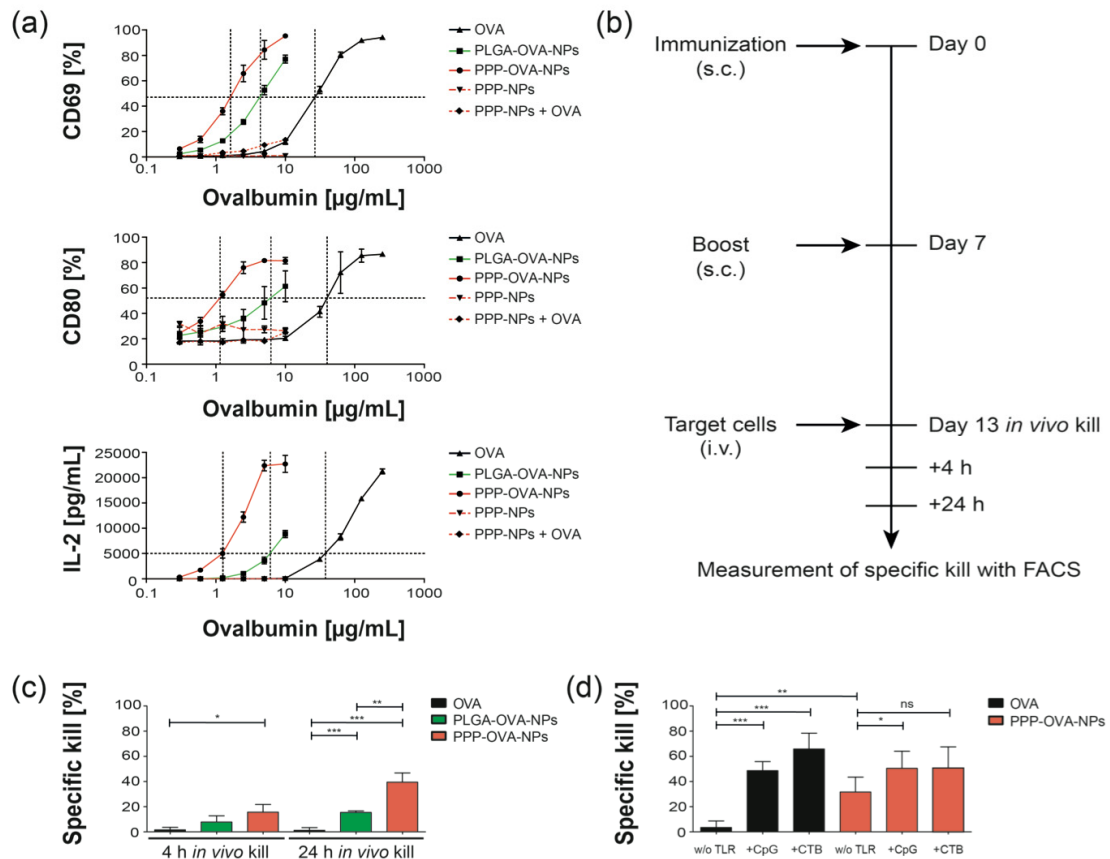


**Figure 6: OVA-loaded PPP-NPs significantly increase T cell/macrophage activation and in vivo kill efficiency.** The NP size for PLGA and PPP is  $250 \pm 30$  nm. (a) OTI T cells and APCs were co-incubated with the indicated OVA concentrations either as unbound control (OVA), loaded within NPs of the indicated polymer type or as a co-incubation with unloaded PPP-NPs for 24 h. CD69 and CD80 expression was detected by FACS, IL-2 by ELISA. Mean  $\pm$  SD is shown for the antigen dependent CD69 expression on OTI T cells, CD80 expression on APCs and IL-2 production in the supernatant for all measured concentrations ( $n=4$ ). (b) Immunization scheme for the in vivo kill assay in which C57BL/6 mice were immunized sc with PBS, OVA, PLGA-OVA or PPP-OVA-NPs  $\pm$  TLR agonist. (c) 4 h and 24 h in vivo kill for OVA, PLGA-OVA-NPs and PPP-OVA-NPs. The mean  $\pm$  SD is shown ( $n=3-5$ ). (d) 4 h in vivo kill for OVA and PPP-OVA  $\pm$  ODN CpG1826 (CpG) or Cholera toxin subunit B (CTB). The mean  $\pm$  SD is shown ( $n=5$ ).

#### 4.3.6. PLGA-OVA-NPs improve generation of cytotoxic CD8 T cells in vivo

PLGA-OVA-NPs and PPP-OVA-NPs were superior to soluble OVA to elicit antigen-specific T cell activation in vitro by myeloid APCs. In vivo this may be different as the NPs might encounter additional hurdles, such as attachment to endothelial cells. We immunized wild-type BL6 mice twice sc with OVA, PLGA-OVA-NPs or PPP-OVA-NPs in PBS at day 0 and day 7 to induce the activation and proliferation of endogenous SIINFEKL-specific T cells. After additional 6 days we analyzed antigen-specific cytotoxicity in vivo by injecting differentially labeled target cells (Figure 6b). In OVA-immunized mice we did not detect any OVA-specific T cell-mediated cytotoxicity, neither 4 h nor 24 h after injection of target

cells (Figure 6c). This was expected as it is known that antigen alone in the absence of adjuvants, does not elicit T cell activation and formation of cytotoxic effector T cells [1]. PLGA-OVA-NPs did not significantly increase the specific cytotoxicity after 4 h but did so after 24 h (15.4%). PPP-OVA-NPs on the other hand not only increased the specific kill significantly after 4 h (15.6%) compared with soluble OVA, but also elicited an increased cytotoxicity compared with PLGA-OVA-NPs injected mice (39.5%). These results confirm our in vitro data and demonstrate that PLGA-based NPs can be used as carrier for prophylactic vaccination strategies. As the state-of-the-art vaccine requires adjuvants to elicit functional maturation of APCs and PLGA-based NPs could also be used as carrier for additional adjuvants, we repeated the above mentioned immunization scheme for OVA and PPP-OVA-NPs in a mix with the TLR9-ligand ODN-CpG and cholera toxin subunit B (CTB) which both are commonly used adjuvants for in vivo experiments. The addition of CpG or CTB increased the specific kill for PPP-OVA-NPs only slightly while the OVA/adjuvant mix did increase more than 50% reaching the same level as PPP-OVA-NPs with adjuvant. Thus, loading of OVA into PPP-NPs increased the T cell response to such an extent that there was only some benefit from additional adjuvant (Figure 6c). Our findings are of interest for the formulation process of vaccines since it may reduce the number of components required and could reduce adjuvant-induced side effects. It is possible that the further addition of an adjuvant to the NP/antigen formulation may strengthen the T cell response even further. Although the difference between OVA+adjuvant versus PPP-OVA-NPs+adjuvant is not significant it is possible that the combinatorial use of PPP-OVA-adjuvant-NPs may provide a further beneficial effect on vaccination efficiency. Similar to the increase in antigen-presentation if antigen is complexed with NP, encapsulated adjuvant within the NP may increase vaccination efficiency. It was shown that inclusion of the adjuvant together with the antigen inside the same NPs leads to an increased stimulation of APCs, because it elicits functional maturation in the same cell that processes the antigen for T cell activation [48,49].

#### 4.4. Conclusion

We observed a significantly increased release of antigen from NPs, which was expected for PEG-*b*-PLGA NPs. Our study shows that the NP uptake in myeloid derived antigen presenting cells is independent from different PLGA polymers, while NP concentration and

size determine the uptake by APCs, with NP sizes ranging between 250-400 nm showing the best cellular uptake. Using in vitro and in vivo experimental models for antigen-specific T cell activation, we show that OVA-loaded PLGA-based NPs increase antigen presentation by APCs and thus cause CD8 T cell activation determined by measuring CD69 and IL-2 production. Furthermore we observed the generation of CD8 T cells in vivo through OVA formulated to PEG-*b*-PAGE-*b*-PLGA that led to potent antigen-specific cytotoxicity. Thus, PPP-NPs appear as a suitable platform for future vaccination formulations as they already contain adjuvant-effects and may serve as carrier for cancer-derived antigens in order to improve tumor-specific immunity. The use of TLR ligands, loaded inside the NPs, may further strengthen the outcome of vaccination. Further experiments need to address whether those additional modifications may improve the success of vaccination also in a therapeutic setting, where conventional vaccination protocols have failed.

## 4.5. References

1. Pulendran B, Ahmed R. Immunological mechanisms of vaccination. *Nat. Immunol.* 2011;12:509–17.
2. Zhao L, Seth A, Wibowo N, Zhao C-X, Mitter N, Yu C, et al. Nanoparticle vaccines. *Vaccine.* 2014;32:327–37.
3. Zhu Q, Talton J, Zhang G, Cunningham T, Wang Z, Waters RC, et al. Large intestine-targeted, nanoparticle-releasing oral vaccine to control genitorectal viral infection. *Nat. Med. Nature Publishing Group*; 2012;18:1291–6.
4. Slütter B, Bal S, Keijzer C, Mallants R, Hagenaars N, Que I, et al. Nasal vaccination with N-trimethyl chitosan and PLGA based nanoparticles: nanoparticle characteristics determine quality and strength of the antibody response in mice against the encapsulated antigen. *Vaccine.* 2010;28:6282–91.
5. Chong CSW, Cao M, Wong WW, Fischer KP, Addison WR, Kwon GS, et al. Enhancement of T helper type 1 immune responses against hepatitis B virus core antigen by PLGA nanoparticle vaccine delivery. *J. Control. Release.* 2005;102:85–99.
6. Slütter B, Plapied L, Fievez V, Sande MA, des Rieux A, Schneider Y-J, et al. Mechanistic study of the adjuvant effect of biodegradable nanoparticles in mucosal vaccination. *J. Control. Release.* 2009;138:113–21.
7. Janes KA, Fresneau MP, Marazuela A, Fabra A, Alonso MJ. Chitosan nanoparticles as delivery systems for doxorubicin. *J. Control. Release.*; 2001;73:255–67.
8. Gan Z, Yu D, Zhong Z, Liang Q, Jing X. Enzymatic degradation of poly( $\epsilon$ -caprolactone)/poly(DL-lactide) blends in phosphate buffer solution. *Polymer (Guildf).* 1999;40:2859–62.



9. Leroueil-Le Verger M, Fluckiger L, Kim Y-I, Hoffman M, Maincent P. Preparation and characterization of nanoparticles containing an antihypertensive agent. *Eur. J. Pharm. Biopharm.* 1998;46:137–43.
10. Sarmento B, Ferreira D, Veiga F, Ribeiro A. Characterization of insulin-loaded alginate nanoparticles produced by ionotropic pre-gelation through DSC and FTIR studies. *Carbohydr. Polym.*; 2006;66:1–7.
11. Balthasar S, Michaelis K, Dinauer N, von Briesen H, Kreuter J, Langer K. Preparation and characterisation of antibody modified gelatin nanoparticles as drug carrier system for uptake in lymphocytes. *Biomaterials.* 2005;26:2723–32.
12. Dillen K, Vandervoort J, Van den Mooter G, Verheyden L, Ludwig A. Factorial design, physicochemical characterisation and activity of ciprofloxacin-PLGA nanoparticles. *Int. J. Pharm.* 2004;275:171–87.
13. Fonseca C, Simões S, Gaspar R. Paclitaxel-loaded PLGA nanoparticles: preparation, physicochemical characterization and in vitro anti-tumoral activity. *J. Control. Release.* 2002;83:273–86.
14. Govender T, Stolnik S, Garnett MC, Illum L, Davis SS. PLGA nanoparticles prepared by nanoprecipitation: drug loading and release studies of a water soluble drug. *J. Control. Release.* 1999;57:171–85.
15. Lemoine D, Pr  at V. Polymeric nanoparticles as delivery system for influenza virus glycoproteins. *J. Control. Release.* 1998;54:15–27.
16. Schuette V, Burgdorf S. The ins-and-outs of endosomal antigens for cross-presentation. *Curr. Opin. Immunol.* 2014;26:63–8.
17. Akagi T, Wang X, Uto T, Baba M, Akashi M. Protein direct delivery to dendritic cells using nanoparticles based on amphiphilic poly(amino acid) derivatives. *Biomaterials.* 2007;28:3427–36.
18. Reisacher WR, Liotta D, Yazdi S, Putnam D. Desensitizing mice to ovalbumin through subcutaneous microsphere immunotherapy (SMITH). *Int. Forum Allergy Rhinol.* 2011;1:390–5.
19. Moingeon P, Batard T, Fadel R, Frati F, Sieber J, Van Overtvelt L. Immune mechanisms of allergen-specific sublingual immunotherapy. *Allergy.* 2006;61:151–65.
20. Dumitriu S, Popa VI. *Polymeric Nanoparticles for Drug Delivery.* Polym. Biomater. Vol. 1. CRC Press; 2013.
21. Pai SS, Tilton RD, Przybycien TM. Poly(ethylene glycol)-modified proteins: implications for poly(lactide-co-glycolide)-based microsphere delivery. *AAPS J.* 2009;11:88–98.
22. Harris JM, Martin NE, Modi M. Pegylation: a novel process for modifying pharmacokinetics. *Clin. Pharmacokinet.* 2001;40:539–51.
23. Bazile D, Prud'homme C, Bassoullet MT, Marlard M, Spenlehauer G, Veillard M. Stealth Me.PEG-PLA nanoparticles avoid uptake by the mononuclear phagocytes system. *J. Pharm. Sci.* 1995;84:493–8.

24. Marepally S, Boakye CHA, Shah PP, Etukala JR, Vemuri A, Singh M. Design, synthesis of novel lipids as chemical permeation enhancers and development of nanoparticle system for transdermal drug delivery. *PLoS One.*; 2013;8:e82581.
25. Byrne JD, Betancourt T, Brannon-Peppas L. Active targeting schemes for nanoparticle systems in cancer therapeutics. *Adv. Drug Deliv. Rev.*; 2008;60:1615–26.
26. Wang M, Thanou M. Targeting nanoparticles to cancer. *Pharmacol. Res.*; 2010;62:90–9.
27. Justyna A. Czaplewska, Tobias C. Majdanski, Markus J. Barthel, Michael Gottschaldt USS. Functionalized PEG-b-PAGE-b-PLGA Triblock Terpolymers as Materials for Nanoparticle Preparation. *J. Polym. Sci. Part A Polym. Chem.* 2015;
28. Horisawa E, Kubota K, Tuboi I, Sato K, Yamamoto H, Takeuchi H, et al. Size-dependency of DL-lactide/glycolide copolymer particulates for intra-articular delivery system on phagocytosis in rat synovium. *Pharm. Res.* 2002;19:132–9.
29. Weiss B, Schaefer UF, Zapp J, Lamprecht A, Stallmach A, Lehr C-M. Nanoparticles made of Fluorescence-Labelled Poly(L-lactide-co-glycolide): Preparation, Stability, and Biocompatibility. *J. Nanosci. Nanotechnol.* American Scientific Publishers; 2006;6:3048–56.
30. Schröder M, Richter C, Juan MHS, Maltusch K, Giegold O, Quintini G, et al. The sphingosine kinase 1 and S1P1 axis specifically counteracts LPS-induced IL-12p70 production in immune cells of the spleen. *Mol. Immunol.* 2011;48:1139–48.
31. Cruz LJ, Tacke PJ, Fokkink R, Figdor CG. The influence of PEG chain length and targeting moiety on antibody-mediated delivery of nanoparticle vaccines to human dendritic cells. *Biomaterials.* Elsevier Ltd; 2011;32:6791–803.
32. Li Y, Pei Y, Zhang X, Gu Z, Zhou Z, Yuan W, et al. PEGylated PLGA nanoparticles as protein carriers: synthesis, preparation and biodistribution in rats. *J. Control. Release.* 2001;71:203–11.
33. Panyam J, Zhou W-Z, Prabha S, Sahoo SK, Labhasetwar V. Rapid endo-lysosomal escape of poly(DL-lactide-co-glycolide) nanoparticles: implications for drug and gene delivery. *FASEB J.* 2002;16:1217–26.
34. Harush-Frenkel O, Rozentur E, Benita S, Altschuler Y. Surface Charge of Nanoparticles Determines Their Endocytic and Transcytotic Pathway in Polarized MDCK Cells. *Biomacromolecules.* 2008;9:435–43.
35. De Feijter, J. A., & Benjamins J. Adsorption kinetics of proteins at the air–water interface. *Food Emuls. Foam.* 1987. p. 72–85.
36. Stevens L. Egg white proteins. *Comp. Biochem. Physiol. Part B Comp. Biochem.* 1991;100:1–9.
37. Sorkin A, Von Zastrow M. Signal transduction and endocytosis: close encounters of many kinds. *Nat. Rev. Mol. Cell Biol.* Nature Publishing Group; 2002;3:600–14.
38. Hammer GE, Ma A. Molecular control of steady-state dendritic cell maturation and immune homeostasis. *Annu. Rev. Immunol. Annual Reviews*; 2013;31:743–91.

39. Blanco D, Alonso MJ. Protein encapsulation and release from poly(lactide-co-glycolide) microspheres: effect of the protein and polymer properties and of the co-encapsulation of surfactants. *Eur. J. Pharm. Biopharm.* 1998;45:285–94.
40. FDA. Inspection Technical Guides: Bacterial Endotoxins / Pyrogens. 2013;1–5.
41. Uto T, Akagi T, Toyama M, Nishi Y, Shima F, Akashi M, et al. Comparative activity of biodegradable nanoparticles with aluminum adjuvants: antigen uptake by dendritic cells and induction of immune response in mice. *Immunol. Lett.* 2011;140:36–43.
42. Akagi T, Baba M, Akashi M. *Polymers in Nanomedicine*. Kunugi S, Yamaoka T, editors. Polym. NANOMEDICINE. Berlin, Heidelberg: Springer Berlin Heidelberg; 2012.
43. Goldberg AL, Cascio P, Saric T, Rock KL. The importance of the proteasome and subsequent proteolytic steps in the generation of antigenic peptides. *Mol. Immunol.* 2002;39:147–64.
44. Foged C, Brodin B, Frokjaer S, Sundblad A. Particle size and surface charge affect particle uptake by human dendritic cells in an in vitro model. *Int. J. Pharm.* 2005;298:315–22.
45. Fontana G, Licciardi M, Mansueto S, Schillaci D, Giammona G. Amoxicillin-loaded polyethylcyanoacrylate nanoparticles: Influence of PEG coating on the particle size, drug release rate and phagocytic uptake. *Biomaterials.* 2001;22:2857–65.
46. Yang A, Yang L, Liu W, Li Z, Xu H, Yang X. Tumor necrosis factor alpha blocking peptide loaded PEG-PLGA nanoparticles: preparation and in vitro evaluation. *Int. J. Pharm.* 2007;331:123–32.
47. Roser M, Fischer D, Kissel T. Surface-modified biodegradable albumin nano- and microspheres. II: effect of surface charges on in vitro phagocytosis and biodistribution in rats. *Eur. J. Pharm. Biopharm.* 1998;46:255–63.
48. Diwan M, Elamanchili P, Lane H, Gainer A, Samuel J. Biodegradable nanoparticle mediated antigen delivery to human cord blood derived dendritic cells for induction of primary T cell responses. *J. Drug Target.* 2003;11:495–507.
49. Ramachandra L, Chu RS, Askew D, Noss EH, Canaday DH, Potter NS, et al. Phagocytic antigen processing and effects of microbial products on antigen processing and T-cell responses. *Immunol. Rev.* 1999;168:217–39.

## 5. Semi-Automated Nanoprecipitation-System - an option for operator independent, scalable and size adjustable nanoparticle synthesis

Parts of this Chapter were published in:

René Rietscher\*, Carolin Thum\*, Claus-Michael Lehr, Marc Schneider;

***Semi-Automated Nanoprecipitation-System - an option for operator independent, scalable and size adjustable nanoparticle synthesis***; Pharmaceutical Research;

DOI: 10.1007/s11095-014-1612-z

\*These authors contributed equally to this work

The author of the thesis made the following contribution to the publication: Planned and designed all experiments, performed experiments related to particle preparation and characterization, analyzed data from the above mentioned studies, interpreted experimental data and wrote the manuscript.

Carolin Thum, instructed by the author of the thesis, contributed to the publication by performing parts of the experiments related to particle preparation and characterization as well and by analyzing data from the above mentioned studies and interpreting experimental data. The author thanks Carolin Thum for the great collaboration.

## **5.1. Introduction**

Nano drug carrier systems increasingly gain influence in the field of galenic drug formulations. By the use of drug carrier systems in general, problems associated with the free drug or therapeutic ineffectiveness can be solved. Problems that can be addressed, are for example an unfavorable pharmacokinetic, a faster in vivo degradation, poor biodistribution or even a lack of selectivity for the target tissue [1]. In short, these carrier systems can improve the bioavailability and significantly reduce the toxicity of the free drug [2]. Especially great potential promises nanoscale carrier systems, so-called nanocarriers. The term nanoscale defines a size range of approximately 1-100 nm. However, even though nanocarriers are systems which can be in this size range the term also describes systems in the sub-micrometer from 1-1000 nm [3]. Major disadvantages of most nanocarriers are the poor scale-up possibility and bad reproducibility of particle production precluding a commercial or clinical use of nanoparticles [4]. Depending on the encapsulated drug, especially colloidal systems based on lipids or polymers are most likely suitable. Consequently, such systems are well studied in recent years [5–7]. The enormous potential of nanocarriers is due to their small size and large surface-to-volume ratio enabling a good tissue penetration and a high cellular uptake. Both are important aspects in order to allow a carrier system to effectively deliver a drug to the site of action. For the preparation of such nanoscaled carrier systems the nanoprecipitation method is one of the most prevalent and commonly used method [5]. The nanoprecipitation method, investigated by Fessi in the end of the 1980s [8], is a simple, rapid, inexpensive and due to the low energy input an especially gentle manufacturing process for polymer-based nanoparticles. Specific for the nanoprecipitation method is the precipitation of a dissolved polymer forming particles, after mixing the solvent with a non-solvent for the polymer containing stabilizing agents. The solvent is thereby totally miscible with the non-solvent. The nanoparticles are formed immediately by fast diffusion of the solvent into the non-solvent forming small nano-droplets, which are directly coated by stabilizer [9–11]. This method is not limited to a specific polymer but can be transferred to many synthetic or natural polymers which are relevant as drug carrier materials [12]. In literature already a multitude of parameters influencing the nanoparticle sizes are extensively discussed. Besides the polymer, solvent and non-solvent, also process parameters, like injection speed of the solvent, FR of the non-solvent and the hydrodynamic forces and their

distribution in the non-solvent with respect to IP influence the particle formation. Most of the parameters are considerably depending on the operator and are difficult to control [12]. To overcome this operator dependency can be avoided using an automated system for nanoparticle preparation, which would also allow for scale-up. Therefore, a fluidic nanoprecipitation system was established by Xie and Smith in 2010 [13] without evaluation and identification of production-influencing process parameters. The present work, focus on a broader understanding of the SAN-System and the impact of the process parameters on the formation of a model drug carrier system. Hence the preparation of blank PLGA particles was investigated analyzing size, size distribution and morphology of the particles. This system can be a viable step on the road to commercialized nanoparticle production for nanomedicines of sufficient pharmaceutical quality.

## **5.2. Materials and method**

### **5.2.1. Materials**

PLGA - Resomer RG 503 H was supplied by Evonik Industries AG (Darmstadt, Germany). DMSO (HPLC grade) and Spectra/Por® 7 - dialysis membrane was purchased from Sigma-Aldrich Chemie GmbH (Steinheim, Germany). PVA (Mowiol 4-88) was purchased from Kuraray Europe GmbH (Hattersheim, Germany). Water used for all preparations and investigations was Millipore Q-Gard 2 (Merck Millipore, Billerica, United States). All other chemicals used were of analytical grade.

### **5.2.2. Experimental setup – SAN-System**

The developed SAN-System is composed of several modules (Figure 1). The relevant parts of the system are the syringe pump (Harvard Apparatus PHD ULTRA, Harvard Apparatus Inc., Holliston, USA), the syringe (Hamilton 1005 TLL, CS-Chromatographie Service GmbH, Langerwehe, Germany), and the gear pump (Ismatec SA MC-Z, IDEX Health & Science GmbH, Wertheim, Germany) with the respective tubing ( $\varnothing_{\text{inner}} = 4.8$  mm, Norprene Chemical, VWR, Darmstadt, Germany). The syringe pump is controlling the IR of the polymer solvent, by a needle with a straight needle head (Metal (N) Hub Needle 0.72x0.41, ps 3, CS-Chromatographie Service GmbH, Langerwehe, Germany), into the tubing. The gear pump is controlling the FR of the polymer non-solvent within the tubing (0.1 to

100 ml/min). The beginning and end of the tubing's are placed into a beaker with stir bar, for sampling. To avoid bending influenced turbulences [14] at the injection point and to keep the injection point and angle always constant a tube straightener module is used. The needle penetration depth is thereby controlled by a spacer bar (Figure 1A).

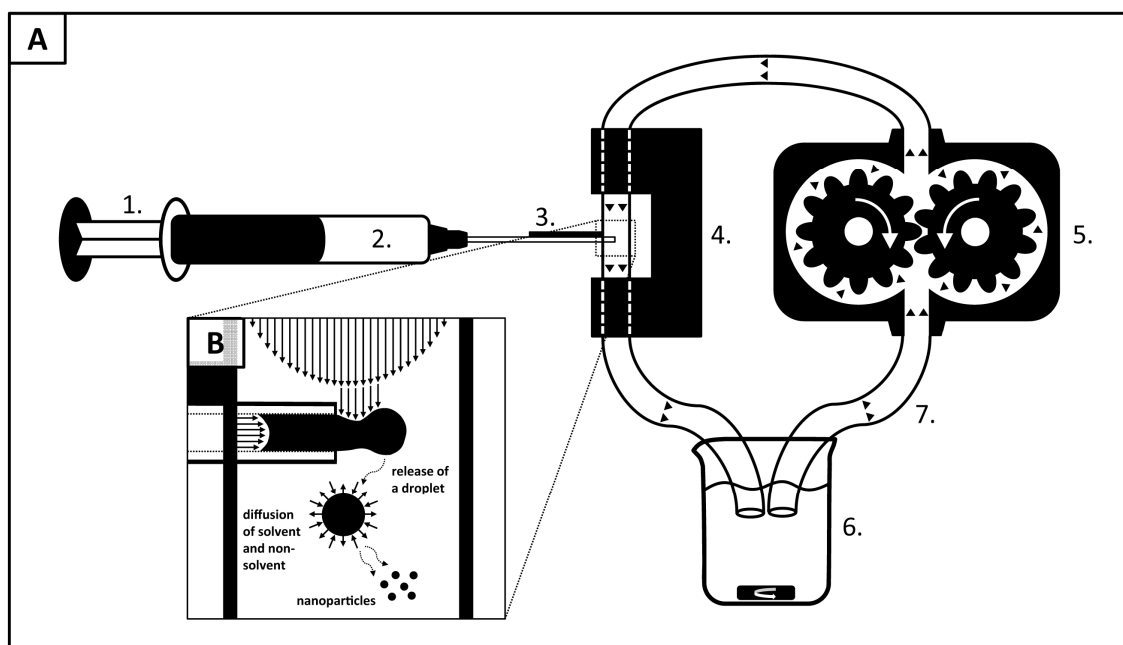


**Figure 1** | A) Schematic presentation of the Semi-Automated Nanoprecipitation-System consisting of a syringe pump with a syringe (1), polymer solution to inject (2), a spacer at a needle with a straight head (3), a tube straightener module (4) a gear pump (5), a beaker with stir bar (6), and the tubing (7) B) Schematic presentation of the nanoparticle formation.

### 5.2.3. Preparation and washing of nanoparticles

Nanoparticles were prepared with by the SAN-System. Different concentrations of PLGA polymer (16.6-100 mg/ml) were dissolved in 3 ml DMSO, drawn up into a 5 ml syringe with a straight needle head and plugged in a syringe pump. 40 ml of a 2% PVA solution was used to fill the tubing beaker and gear pump. The resulting nanoparticle solution was purified by dialysis (Molecular weight cut off 15,000 Da) in water (in 2 liters for 2 hours) to reduce the amount of DMSO for improved lyophilization. Finally, the nanoparticles were purified by centrifugation at 15,000 g for 10 min (Rotina 420 R, Hettich Lab Technology, Tuttlingen, Germany) and washed twice with water to remove excess PVA. After purification Trehalose (w/w) was added as a cryoprotectant for lyophilization. Three independent batches for each formulation were prepared and stored at 6 °C after lyophilization.

#### **5.2.4. Characterization of nanoparticles**

The average size (in nm) and size distribution (polydispersity index - PDI) of the polymeric nanoparticles were measured using DLS (Zetasizer Nano ZSP, Malvern Instruments, Herrenberg, Germany) at 25°C. The measurements were performed with aqueous dispersions of nanoparticles (~ 0.1 mg/ml) before lyophilization. The surface morphology was determined by SEM (Zeiss EVO HD15, Jena, Germany) after sample coating with a 10 nm gold layer (Q150R Rotary-Pumped Sputter Coater, Quorum Technologies, UK) at a focal distance of 10 mm and an acceleration voltage of 5 kV.

#### **5.3. Results and Discussion**

The primary objective of our study is the evaluation of the relevant parameters of the SAN-System to control particle size. Several parameters were investigated to show the influence on particle formation. These are the needle position inside of the tube moving the drop formation to different flow conditions of the non-solvent, the IR of the solvent from the syringe, the FR of the non-solvent in the tubes and the polymer concentration. As standard parameters an aqueous 2% PVA solution as non-solvent with a FR of 20 ml/min 50 mg PLGA in 3 ml DMSO as solvent for injection into the non-solvent with an IR of 0.05 ml/min at a fixed needle position in the center of the tubing was used. The size and PDI of the resulting nanoparticles were evaluated as key parameters for comparing the particles supported by scanning electron microscope micrographs.

Based on the laminar flow profile inside the tubes which was estimated by calculating the Reynolds number (< critical Reynolds number of ~2,300 for all flow rates investigated [15]) it was assumed that the drop formation and as a consequence particle formation is influenced by the IP. The reason for this assumption is the different flow speed in the center or near the edge of the tube. The head of the needle was placed in the center or near the tube wall at the injection point of the tube or the opposite side of the IP. The penetration depth of the needle was controlled by a spacer and all other parameters, IR, FR and PLGA concentration were kept constant. Smaller and more uniform droplets/particles are estimated for the centered position because of the higher flow speed in the center of the tube. The difference between the centered and the edge position was 1.5 millimeter. Independently from the needle position no significant smaller particles for



the centered position (size  $208.1 \pm 4.7$  nm, PDI  $0.09 \pm 0.03$ ) compared to the edge positions (size  $213.4 \pm 14.7$  nm, PDI  $0.07 \pm 0.03$ ) were found. This is supported by calculations of flow speeds in the center and near the edge of the tubes that show only a difference of 5%. Due to the better handling and no significance of the IP, for all other experiments the center position was used.

To clarify the influence of different IR of the syringe pump, 0.01, 0.05 and 0.25 ml/min were used, with a constant FR of 20 ml/min and PLGA concentration of 50 mg/ml. The needle diameter was also kept constant, because bigger or smaller diameter would only lead to higher or lower speed using the same IR. In detail, the bypassing circulation of non-solvent in the tubes tears off a solvent droplet from the needle exit (Figure 1B). With higher IR bigger droplets will be formed and as a consequence bigger particles as the FR was kept constant and hence the force to tear off a drop. As expected an increased size from 145 nm at 0.01 ml/min IR, 154 nm for 0.05 ml/min IR up to 179 nm for 0.25 ml/min IR, with a PDI for all results always below 0.1 was found. Consequently, by using different IR the experimental time increases. With the same amount of 50 mg PLGA polymer in 1 ml DMSO, with a decreasing IR from 0.25 ml/min to 0.01 ml/min, the experimental time increases from 4 min up to 100 min. As a perspective also a run with an IR of 0.1 ml/min, PLGA concentration of 50 mg/ml and FR of 20 ml/min with an extended time over 8 h was performed. Compared to our short runs, we found no major difference in size ( $148.1 \pm 2.5$  nm), by scaling up the amount of polymer and injection time.

For the control of the FR a gear pump was used. The use of a peristaltic pump was excluded due to the non-constant and pulsatile flow, which would have complicated or even dismantled the analysis of this parameter. The use of different tube diameters was also not necessary, because thinner or thicker tubes would only result in a changed overall flow speed. Representatively the adjusted flow rates of 1, 4, 8 and 20 ml/min lead to flow speeds of 5.76, 23.06, 46.11 and 115.28 cm/min. The FR used - 1, 4, 8 and 20 ml/min for 50 mg/ml PLGA resulted in a steady increase of particles size from 155.6 nm for 1 ml/min up to 228.3 nm for 20 ml/min. This trend is also observed for other PLGA concentrations (Figure 2). Furthermore it is evident, that with a decrease in FR the particle distribution is increasing. Starting from a PDI with 0.03, which represents a uniform distribution the PDI raises up to 0.15 indicating a more polydisperse size distribution [16]. Due to the higher

polydispersity of particles prepared with the FR of 1 ml/min this FR was not used for later experiments.

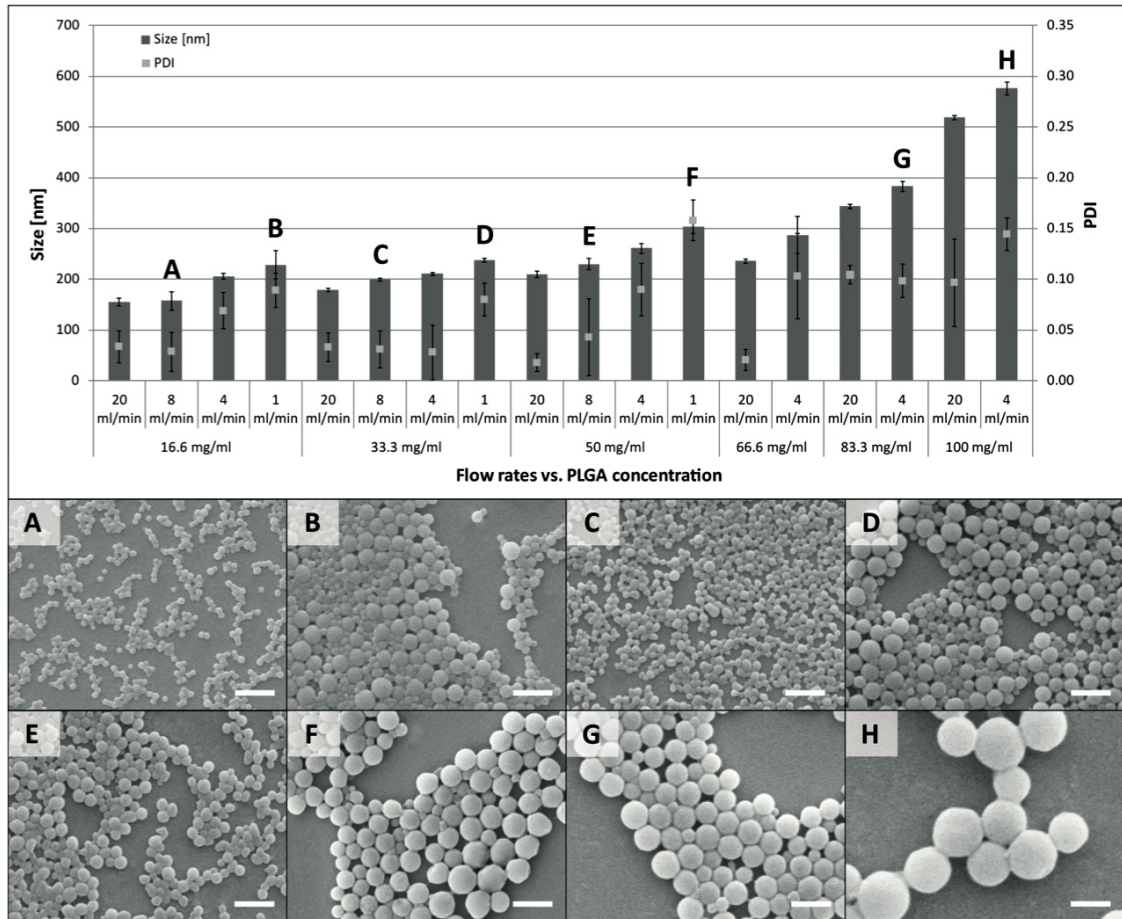


**Figure 2 |** Bar chart with particle size and PDI as a function of FR and polymer concentration. SEM images A-H to the corresponding DLS measurements. Size of the scale bar = 500 nm.

Regarding the influence of the polymer concentration six different PLGA concentrations from 16.6 mg/ml to 100 mg/ml dissolved in DMSO were tested, while keeping the other parameters constant. The effect of different PLGA concentrations in combination with different FRs for the non-solvent can be seen in Figure 2. For lower PLGA concentrations 16.6 and 33 mg/ml no change in the size was observed. By increasing the PLGA concentration further from 50 to 100 mg/ml the size of the particles increased up to 580 nm. For higher PLGA concentrations 1 ml/min FR were excluded due to the too high polydispersity. The effect of the concentration on particle size is most likely due to an increase of the viscosity of the solvent, with a higher amount of dissolved polymer. The injected polymer stream from the syringe is still the same, but with a higher viscosity of the solvent more force is needed to tear off a drop from the stream.

Additionally to DLS the size measurements were evaluated with SEM images (Figure 2). The particles are spherical and image analyses by Image J revealed 10-20 nm smaller particles. This difference is due to hydrodynamic diameter obtained in DLS, compared to diameters measured under dried conditions with SEM. To summarize, it was possible to generate particles from 150 to 600 nm. The strong influence of the polymer concentration by bench-top (manual) performance of nanoprecipitation was already claimed in literature [17,18].

## **5.4. Conclusion**

In summary, it can be concluded that the particle size and distribution of the PLGA nanoparticles can be controlled by varying the FR, IR and polymer concentration using the SAN-System in a large range from 150 to 600 nm. The influence can be ranked from IP with no influence under the experimental conditions chosen and to an increasing influence for IR, to FR to polymer concentration. With increasing FR, the resulting particles are smaller. By increasing the IR, the resulting particle size of the prepared PLGA nanoparticles increases (increase of nanoparticles particle size:  $0 \sim I < IR < FR-1 < c_{\text{polymer}}$ ). In the present work the polymer concentration was identified as the most relevant process parameter regarding size and size distribution of the particles. The results demonstrate that the developed and validated SAN-system is able to produce particles in a reproducible and controllable manner by the principle of nanoprecipitation without any influence of the operator. Additionally a larger scale-up for the production of nanoparticles with no restrictions is possible, because the quantities of solvent and non-solvent are not limited to a certain extend. Sizes between 100 to 600 nm can be specifically produced for the respective application requirement.

## **5.5. References**

1. Allen TM, Cullis PR. Drug delivery systems: entering the mainstream. *Science*. 2004;303:1818–22.
2. Kammona O, Kiparissides C. Recent advances in nanocarrier-based mucosal delivery of biomolecules. *J. Control. Release*. 2012;161:781–94.
3. Goeran L, Hubert R, Gert R, Birgit S-K, Peter G, Jean-Philippe P, et al. Considerations on a Definition of Nanomaterial for Regulatory Purposes. Publications Office of the European Union; 2010.

4. Davis ME, Chen ZG, Shin DM. Nanoparticle therapeutics: an emerging treatment modality for cancer. *Nat. Rev. Drug Discov.* Nature Publishing Group; 2008;7:771–82.
5. Soppimath KS, Aminabhavi TM, Kulkarni AR, Rudzinski WE. Biodegradable polymeric nanoparticles as drug delivery devices. *J. Control. Release.* 2001;70:1–20.
6. Des Rieux A, Fievez V, Garinot M, Schneider Y-J, Préat V. Nanoparticles as potential oral delivery systems of proteins and vaccines: a mechanistic approach. *J. Control. Release.* 2006;116:1–27.
7. Swaminathan J, Ehrhardt C. Liposomal delivery of proteins and peptides. Informa UK, Ltd. London; 2012;
8. Fessi H, Puisieux F, Devissaguet JP, Ammoury N, Benita S. Nanocapsule formation by interfacial polymer deposition following solvent displacement. *Int. J. Pharm.* 1989;55:R1–4.
9. Beck-Broichsitter M, Rytting E, Lebhadt T, Wang X, Kissel T. Preparation of nanoparticles by solvent displacement for drug delivery: a shift in the “ouzo region” upon drug loading. *Eur. J. Pharm. Sci.* 2010;41:244–53.
10. François G, Katz JL. Nanoparticles and nanocapsules created using the Ouzo effect: spontaneous emulsification as an alternative to ultrasonic and high-shear devices. *Chemphyschem.* 2005;6:209–16.
11. Quintanar-Guerrero D, Allémann E, Doelker E, Fessi H. Preparation and Characterization of Nanocapsules from Preformed Polymers by a New Process Based on Emulsification-Diffusion Technique. *Pharm. Res.* Kluwer Academic Publishers-Plenum Publishers; 1998;15:1056–62.
12. Mora-Huertas CE, Fessi H, Elaissari A. Polymer-based nanocapsules for drug delivery. *Int. J. Pharm.*; 2010;385:113–42.
13. Xie H, Smith JW. Fabrication of PLGA nanoparticles with a fluidic nanoprecipitation system. *J. Nanobiotechnology.* 2010;8:18.
14. Guan X, Martonen TB. Simulations of Flow in Curved Tubes. *Aerosol Sci. Technol.* Taylor & Francis; 1997;26:485–504.
15. Avila K, Moxey D, de Lozar A, Avila M, Barkley D, Hof B. The onset of turbulence in pipe flow. *Science.* 2011;333:192–6.
16. Keck, C.M., Müller RH. Photonenkorrelationsspektroskopie. *Mod. Pharm. Technol.* 2009. p. 56–60.
17. Plasari E, Grisoni PH, Villermaux J. Influence of Process Parameters on the Precipitation of Organic Nanoparticles by Drowning-Out. *Chem. Eng. Res. Des.* 1997;75:237–44.
18. Chorny M, Fishbein I, Danenberg HD, Golomb G. Lipophilic drug loaded nanospheres prepared by nanoprecipitation: effect of formulation variables on size, drug recovery and release kinetics. *J. Control. Release.* 2002;83:389–400.

## 6. Overall Conclusion and Outlook

The major aim of the thesis was to show the potential of oral vaccine delivery using nanoparticulate delivery systems for vaccination. Therefore the model protein OVA was used, which can be either used for method development, but also for *in vivo* murine studies. NPs are an ideal protective vehicle for oral vaccine delivery as they protect the vaccine from harsh gastrointestinal environment and can be taken up efficiently by APCs to induce immunological responses. In literature oral vaccination plays an important role in current research, due to the huge advantages. Nevertheless, disadvantages like potential degradation of the vaccine based protein, with probably inefficient uptake through the intestinal wall and APCs or low immune response need to be considered. With regard on these specific issues, we investigated different approaches, like usage of different adjuvants and polymers with passive and active drug targeting properties. We focused with our work on the *in vitro* and *in vivo* evaluation of a nanoparticulate vaccine delivery system as a platform for oral vaccination.

For our research the well-known and FDA approved polymer PLGA was used, to create modified PLGA derivatives for passive and active drug targeting, to further improve NP uptake and achieve higher immune response. Specific modifications of PLGA should lead to lower regulatory obstacles for registration, of a new vaccine delivery system, and clinical trials, rather than using an unknown and maybe unsafe polymer. Besides the basic PLGA polymer, the following modified PLGA derivatives were used for our research: PEG-*b*-PLGA, unmodified PEG-*b*-PAGE-*b*-PLGA, Mannose-PEG-*b*-PAGE-*b*-PLGA and Amine-PEG-*b*-PAGE-*b*-PLGA polymer. On the one hand the PEGylation was added in order to increase the hydrophilic character of the polymer (PEG-*b*-PLGA polymer) and consequently enhance the encapsulation and release properties for proteins. On the other hand the PEGylation forms a shell on the NP surface and can mask the NPs from host's immune system, prolonging the presence of the PEGylated NPs in the human body (passive drug targeting). For our *in vitro* and *in vivo* studies different PLGA, PEG-*b*-PLGA and unmodified PEG-*b*-PAGE-*b*-PLGA polymers were available in sufficient large quantities. As the Mannose-PEG-*b*-PAGE-*b*-PLGA and Amine-PEG-*b*-PAGE-*b*-PLGA polymers were only accessible during later stages of the experiments and also only in small quantities, the prepared NPs with the model proteins OVA and Her-2/neu were directly send to partners,

for further characterization and *in vitro* and *in vivo* studies.

For active drug targeting a PAGE group was added between the PEG and PLGA building block (PEG-*b*-PAGE-*b*-PLGA polymer) to link covalently functional groups to the polymer. Functional groups or ligands can reduce associated side effects and furthermore the total dose of NPs needed for vaccination. Tested side-chain functionalizations are the Mannose functionalized Mannose-PEG-*b*-PAGE-*b*-PLGA and the Amine functionalized Amine-PEG-*b*-PAGE-*b*-PLGA polymer. As mentioned before in the main introduction part the Mannose functionalization can target the Mannose receptor of APCs, facilitating the NP uptake in APCs, whereas the Amine functionalization was introduced to mimic the properties of starch or chitosan NPs, which are able to open the tight junctions, due to their cationic surface charge and increase the uptake through the intestinal wall. The results of the thesis demonstrate the potential of modified PLGA polymers, PEG-*b*-PLGA and PEG-*b*-PAGE-*b*-PLGA, for the protection of the protein from degradation and for the induction of higher immune responses, in contrast to the basic PLGA polymer. Furthermore adjuvant-effects of the nanoparticulate vaccine delivery systems made of the unmodified PEG-*b*-PAGE-*b*-PLGA polymer were demonstrated. Unfortunately, the Amine-PEG-*b*-PAGE-*b*-PLGA could not show any benefit in the performed studies. A possible explanation is the pH dependency of the amine functionality and the absence of the permanent, cationic charge of the amine, to mimic the cationic Chitosan. For Mannose-PEG-*b*-PAGE-*b*-PLGA NPs a different routing of NP uptake was observed. Walden et al. recently found the uptake of these NPs in early endosomes rather than acidified endosomes, in comparison to already published studies (paper still under review). However, a significant higher efficiency of T cell stimulation of Mannose-PEG-*b*-PAGE-*b*-PLGA NPs was determined, than with PLGA NPs.

As shown in the third chapter of the thesis even the unmodified PEG-*b*-PAGE-*b*-PLGA polymer shows in first *in vitro* studies, with the model protein OVA, superior properties over the basic PLGA and PEG-*b*-PLGA polymer. A significantly increased loading for the PEG-*b*-PAGE-*b*-PLGA polymer was observed, with lower tendency to degrade the encapsulated protein. The PEGylation alone had no major impact on OVA loading, however the addition of the PAGE building block between PEG and PLGA, increased the OVA loading significantly. For the release of protein a minor impact of the PEG group was

observed by increasing the OVA release slightly. However the burst and sustained release from PEG-*b*-PAGE-*b*-PLGA NPs was roughly 50 to 100% higher compared to PEG-*b*-PLGA and PLGA NPs. Initially the PAGE group was inserted to add functionalities to the polymer. Surprisingly the non-functionalized PAGE group added already major benefits in loading and release of the model protein, what can be only attributed to the combined PEG-*b*-PAGE functionality.

As the unmodified PEG-*b*-PAGE-*b*-PLGA polymer shows in *in vitro* systems potential benefits, the polymer has been also evaluated within an *in vivo* mouse vaccination study. Therefore, in the fourth chapter of this thesis, PLGA and PEG-*b*-PAGE-*b*-PLGA NPs were used in *in vitro* and *in vivo* mouse vaccination studies. First the safety of the NPs was proven, regarding cytotoxicity, endotoxin content and stability. As almost the same polymers were used, from the chapter before, the same favorable loading and release characteristics were found for PEG-*b*-PAGE-*b*-PLGA, compared to PLGA. With different PLGA and PEG-*b*-PAGE-*b*-PLGA NP sizes a polymer independent and size dependent uptake optimum between 250-400 nm in macrophages (APC) *in vitro* was found. The following cross presentation of antigen on MHC I molecules and subsequent CD8<sup>+</sup> T cell activation was highly dependent on the polymer type. PEG-*b*-PAGE-*b*-PLGA NP showed *in vitro* a significant increased T cell activation, determined by CD69 up-regulation on T cells, CD80 expression on macrophages and a higher IL-2 production of T cells. In *in vivo* mouse studies, sc application of PEG-*b*-PAGE-*b*-PLGA NPs, resulted in the generation of CD8<sup>+</sup> T cell-mediated OVA-specific cytotoxicity, that was more pronounced than after application of OVA alone or PLGA-OVA-NPs. Additionally an intrinsic adjuvant-function of PEG-*b*-PAGE-*b*-PLGA NPs was found, because the NPs were as good as OVA alone with additional adjuvant.

For the vaccination study the synthesis of PLGA NPs with increasing sizes for size dependent uptake studies in APCs were necessary. The standard methods for the preparation of NPs are the double emulsion or nanoprecipitation method, which are commonly used to produce NPs in a size range of 150-250 nm. However these methods lack in the preparation of NPs with different sizes in a controlled manner, especially in terms of reproducibility and scale-up possibility. Therefore, in the fifth chapter of this thesis, a semi-automated system for an operator independent, scalable and size-

adjustable nanoparticle synthesis, on the bases of the nanoprecipitation method, was investigated. With the “Semi-Automated Nanoprecipitation System”, by varying process parameters, NPs in a size range of 150 to 600 nm with a narrow size distribution ( $PDI < 0.15$ ) were achievable. Furthermore, a production of NPs in a larger scale was possible with this SAN-System. As the principles of the nanoprecipitation were used for the SAN-System, encapsulation of hydrophilic substances, like proteins was not achieved.

### **Suggestions for future work**

Based on our studies and literature survey, vaccination via the oral route shows great potential to develop effective immune responses, with all mentioned benefits. However, the major challenge is the delivery of the vaccine via the oral route to APCs to generate an efficient immune response. From our studies, we have shown the great potential of our nanoparticulate vaccine carriers, nevertheless the proof of concept for a successful oral vaccination is still an unresolved issue. The focus of future work should be:

- I. Mechanistic studies of the PAGE building block for the *in vitro* characterization of the new PLGA derivatives. The influence and mechanistic action of the PAGE group is still unclear. Therefore polymers with different molecular weight of PLGA, PEG and also PAGE should be synthesized, in comparison to a PAGE-*b*-PLGA polymer, without PEGylation.
- II. Expansion of the mouse vaccination studies to a broad setup with oral and rectal immunization, in comparison to sc vaccination, with PLGA, unmodified PEG-*b*-PAGE-*b*-PLGA and Mannose-PEG-*b*-PAGE-*b*-PLGA and Amine-PEG-*b*-PAGE-*b*-PLGA polymers.
- III. Expansion of the SAN-System, to drug loaded nanoparticle, with a relevant indication



## List of Abbreviations

2D	two-dimensional
3D	three-dimensional
AFM	atomic force microscopy
AIN	antigen loaded nanoparticle
ANOVA	analysis of variance
APC	antigen presenting cell
API	active pharmaceutical ingredient
BCA	bicinchoninic acid
BSA	bovine serum albumin
CFSE	carboxyfluorescein succinimidyl ester
CpG ODN	CpG oligodeoxynucleotides
CTB	cholera toxin B
DC	dendritic cell
DCM	dichloromethane
DDS	drug delivery system
DLS	dynamic light scattering
DMEM	Dulbecco's Modified Eagle Medium
DMSO	dimethyl sulfoxide
DNA	deoxyribonucleic acid
ELISA	enzyme-linked immunosorbent assay
FCS	fetal calf serum
FA	fluoresceinamine
FACS	fluorescence-activated cell sorting
FDA	Food and Drug Administration
FR	flow rate

---

GALT	gut associated lymphoid tissue
GIT	gastrointestinal tract
GM 1	monosialotetrahexosylganglioside 1
HBSS	Hank's Balanced Salt Solution
Her2	human epidermal growth factor receptor 2
IL-2	interleukin 2
i.e.	id est
im	intramuscular
IP	injection position
IR	injection rate
iv	intravenous
LAL	limulus amebocyte lysate
LLOD	lower limit of detection
M-CSF	macrophage colony-stimulating factor
MFI	mean fluorescence intensity
MHC	major histocompatibility complex
Mn	molecular weight
MP	microparticle
MTT	3-(4,5-dimethylthiazol-2-yl)-2,5-diphenyltetrazolium bromide
NEAA	non-essential amino acids
nm	nano meter
NP	nanoparticle
OVA	ovalbumin
o/w	oil-in-water
PAGE	poly(allyl glycidyl ether)
PAMP	pathogen-associated molecular pattern

---

PEG	polyethylene glycol
PB	phosphate buffered
PBS	phosphate buffered saline
PCL	poly- $\epsilon$ -lactone
PDI	polydispersity index
PE	phycoerythrin
PLGA	poly(D,L-lactide- <i>co</i> -glycolide)
PP	PEG- <i>b</i> -PLGA
PPP	PEG- <i>b</i> -PAGE- <i>b</i> -PLGA
PQ	partitioning coefficient
PRR	pattern recognition receptor
PVA	polyvinyl alcohol
RB	Rose Bengal
RPMI	Roswell Park Memorial Institute medium
RNA	ribonucleic acid
RT	room temperature
SAN	Semi-Automated Nanoprecipitation
sc	subcutaneous
SEM	scanning electron microscopy
SEC	size exclusion chromatography
TEM	transmission electron microscopy
TCR	T cell receptor
TLR	Toll-like receptor
w/o	water-in-oil
w/o/w	water-in-oil-in-water

## Curriculum vitae

### Personal Information

---

Name	René Rietscher
Date of birth	March 12 <sup>th</sup> 1986
Place of birth	Räckelwitz
Nationality	German

### Doctoral Thesis

---

04/2011 - 10/2014	Helmholtz Institute for Pharmaceutical Research Saarland (HIPS)/ Institute for Biopharmaceutics and Pharmaceutical Technology, Saarland University, Saarbrücken
-------------------	---

### Academic education/ professional activities

---

12/2010 - 03/2011	Pharmacist at Medicon pharmacies in Nuremberg
12/2010	Pharmaceutical license (Approbation)
05/2010 - 11/2010	Practical training as a pharmacist, Medicon pharmacy in Nuremberg - Eibacher Hauptstrasse
11/2009 - 04/2010	Diploma thesis at the Institute for Pharmaceutical Science/ University of Freiburg and Department of Pharmaceutical and Medical Chemistry/ University of Erlangen-Nuremberg
10/2005 - 10/2009	Pharmaceutical studies at the University of Erlangen-Nuremberg

## List of Publications

- I. **Rietscher R**, Thum C, Lehr CM, Schneider M  
„Semi-Automated Nanoprecipitation-System - an option for operator independent, scalable and size adjustable nanoparticle synthesis”; published in Pharmaceutical Research 2014; DOI: 10.1007/s11095-014-1612-z
- II. **Rietscher R**, Czaplewska JA, Majdanski TC, Gottschaldt M, Schubert US, Schneider M, Lehr CM  
„Impact of hydrophilic-modified PLGA on particle formation, protein loading and release”; submitted to European Journal of Pharmaceutics and Biopharmaceutics 2015
- III. **Rietscher R**, Schröder M, Janke J, Czaplewska JA, Gottschaldt M, Scherließ R, Hanefeld A, Schneider M, Knolle PA, Lehr CM  
“Tunable hydrophilic PLGA nanoparticles for protein delivery - a drug delivery system for improved vaccination efficiency”; submitted to European Journal of Pharmaceutics and Biopharmaceutics 2015
- IV. Baleeiro RB, **Rietscher R**, Diedrich A, Czaplewska JA, Lehr CM, Scherließ R, Hanefeld A, Gottschaldt M, Walden P  
“Spatial separation of the processing and MHC class I loading compartments for cross-presentation of the tumor-associated antigen HER2/neu by human dendritic cells”; published in OncoImmunology 2015; DOI: 10.1080/2162402X.2015.1047585
- V. Baleeiro RB, Schweinlin M, **Rietscher R**, Diedrich A, Metzger M, Lehr CM, Scherließ R, Hanefeld A, Walden P  
“Nanoparticle-based mucosal vaccines targeting tumor-associated antigens to human dendritic cells”; submitted to Journal of Biomedicine and Nanotechnology

**Conference contributions**

- I. **Rietscher R**, Thum C, Lehr CM, Schneider M  
“Semi-Automated Nanoprecipitation System” for the Formulation of Protein loaded PLGA Nanoparticles”; poster presentation at 9th World Meeting on Pharmaceutics, Biopharmaceutics and Pharmaceutical Technology; Lisbon, Portugal; 2014
- II. **Rietscher R**, Collnot E-M, Lehr C-M  
“Saponins as dual purpose excipients in the formulation of antigen loaded PLGA nanoparticles”; poster presentation at CRS Local Chapter Germany; Würzburg, Germany; 2012
- III. Baleeiro RB, **Rietscher R**, Diedrich A, Scherließ R, Hanefeld A, Walden P  
“Cross-presentation of the tumor antigen Her2/neu involves neither the canonical nor the endosomal pathway – A novel MHC class I cross-presentation compartment in DCs”; poster presentation at 13th International Symposium on Dendritic Cells; Tours, France; 2014
- IV. Hanefeld A, Schiller S, Wolf A, Weigandt M, Scherließ R, Diedrich A, Janke J, Knolle P, Schröder M, Walden P, Baleerio R, Lehr CM, **Rietscher R**, Schneider M,  
“Dendritic cell-targeting cancer vaccine formulations for pulmonary and peroral delivery”; presentation at DPhG annual meeting, Frankfurt, Germany; 2014

## Acknowledgements

Rückblickend auf die vergangen Jahre kann ich sagen, dass die hier vorliegende Arbeit ohne die Hilfe und Unterstützung von so vielen verschiedenen Menschen, wie meiner Familie, Freunden, Betreuern und Kollegen, nicht hätte entstehen können. Deshalb möchte ich an dieser Stelle meine Dankbarkeit gegenüber diesen wichtigen Menschen zum Ausdruck bringen. In 3-4 Jahren der Promotion lernt man unzählige Menschen kennen, die auf jeglicher Art und Weise ihren Beitrag zum Entstehen meiner Arbeit beigetragen haben. Jene Menschen, die ich hier nicht namentlich erwähnt habe, da ich diese beim Verfassen dieser Zeilen nicht immer alle vor Augen habe, bitte ich bereits jetzt um Verzeihung! Auch euch gebührt natürlich meine Dankbarkeit und Wertschätzung.

Vor allen anderen möchte ich mich ganz herzlich bei meinem Doktorvater Herrn Prof. Dr. Claus-Michael Lehr bedanken, der es mir ermöglicht hat an einem so interessanten Thema forschen zu dürfen. Ich konnte mir stets seiner Bereitschaft sich gemeinsam über mein Thema auszutauschen und seiner Unterstützung und Förderung gewiss sein. Vor allem danke ich ihm aber für seine stets offene Art als Mentor und Betreuer.

Mein besonderer Dank gilt meinen beiden Betreuern im wissenschaftlichen Alltag, Prof. Dr. Marc Schneider und Dr. Eva-Maria Collnot. Beide haben mich vor allen Dingen in meinen schwersten Zeiten zu Beginn und zum Ende meiner Promotion begleitet. Prof. Dr. Marc Schneider, mit dem ich die letzten 2 Jahre intensiver zusammen arbeiten durfte, danke ich im besonderen Maße für seine immerwährende Diskussionsbereitschaft, E-mails und Telefonate jenseits der normalen Arbeitszeiten, dem wiederholten Review meiner Erstlingswerke, sein Auge fürs Detail (Ja, ich werde nie wieder „.“ und „.“ im Englischen missachten bzw. das Leerzeichen zwischen Zahl und Einheit vergessen), sowie seine fortwährende Unterstützung und Offenheit. Natürlich möchte ich mich an dieser Stelle auch bei Frau Dr. Eva Maria Collnot bedanken, die mir zu Beginn meiner Promotion eine große Hilfe war, um mich schnell in Saarbrücken, der Arbeitsgruppe und auch in meinem Thema einzufinden.

Prof. Dr. Elmar Heinzle danke ich recht herzlich für die Übernahme des Zweitgutachtens und seine wertvollen Ratschläge und Fragen zu unseren gemeinsamen Treffen während meiner Promotionszeit. Des Weiteren bedanke ich mich bei allen weiteren Mitgliedern der Prüfungskommission.

Meine Arbeit wäre ohne die entsprechende Finanzierung meines Projektes auch nicht zu Stande gekommen. Daher möchte ich mich herzlich beim BMBF (Bundesministerium für Bildung und Forschung) für die finanzielle Förderung meiner Arbeit im Zusammenhang mit dem „PeTrA“ Projekt bedanken. Zusätzlich möchte ich mich bei allen Wissenschaftlern, die zum Erfolg dieses Projektes beigetragen haben, bedanken. Insbesondere danke ich hier Stefan Schiller von der Firma Merck für die gemeinsame Entwicklung der Nano- und Mikropartikel sowie Dr. Matthias Schröder von der Uni Bonn, für die Durchführung der zahlreichen immunologischen Experimente und für das gemeinsame Niederschreiben unserer Publikation.

Ein besonderer Dank gilt natürlich auch unserem „Office“. Dazu gehören Isabelle Conrad, Karin Groß, Sarah Müller und Stephanie Kallenborn, auf deren organisatorische Unterstützung ich immer zählen konnte.

Weiterhin möchte ich mich bei unseren Technikern, insbesondere Dr. Chiara De Rossi, Petra König, Leon Muijs, Peter Meiers, Heike Stumpf und Chris Schild für ihre Unterstützung in der Zellkultur, dem Praktikum und für elektronenmikroskopische Aufnahmen, bedanken.

Ein großer Dank geht selbstverständlich an meine ehemaligen Kollegen, besonders Ankit, Nico, Sarah, Steffi, Nici, Caro, Hagar, Xavier, Chrissi, Saeed, Daniel, Efrat, Birthe, Nadia, Salem, Lutz, Christina, Maïke, Hiroe, Clemens und Mardiyanto. Mit eurer neu gewonnen Freundschaft und Hilfe für wissenschaftliche, aber auch alltägliche Dinge, war so manches Problem leichter zu bewältigen. Es hat Spaß gemacht mit euch zusammen zu arbeiten und wenn ich eines in der kleinen Welt der pharmazeutischen Wissenschaft gelernt habe, dann dass man sich mindestens zweimal im Leben trifft. Ich freue mich darauf!!

Der bedeutendsten Dank gilt aber den mir wichtigsten Personen in meinem jetzigen Leben. Dies sind an erster Stelle meine Eltern, die mich stets in allem unterstützt und an mich geglaubt haben und mich meinen eigenen Weg gehen ließen, auch wenn dieser



fernab meiner Heimat ist. Den wohl größten Anteil daran, dass ich mich überhaupt für die Promotion und nicht für die Leitung einer Apotheke entschieden habe, hatte meine Schwester Anja. Dafür und für jegliche Unterstützung in sämtlichen Lebenslagen, möchte ich mich herzlich bedanken. Meiner Freundin Christina, die stets an mich glaubt, mir jederzeit zugehört und so unendlich viel Zeit und arbeitsreiche Wochenenden für mich geopfert hat, danke ich auch von ganzem Herzen! Selbstverständlich darf hier auch der Rest meiner Familie nicht fehlen! Vielen lieben Dank für alles!!!

